

This version of the SI published 30/08/2024 replaces the previous version published 30/07/2024 . It now includes a link to the DRUM repository.

Supplementary Information for

Combining photocontrolled-cationic and anionic-group-transfer polymerizations using a universal mediator: enabling access to two- and three-mechanism block copolymers

Brandon M. Hosford^{‡, [a]} William Ramos^{‡, [a]} and Jessica R. Lamb^{*[a]}

[‡]Contributed equally to this work

^[a]*Department of Chemistry, University of Minnesota—Twin Cities, 207 Pleasant Street SE, Minneapolis, MN 55455, United States*

*Corresponding author. Email: jrlamb@umn.edu

Data for this paper, including raw data for NMR spectroscopy, SEC, TGA, DSC, MALDI-TOF, and copies of figures are available at the Data Repository for the University of Minnesota (DRUM) at <https://doi.org/10.13020/jqbp-3e81>.

Table of Contents

1. General information	S2
A. Instrumentation and methods.....	S2
B. Sources of solvents and reagents	S4
2. Supplemental data	S6
A. Exploring the effects of the pyrylium photocatalyst on TAGT homopolymerization	S6
B. Homopolymerization screen and associated SEC traces.....	S7
C. Vinyl ether monomer screen and associated SEC traces	S9
D. Thiirane monomer screen and associated SEC traces.....	S10
E. Initial chain extension screen and associated SEC traces	S12
F. Evidence for fractionation by solubility upon precipitation	S16
G. SEC traces of block copolymers purified by prepSEC.....	S21
H. Verification of polymer end-groups	S24
I. Thermal characterization of polymers.....	S32
J. Triblock terpolymer synthesis and associated SEC traces.....	S48
K. Polymerization mechanisms.....	S50
3. General synthetic procedures	S51

A.	Photoreactor setup	S51
B.	General procedure for photo-CP of vinyl ethers.....	S51
C.	General procedure for TAGT of thiiranes	S54
D.	General procedure for anionic chain extensions of p(EVE)	S57
E.	Procedure for radical chain extension of p(EVE)- <i>b</i> -p(POPS)	S59
4.	Compound synthesis and characterization.....	S60
A.	1-(2-Methylpropoxy)ethyl <i>N,N</i> -diethylcarbamodithioate (TCT1).....	S60
B.	3-Phenoxypropylene sulfide (POPS)	S62
C.	Propylene sulfide (PS).....	S63
D.	3-(Allyloxy) propylene sulfide (AOPS).....	S64
E.	3-Phenylpropylene oxide	S65
F.	3-Phenylpropylene sulfide (PPS)	S66
5.	References	S67

1. General information

A. Instrumentation and methods

All polymerizations were set up in an MBraun Unilab glovebox with a nitrogen atmosphere. Cationic and radical polymerizations were irradiated in a photoreactor setup (see Section S3.A for more details) under nitrogen atmosphere outside the glovebox. Thioacyl anionic group transfer polymerizations (TAGTs) were carried out inside the glovebox. Column chromatography was performed with silica gel (particle size 3–200 μm , 70–320 mesh) using mixtures of ethyl acetate (EtOAc) and hexanes. All work-up and purification was carried out in reagent grade solvents (purchased from Fisher, Oakwood, Sigma Aldrich, and TCI) in air.

NMR spectra were recorded on a Bruker 500 MHz Avance III HD instrument with a Prodigy TCI cryoprobe [^1H , 500 MHz), (^{13}C , 126 MHz)] or a Bruker 600 MHz Avance Neo instrument with a 5 mm triple resonance cryoprobe [^1H , 600 MHz), (^{13}C , 151 MHz)] at 22 °C with shifts reported relative to the residual solvent peak [CDCl_3 : 7.26 ppm (^1H), 77.16 ppm (^{13}C)]. Data are reported as follows: chemical shift, multiplicity (s = singlet, d = doublet, t = triplet, q = quartet, h = hexet, sep = septet, m = multiplet), coupling constants (in Hz), and integration. Deuterated chloroform was purchased from Cambridge Isotope Laboratories.

Size-exclusion chromatography (SEC) analyses for polymers soluble in dimethylformamide (DMF) were performed on an Agilent 1260 LC system with two Agilent PolarGel-M (300 x 7.5 mm) columns in series at 40 °C and a flow rate of 1 mL/min with 0.025 M LiBr in DMF as the eluent. Wyatt Optilab differential refractive index (dRI), DAWN 8 angle light scattering (MALS), and Agilent 1260 Infinity UV detectors were used. The SEC was calibrated with poly(methyl methacrylate) (PMMA) standards in the same solvent. DMF (HPLC grade) was

purchased from VWR and lithium bromide was purchased from Sigma Aldrich. Samples were filtered through 0.2 μm poly(tetrafluoroethylene) (PTFE) syringe filters.

SEC analyses for poly(cyclohexyl vinyl ether) and poly(2,3-dihydrofuran) were performed on an Agilent Infinity 1260 series HPLC system with three Styragel HR columns in series at 35 $^{\circ}\text{C}$ and a flow rate of 1 mL/min with THF as the eluent. Wyatt differential refractive index and Wyatt multiangle laser light scattering detectors were used. The SEC was calibrated with poly(styrene) standards in the same solvent. THF (HPLC grade) was purchased from Fisher. Samples were filtered through 0.2 μm PTFE syringe filters.

Preparative SEC (prepSEC) was performed on a Recycling Preparative HPLC LaboACE LC-5060 Series equipped with JAIGEL-2HR column with UV and RI detectors. Dichloromethane (DCM) was used as the eluent. Samples were prepared by dissolution of the polymer samples up to a concentration of 10 mg/mL in HPLC-grade DCM stabilized with amylene, followed by filtration through a 0.2 μm syringe filter. Samples were injected into the sample loop and collected without recycling.

Thermogravimetric analyses (TGA) were performed on a TA TGA 5500 with the sample placed in an aluminum TA Classic pan inside TA platinum TGA pans (for ease of cleaning) at a heating rate of 20 $^{\circ}\text{C}/\text{min}$ under a nitrogen atmosphere. Extrapolated onset temperatures of degradation (T_0) were calculated by the intersection of the tangent lines of the pre-degradation baseline and the point of maximum gradient using the TA TRIOS software (Figure S1).

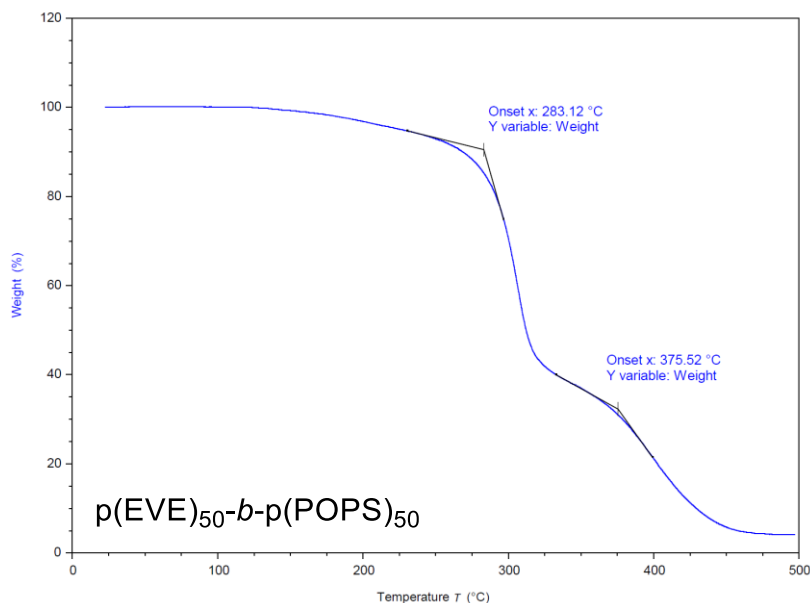


Figure S1. Example calculation of T_0 using TRIOS software.

Differential scanning calorimetry (DSC) analyses were performed on a TA 2500 under a nitrogen atmosphere. Samples were sealed inside TA Tzero pans with a hole punctured in the lid with an 18 gauge needle to allow the nitrogen atmosphere to blanket the sample. Heating and

cooling rates were set to 10 °C/min. Glass transition temperature (T_g) features were determined during the second heating cycle.

Photochemical reactions were performed using a Kessil PR160L 50W 456 nm lamp at 100% power placed in an EvoluChem PhotoRedOx Box. The box is placed on top of a magnetic stirrer inside of a fume hood. For more details and pictures, see Section S3.A.

Centrifugation of precipitated polymers was performed in 15 mL centrifuge tubes using a VWR 76019-132 Fixed Angle General Purpose Centrifuge with a 12 x 15 mL rotor spun at 4500 RPM for 1 hour.

Drying of polymer samples was performed using a Fisherbrand Isotemp Model 281A Vacuum Oven at 70 °C overnight equipped with an external trap attached to a Welch 1402B-01 DuoSeal Vacuum Pump.

Solvent purification system was purchased from Pure Process Technology (PPT) and features two packed columns of neutral alumina for each solvent. Argon is used as the inert gas.

Solubility tests were conducted by combining polymer (0.2–4.6 mg) and solvent (10 mg/mL) in a 1 dram vial and vortex mixing for 5 min. Polymers that were insoluble after vortex mixing were then sonicated for 15 min. Polymers that were still insoluble were diluted to 2 mg/mL followed by 1 mg/mL with the vortex and sonication procedures repeated at each concentration. Polymers were deemed soluble at a given concentration if the solution was clear and homogenous and insoluble if the solution was not. Solubility was then classified into one of three semi-quantitative categories defined by You and coworkers:¹ soluble (≥ 10 mg/mL), partially soluble (1–10 mg/mL), and insoluble (< 1 mg/mL).

Matrix-assisted laser desorption/ionization time-of-flight mass spectrometry (MALDI-TOF MS) was performed on a Bruker autoflex maX instrument. Analysis of poly(ethyl vinyl ether) was performed by mixing 2,5-dihydroxybenzoic acid (DHB) matrix (10 mg/mL in THF), polymer solution (10 mg/mL in THF), and potassium trifluoroacetate (5 mg/mL) at a v:v:v ratio of 1:1:1 matrix:polymer:salt, and 3 μ L were spotted on Bruker MTP 384 polished steel target plate and air-dried.

B. Sources of solvents and reagents

Allyl benzene was purchased from Oakwood Chemical and used as received.

Carbon disulfide (>99.9%) was purchased from Sigma Aldrich and used as received.

2,2'-[Carbonthioylbis(thio)]bis[2-methylpropanoic acid] (TCT2) was synthesized according to previous literature² and dried under high vacuum prior to first use.

meta-Chloroperoxybenzoic acid (<77%) was purchased from Aldrich and used as received.

Cyclohexyl vinyl ether (CHVE) was purchased from TCI and dried over calcium hydride, vacuum transferred, and freeze-pump-thawed (3x) prior to use.

Diethylamine (99%) was purchased from Alfa Aesar and filtered through a basic alumina plug prior to use.

2,5-Dihydrobenzoic acid (DHB) was purchased from Sigma Aldrich and used as received.

2,3-Dihydrofuran (DHF) was purchased from ThermoFisher Scientific and dried over calcium hydride, vacuum transferred, and freeze-pump-thawed (3x) prior to use.

***N,N*-Dimethylacetamide (DMAc) (99.8%, anhydrous)** was purchased from ThermoFisher Scientific and used as received.

Ethyl acetate (EtOAc) was purchased from Sigma Aldrich and used as received.

Ethyl 1-(2-methylpropoxy)ethyl carbonotrithioate (TCT3) was synthesized according to previous literature.³

Ethyl vinyl ether (EVE) was purchased from Sigma Aldrich and dried over calcium hydride, vacuum transferred, and freeze-pump-thawed (3x) prior to use.

Isobutyl vinyl ether (IBVE) was purchased from Sigma Aldrich and dried over calcium hydride, vacuum transferred, and freeze-pump-thawed (3x) prior to use.

***N*-Isopropylacrylamide (NIPAM)** was purchased from Sigma Aldrich and was recrystallized in hexanes prior to use.

2-Methyloxirane was purchased from Acros Organics and used as received.

2-Methylthiirane/Propylene sulfide (PS) was synthesized using a modified procedure⁴ and dried over calcium hydride, vacuum transferred, and freeze-pump-thawed (3x) prior to use. See Section S4.C for more details.

1-(2-Methylpropoxy)ethyl *N,N*-diethylcarbamodithioate (TCT1) was synthesized using a modified procedure⁵ and dried via vacuum before being brought into a nitrogen glovebox for use in polymerizations. See Section S4.A for more details.

2-(Phenoxymethyl)oxirane was purchased from TCI and used as received.

2-(Phenoxymethyl)thiirane/3-Phenoxypropylene sulfide (POPS) was synthesized using a modified procedure⁴ and dried over calcium hydride, cannula transferred and filtered through oven-dried celite, and freeze-pump-thawed (3x) prior to use. See Section S4.B for more details.

2-(Phenylmethyl)oxirane/3-Phenylpropylene oxide was synthesized using a modified procedure.⁶ See Section S4.E for more details.

2-(Phenylmethyl)thiirane/3-Phenylpropylene sulfide (PPS) was synthesized using a modified procedure⁷ and dried over calcium hydride, cannula transferred and filtered through oven-dried celite, and freeze-pump-thawed (3x) prior to use. See Section S4.F for more details.

Potassium thiocyanate was purchased from Oakwood Chemical and used as received.

Potassium trifluoroacetate was synthesized according to previous literature.⁸

2-(Prop-2-enoxymethyl)oxirane (99%) was purchased from Sigma Aldrich and used as received.

2-(Prop-2-enoxymethyl)thiirane/3-Allyloxypropylene sulfide (AOPS) was synthesized using a modified procedure⁹ and dried over calcium hydride, cannula transferred and filter through oven-dried celite, and freeze-pump-thawed (3x) prior to use. See Section S4.D for more details.

Silver nitrate (AgNO₃) was purchased from EM Sciences and used as received.

Tetrahydrofuran (THF) was purchased from Fisher Chemical, passed through two packed columns of neutral alumina and degassed via three freeze-pump-thaw cycles prior to first use.

Tetraphenylphosphonium chloride (TPPCI) was purchased from AA Blocks and used as received.

2,4,6-Tri-(*p*-methoxyphenyl)pyrylium tetrafluoroborate (PC) was synthesized according to previous literature.¹⁰

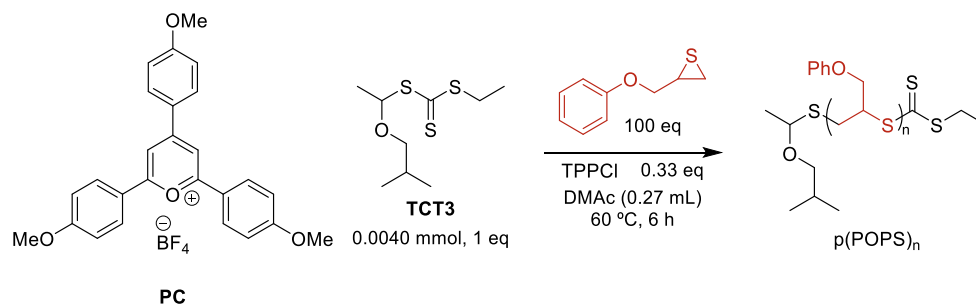
Tris[2-phenylpyridinato-C2,N]iridium(III) (Ir(ppy)₃) was purchased from Strem and was used as received.

2. Supplemental data

A. Exploring the effects of the pyrylium photocatalyst on TAGT homopolymerization

As mentioned in the main text, p(EVE) is difficult to purify due to its high solubility. Thus, the pyrylium photocatalyst (**PC**) remains in the polymer after drying the p(EVE) samples in vacuo. Therefore, the effects of the presence of **PC** needed to be explored.

Table S1. Effect of **PC** on TAGT homopolymerization



entry	mol % of PC ^[a]	conv. (%) ^[b]	<i>M</i> _n (kDa) ^[c]	<i>M</i> _w (kDa) ^[c]	<i>D</i> ^[c]
1	0	88	19.5	26.2	1.35
2	1	60	14.1	23.6	1.67
3	2	22	7.15	11.4	1.60
4	4	13	5.59	8.79	1.57

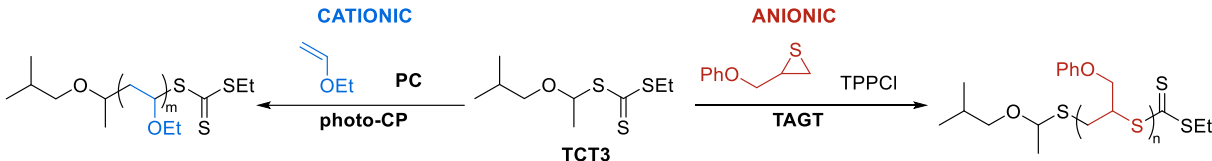
[a] Relative to **TCT3**. [b] Determined via ¹H NMR spectroscopy of the crude reaction mixture. [c] Determined via SEC in DMF with 0.025 M LiBr against PMMA standards.

As the loading of **PC** increased, the conversion of POPS to polymer decreases, which shows that **PC** does inhibit the anionic polymerization. However, limiting the amount of **PC** present in each sample of p(EVE) allows for the TAGT to run with limited effects on the polymerization. To limit the amount of residual **PC** present in the p(EVE) samples, we lowered the **PC** loading to 0.02 mol % (with respect to vinyl ether) in the photo-CP.

B. Homopolymerization screen and associated SEC traces

These studies investigate the effectiveness of both photo-CP and TAGT with a range of [M]:[**TCT3**] ratios in order to understand the limitations of the respective mechanisms. Tabulated data from these polymerizations (Table S2), along with SEC traces (Figure S2–Figure S3) can be found below.

Table S2. Tabulated SEC data from homopolymerization screen



[M]:[TCT3]	entry	photocontrolled cationic ^[a]				entry	anionic group transfer ^[b]			
		conv. (%) ^[c]	$M_{n,theo}$ (kDa)	M_n (kDa) ^[d]	\mathcal{D} ^[d]		conv. (%) ^[c]	$M_{n,theo}$ (kDa)	M_n (kDa) ^[d]	\mathcal{D} ^[d]
50:1	1a	98	3.8	4.5	1.17	1b	90	8.42	10.9	1.29
100:1	2a	99	7.4	7.0	1.26	2b	88	15.6	19.5	1.35
200:1	3a	>99	14.7	8.9	1.35	3b	90	32.0	35.8	1.44
300:1	4a	>99	21.9	11.7	1.47	4b	94	51.2	53.6	1.55

[a] Cationic standard conditions: **TCT3** (1 eq), EVE (m eq), **PC** (0.02 mol % rel. EVE), DCM (100 mM **TCT3**), RT, 456 nm LED, 6 h. [b] Anionic standard conditions: **TCT3** (1 eq), POPS (n eq), TPPCI (0.33 eq), DMAc (0.27 mL), 60 °C, 6 h. [c] Determined via ¹H NMR spectroscopy. [d] Determined via SEC in DMF with 0.025 M LiBr against PMMA standards.

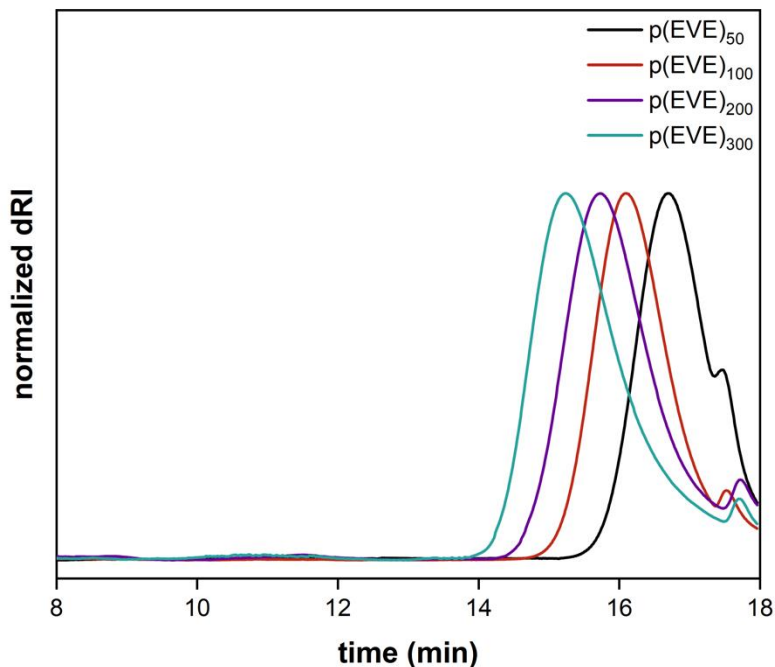


Figure S2. SEC traces of p(EVE) at various [EVE]:[TCT3] ratios. Note that p(EVE)₅₀ (black trace) is slightly overlapping with small molecule peaks.

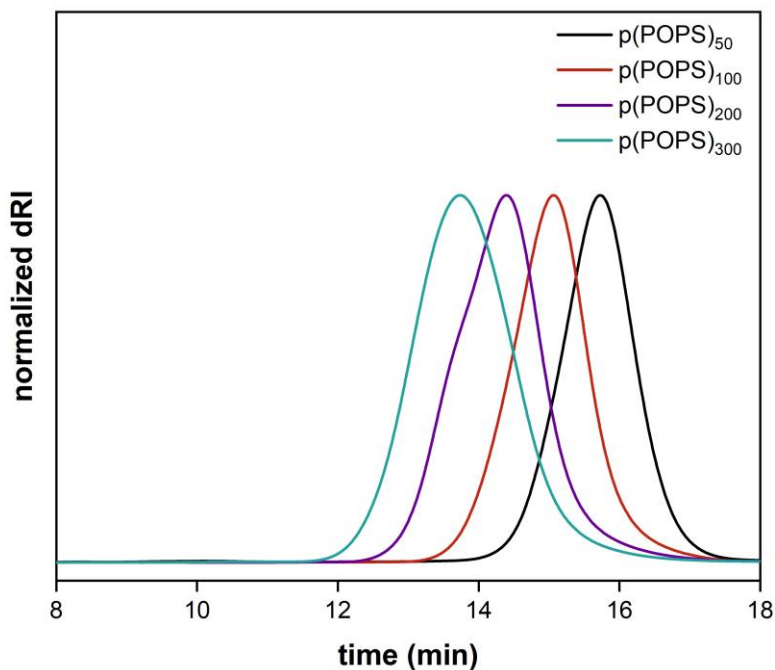


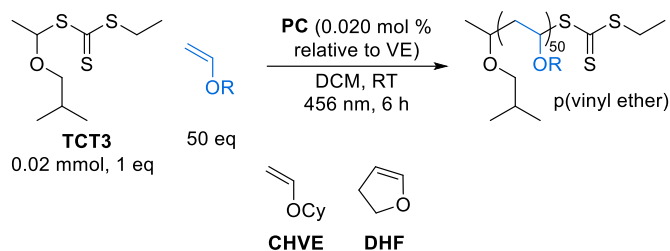
Figure S3. SEC traces of p(POPS) at various [POPS]:[TCT3] ratios.

For photo-CP, control was lost at [M]:[TCT3] greater than 100:1 due to direct monomer oxidation by the photocatalyst. TAGT retained moderate control at higher [M]:[TCT3] with a slight increase in dispersity.

C. Vinyl ether monomer screen and associated SEC traces

We attempted to expand the scope of photo-CP to high T_g poly(vinyl ethers) from cyclohexyl vinyl ether (CHVE) and 2,3-dihydrofuran (DHF), but poor control was observed (see bimodal SEC traces in Figure S4–Figure S5). Additionally, poly(CHVE) and poly(DHF) were found to be insoluble in DMAc and thus would not be suitable for chain extensions with TAGT. Therefore, we did not pursue further optimization of these monomers.

Table S3. Tabulated SEC data from vinyl ether monomer screen



Monomer	% conv. ^[a]	$M_{n,theo}$ (kDa)	M_n (kDa) ^[b]	M_w (kDa) ^[b]	\mathcal{D} ^[b]
CHVE	>99	6.5	17.6	26.6	1.51
DHF	>99	3.7	14.9	18.6	1.25

^[a]Determined via ^1H NMR spectroscopy of the crude reaction mixture. ^[b]Determined via SEC in THF against polystyrene standards.

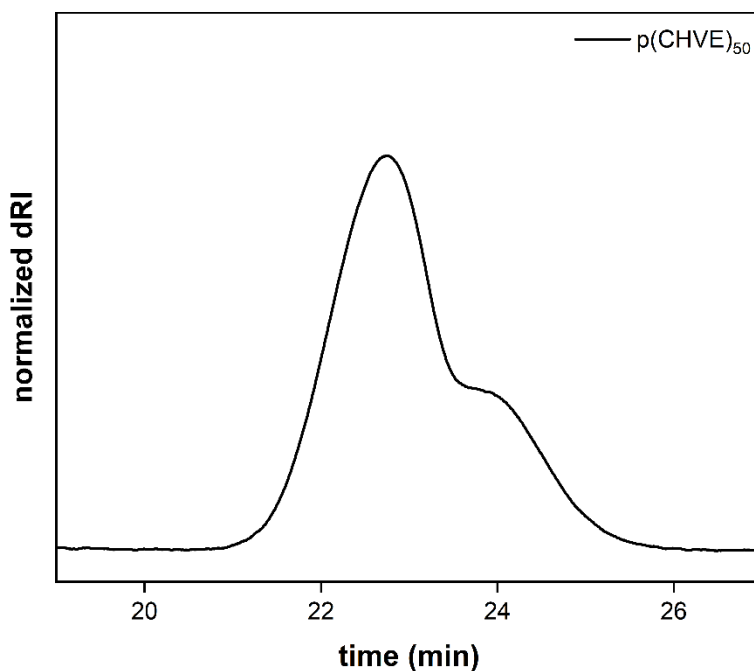


Figure S4. SEC trace of p(CHVE)₅₀.

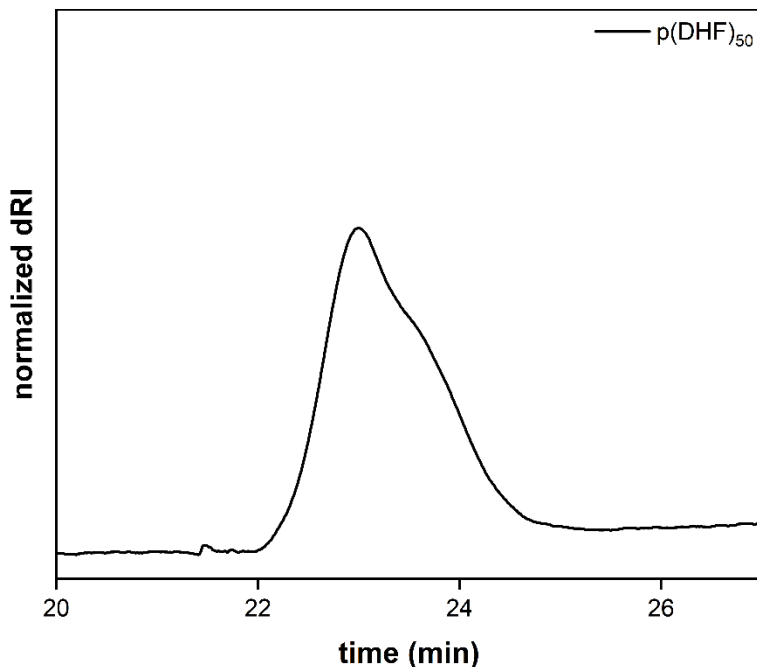
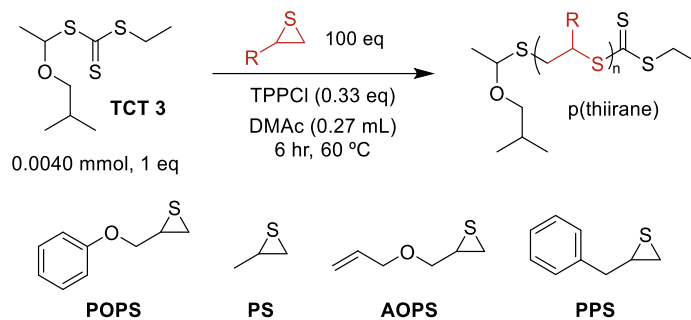


Figure S5. SEC trace of $p(\text{DHF})_{50}$.

D. Thiirane monomer screen and associated SEC traces

TCT3 has never been reported for TAGT so we wanted to test the homopolymerization of common thiirane monomers (Table S4 and Figure S6–Figure S8).

Table S4: Tabulated SEC data from thiirane monomer screen



monomer	% conv. ^[a]	$M_{n,theo}$ (kDa)	M_n (kDa) ^[b]	M_w (kDa) ^[b]	\mathcal{D} ^[b]
POPS	88	15.6	19.5	26.3	1.35
PS	>99	15.5	11.9	14.4	1.20
AOPS^[c]	17	2.66	3.02	4.63	1.54
PPS	66 ^[d]	10.9	14.1	19.6	1.39

^[a]Determined via ^1H NMR spectroscopy of the crude reaction mixture. ^[b]Determined via SEC in DMF with 0.025 M LiBr against PMMA standards. ^[c]24 hr reaction time. ^[d]Estimated due to overlap of polymer and monomer peaks in the ^1H NMR spectrum.

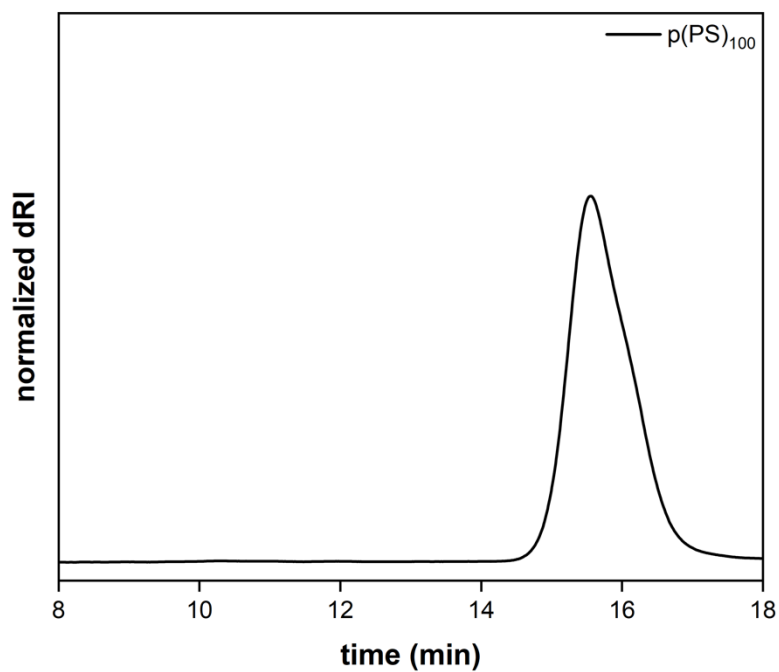


Figure S6. SEC trace of p(PS)₁₀₀.

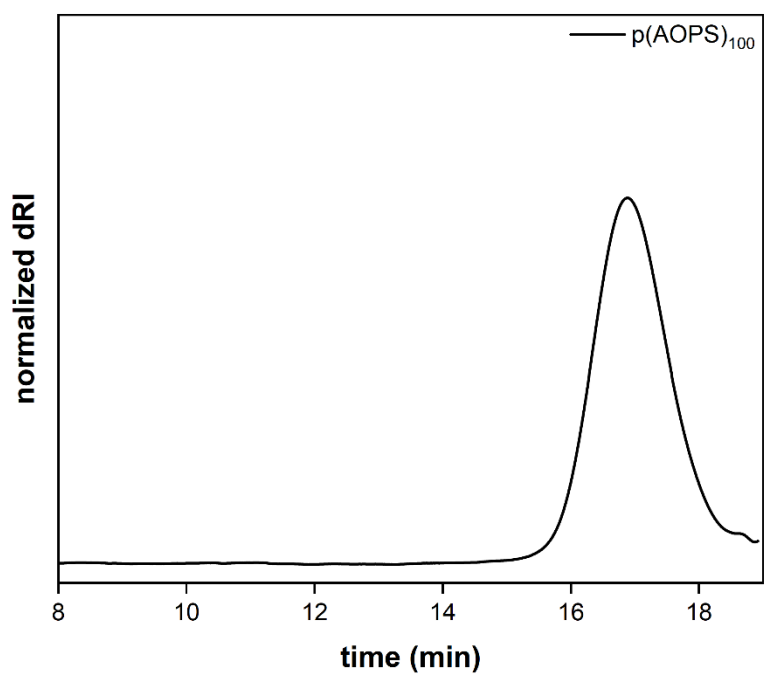


Figure S7. SEC trace of p(AOPS)₁₀₀.

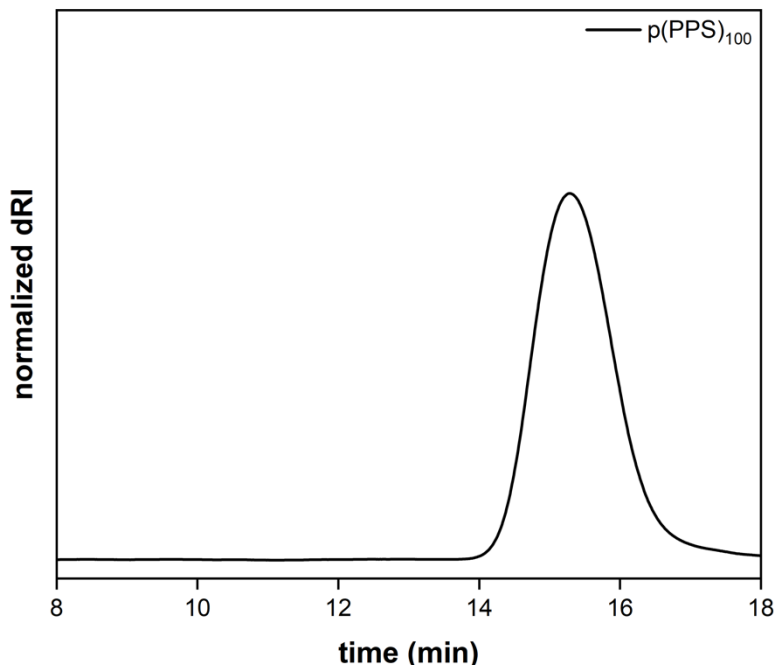


Figure S8. SEC traces of p(PPS)₁₀₀.

E. Initial chain extension screen and associated SEC traces

An initial chain extension screen was performed targeting DP 50, 100, 200, and 300 of each block. For this initial screen, a large-scale photo-CP was performed (4x typical) and the resulting p(EVE) was divided into batches for extension. This chain extension screen used 4 different [EVE]:[TCT3] ratios – 50:1, 100:1, 200:1, and 300:1 (Table S5). The degree of polymerization (DP) for p(EVE) was estimated using M_n from SEC dRI calibrated against PMMA standards.

Procedure for initial chain extensions: The p(EVE) (180–270 mg) was dissolved in DMAc (0.75 mL) to generate a stock solution. A 1 dram screw-top vial was charged with the stock solution (4.0 μ mol, 1 eq) and a stir bar. POPS (50–300 eq) was added to the vial followed by a stock solution (12 mM) of TPPCl in DMAc (0.11 mL, 1.3 μ mol, 0.33 eq). More DMAc was added until the total amount of solvent was 0.27 mL. The solution was homogenized and placed in a pre-heated reaction block at 60 °C. After stirring for 6 hours, the vial was removed from the glovebox, and an aliquot was taken for ¹H NMR analysis. The polymerization was then quenched with the addition of DCM (~100 μ L), followed by isolation via precipitation in cold methanol. The pellet was redissolved in DCM to transfer to a tared vial. Additionally, an aliquot was taken for SEC analysis. The solvent was removed via drying overnight in a vacuum oven set at 70 °C.

The DP of the p(POPS) block was estimated using ¹H NMR spectroscopy. We determined the ratio of the methine and methylene protons adjacent to the ether oxygens in p(EVE) (δ 3.33–3.66, 3H) to the methylene protons adjacent to the phenoxy groups in p(POPS) (δ 3.97–4.15, 2H). The p(POPS) DP was then calculated from this ratio and the estimated DP of the initial p(EVE) block. Due to the challenge in determining accurate DPs in the BCPs, all polymers are labeled with the

monomer equivalents added relative to TCT throughout. Please note that these labels do not correspond to the actual incorporated number of monomers but do correspond to relative length of each block (e.g., p(EVE)₁₀₀ is a larger p(EVE) block than p(EVE)₅₀). The estimated DPs can be found in Table S5. Surprisingly, the calculated DP of p(EVE)₃₀₀ was not higher than p(EVE)₂₀₀. We attribute this to the larger scale on which this screen was run (0.08 mmol TCT). Standard conditions (0.02 mmol TCT) show a slight increase in DP from p(EVE)₂₀₀ to p(EVE)₃₀₀, as expected (see Section S2.B).

Excitingly, for all the chain extensions, p(POPS) peaks were clearly present in the ¹H NMR spectra. Additionally, all SEC traces (Figures S9–S12) completely shifted to a lower retention time – indicating clean block formation. For the lower monomer feeds (50 and 100 eq to TCT), we observe unimodal peaks; conversely, for the higher monomer feeds (200 and 300 eq to TCT), we observe bimodality in the SEC traces. We hypothesize this bimodality is due to loss of control, similar to the loss of control seen in the high [monomer]:[TCT] ratio homopolymerizations (see Section S2.B).

Table S5. Summary of TAGT chain extensions on p(EVE) homopolymers

entry	starting polymer	DP of p(EVE) block ^[a]	[POPS]:[p(EVE)]	conv. (%) ^[b]	DP for p(POPS) block ^[c]	M_n (kDa) ^[d]	M_w (kDa) ^[d]	\bar{D} ^[d]
1	p(EVE) ₅₀	55	50:1	75	54	32.0	42.9	1.31
2			100:1	77	118	53.1	83.1	1.55
3			200:1	85	300	116	189	1.62
4			300:1	85	378	144	252	1.75
5	p(EVE) ₁₀₀	98	50:1	42	29	24.9	32.6	1.31
6			100:1	63	97	57.6	82.4	1.43
7			200:1	72	180	96.6	146	1.51
8			300:1	81	300	159	265	1.67
9	p(EVE) ₂₀₀	130	50:1	31	23	24.8	34.2	1.38
10			100:1	56	71	61.4	96.4	1.57
11			200:1	60	135	100	152	1.51
12			300:1	73	305	183	302	1.64
13	p(EVE) ₃₀₀	129	50:1	11	9	12.7	20.7	1.63
14			100:1	39	63	49.7	67.6	1.26
15			200:1	40	82	77.4	113	1.45
16			300:1	63	279	205	327	1.60

[a] Estimated via M_n of p(EVE) determined by SEC in DMF with 0.025 M LiBr calibrated against PMMA standards. [b] Determined via ¹H NMR spectroscopy of the crude reaction mixture. [c] Estimated via the ratio of p(EVE) to p(POPS) in the ¹H NMR spectrum of the crude reaction mixture. [d] Determined via SEC in DMF with 0.025 M LiBr against PMMA standards. Standard reaction conditions: p(EVE) (4.0 μmol, 1 eq), POPS (n eq), TPPCI (0.33 eq), DMAc (15 μM p(EVE)), 6 h, 60 °C.

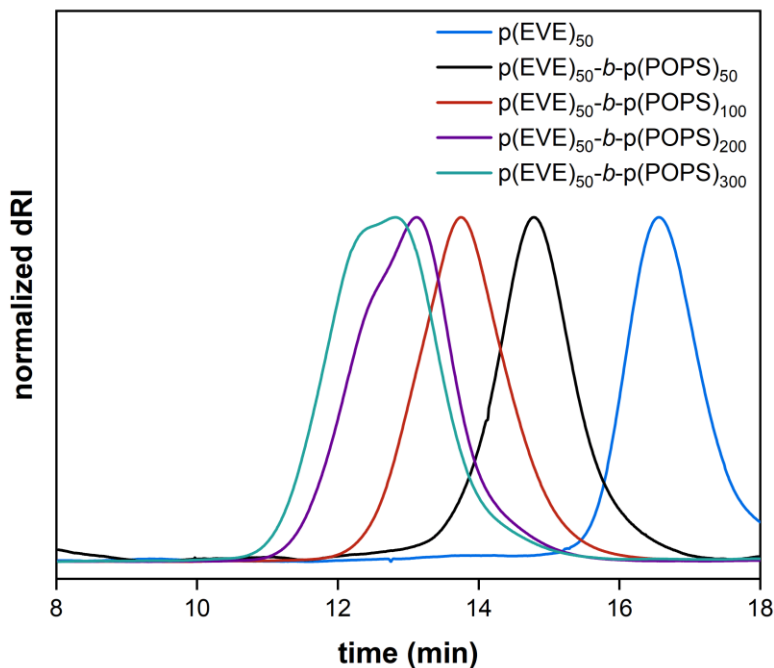


Figure S9. SEC traces of precipitated p(EVE)₅₀-b-p(POPS)_n.

The SEC traces of the p(EVE) homopolymers shown in Figures S10–S12 feature a sloping baseline that was due to contamination of the cationic photocatalyst building up in the columns over time. We learned that a 2 hour flush at the end of the SEC sequence was required to remove the contamination – resulting in better baselines going forward.

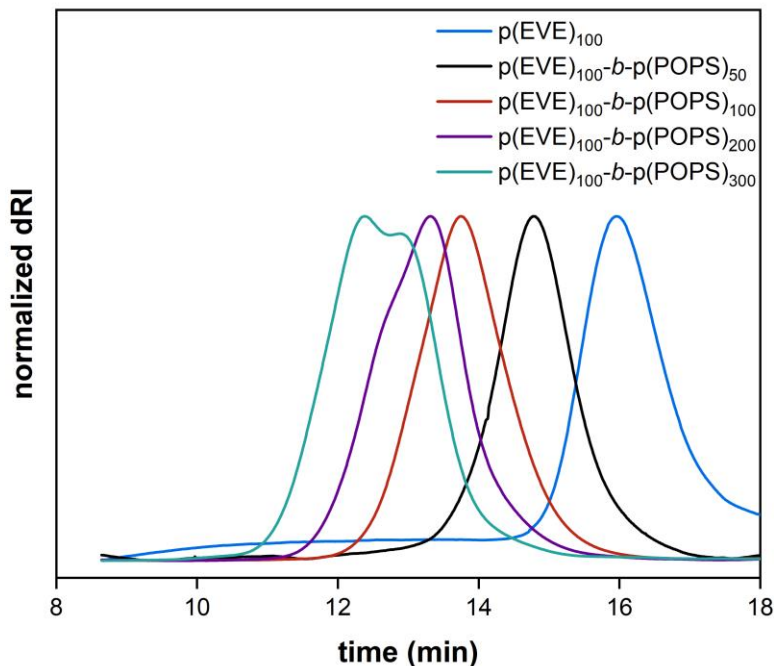


Figure S10. SEC traces of precipitated p(EVE)₁₀₀-b-p(POPS)_n.

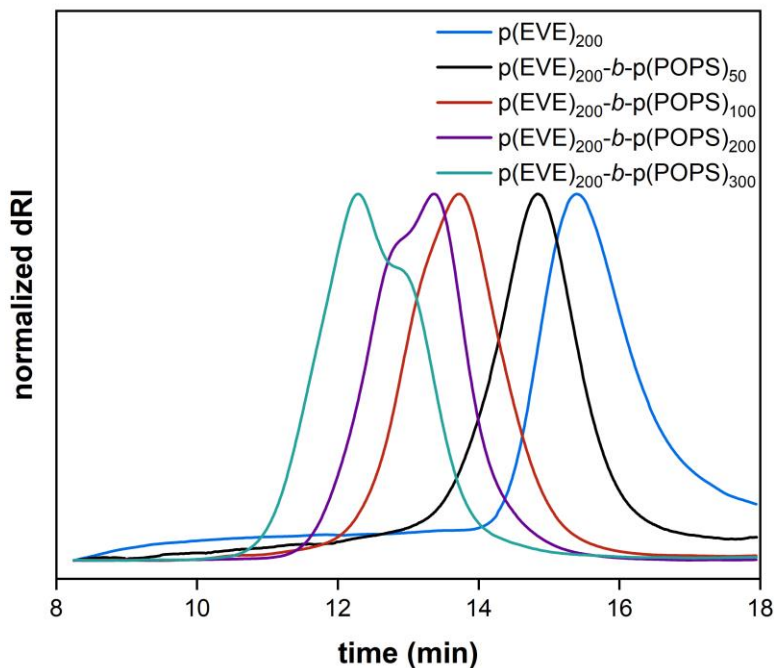


Figure S11. SEC traces of precipitated p(EVE)₂₀₀-b-p(POPS)_n.

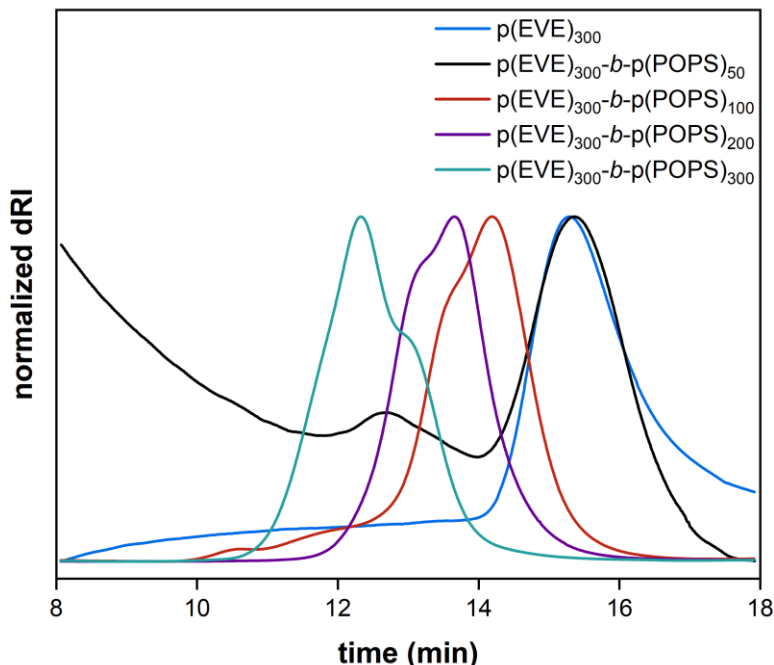


Figure S12. SEC traces of precipitated $p(\text{EVE})_{300}\text{-}b\text{-}p(\text{POPS})_n$.

The amount of recovered polymer following precipitation of $p(\text{EVE})_{300}\text{-}b\text{-}p(\text{POPS})_{50}$ (black trace in Figure S12) was <2 mg – therefore, the SEC sample was very dilute, resulting in the observed unreliable baseline. We now understand this poor recovery to be a consequence of the large $p(\text{EVE})$ fraction relative to the $p(\text{POPS})$ fraction, leading to high solubility of most polymer chains (see Section S2.F).

F. Evidence for fractionation by solubility upon precipitation

When analyzing the ^1H NMR spectra of the crude and precipitated BCPs, we observed the integration of the $p(\text{EVE})$ peaks decreasing significantly relative to the $p(\text{POPS})$ peaks after precipitation in methanol (Figure S13A and B). Furthermore, the material isolated from the supernatant shows an elevated integration of the $p(\text{EVE})$ peaks relative to the $p(\text{POPS})$ peaks (Figure S13C) – suggesting a “migration” of $p(\text{EVE})$ from the crude BCP to the supernatant.

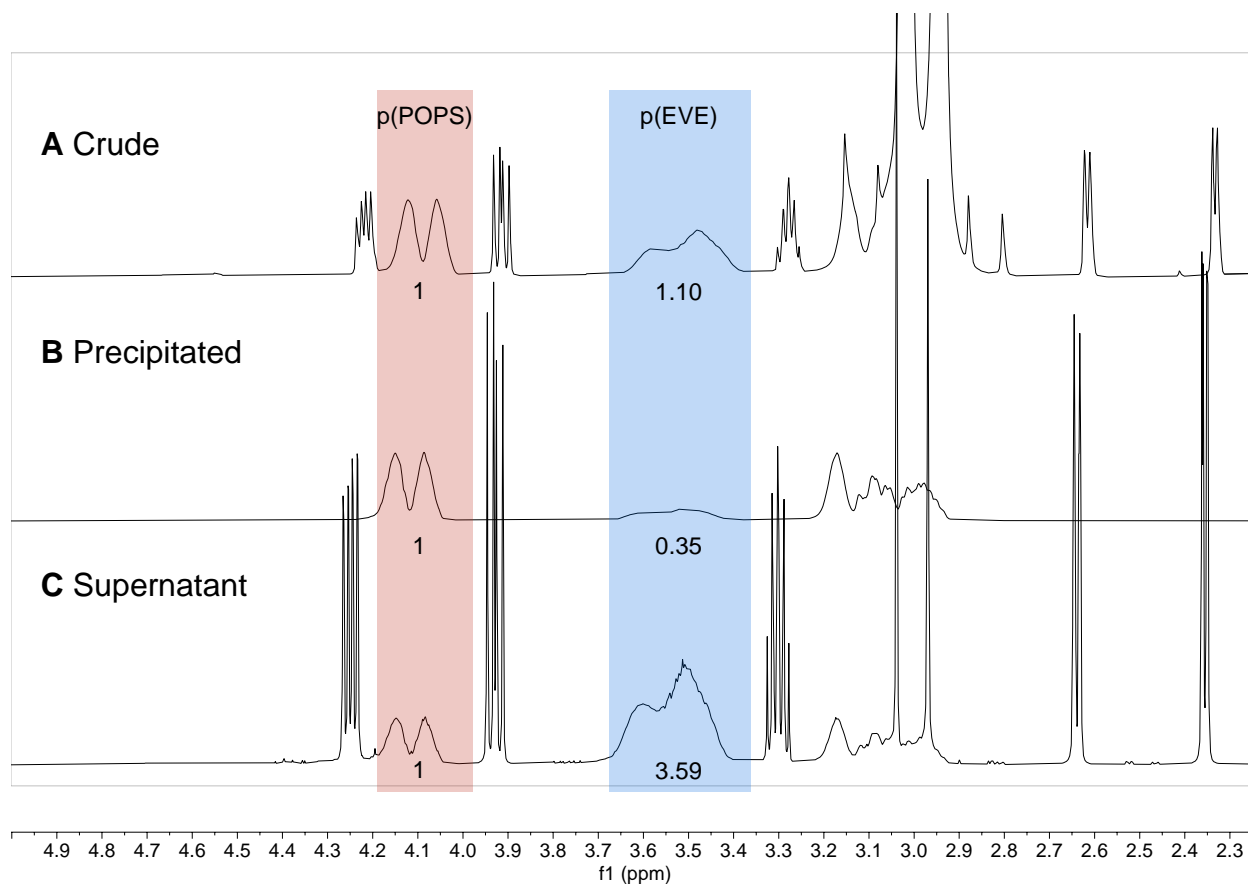


Figure S13. ^1H NMR spectra for $\text{p(EVE)}_{50}\text{-}b\text{-p(POPS)}_{100}$ of (A) the crude polymerization mixture, (B) polymer after precipitation in methanol and drying overnight at $70\text{ }^\circ\text{C}$ in a vacuum oven, and (C) the supernatant after removal of the methanol. Numbers under the highlighted peaks represent relative integrations of p(POPS) (red box) to p(EVE) (blue box).

TGA and DSC support the conclusion that the BCPs after precipitation contain little-to-no p(EVE). A representative TGA from these precipitated polymers (Figure S14) shows a single degradation feature matching the T_o of p(POPS) homopolymer (thermal data for both homopolymers can be found in Section 2.H). Similarly, the DSC of the same precipitated BCP (Figure S15) shows a single T_g similar to the T_g of p(POPS) homopolymer. If the p(EVE) block was of significant length, we would expect it to significantly alter the thermograms of the BCPs compared to the p(POPS) homopolymer. Therefore, it was clear that characterization done post-precipitation was not accurately reflecting the original composition of the BCPs.

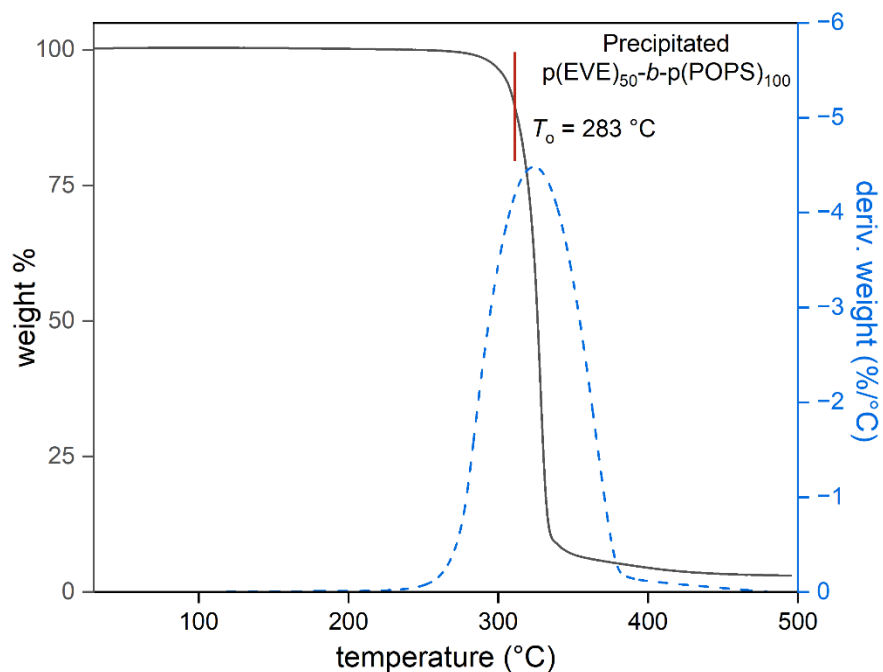


Figure S14. TGA thermogram of precipitated p(EVE)₅₀-b-p(POPS)₁₀₀ featuring a single T_o that matches the T_o of p(POPS) homopolymer.

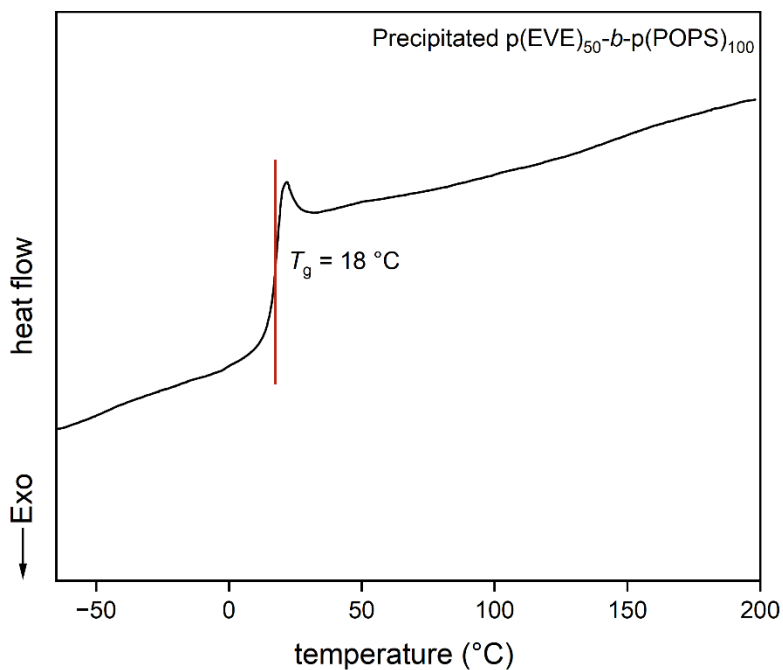


Figure S15. DSC thermogram of precipitated p(EVE)₅₀-b-p(POPS)₁₀₀ featuring a single T_g that matches the T_g of p(POPS) homopolymer.

Because of the aforementioned discrepancies, we initially hypothesized that the thioacetal linkage between the p(EVE) and p(POPS) blocks (highlighted in Figure S16) was cleaved by the methanol during precipitation. However, the SEC traces of the crude and precipitated polymers are nearly identical and only at slightly shorter retention times than that of the material isolated from the supernatant (Figure S17) – which does not support this hypothesis.

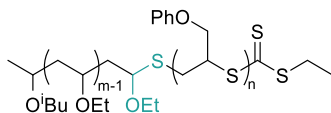


Figure S16. p(EVE)-*b*-p(POPS) BCP with thioacetal linkage highlighted in green.

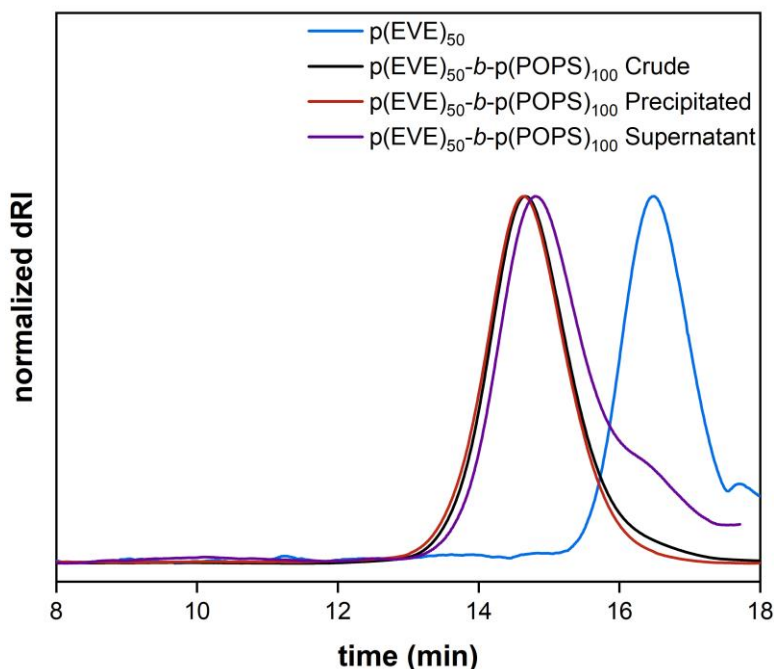
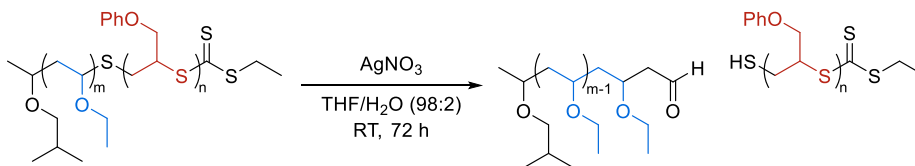


Figure S17. SEC traces of p(EVE)₅₀ and the p(EVE)₅₀-*b*-p(POPS)₁₀₀ crude, precipitated, and supernatant samples.

We collected further evidence against thioacetal methanolysis by intentionally cleaving this linkage (Scheme S1) to compare the SEC traces of the crude diblocks with these degraded samples.



Scheme S1. Cleavage of the thioacetal linkage of p(EVE)-*b*-p(POPS) by AgNO₃ in THF/H₂O.

General procedure for thioacetal hydrolysis: These conditions were adapted from a previous literature procedure.¹¹ A 1 dram screw-top vial was charged with p(EVE)_m-b-p(POPS)_n (10–15 mg) and a stir bar. The vial was sealed with a septum and evacuated and backfilled with N₂ three times on a Schlenk line. The polymer was dissolved in degassed THF (1.5 mL) and 50 μL of AgNO₃ (1 M in H₂O, ~30–50 eq) was added to the vial. The solution was allowed to stir at room temperature for 72 hours. Within 30 minutes of adding AgNO₃, the solution turned cloudy, and upon reaching 72 hours, a black precipitate coated the vial. The THF was removed by a gentle flow of air, and the solid residue was redissolved in DCM (1.5 mL). This solution was washed with water (5 x 0.5 mL) and the DCM was removed by gentle air flow to yield a brown solid. This solid was analyzed by SEC (Figure S18) and ¹H NMR spectroscopy. In the ¹H NMR spectra, the anticipated aldehyde end-group was not observed – likely due to the low abundance relative to the repeat unit protons, which were still present, as expected.

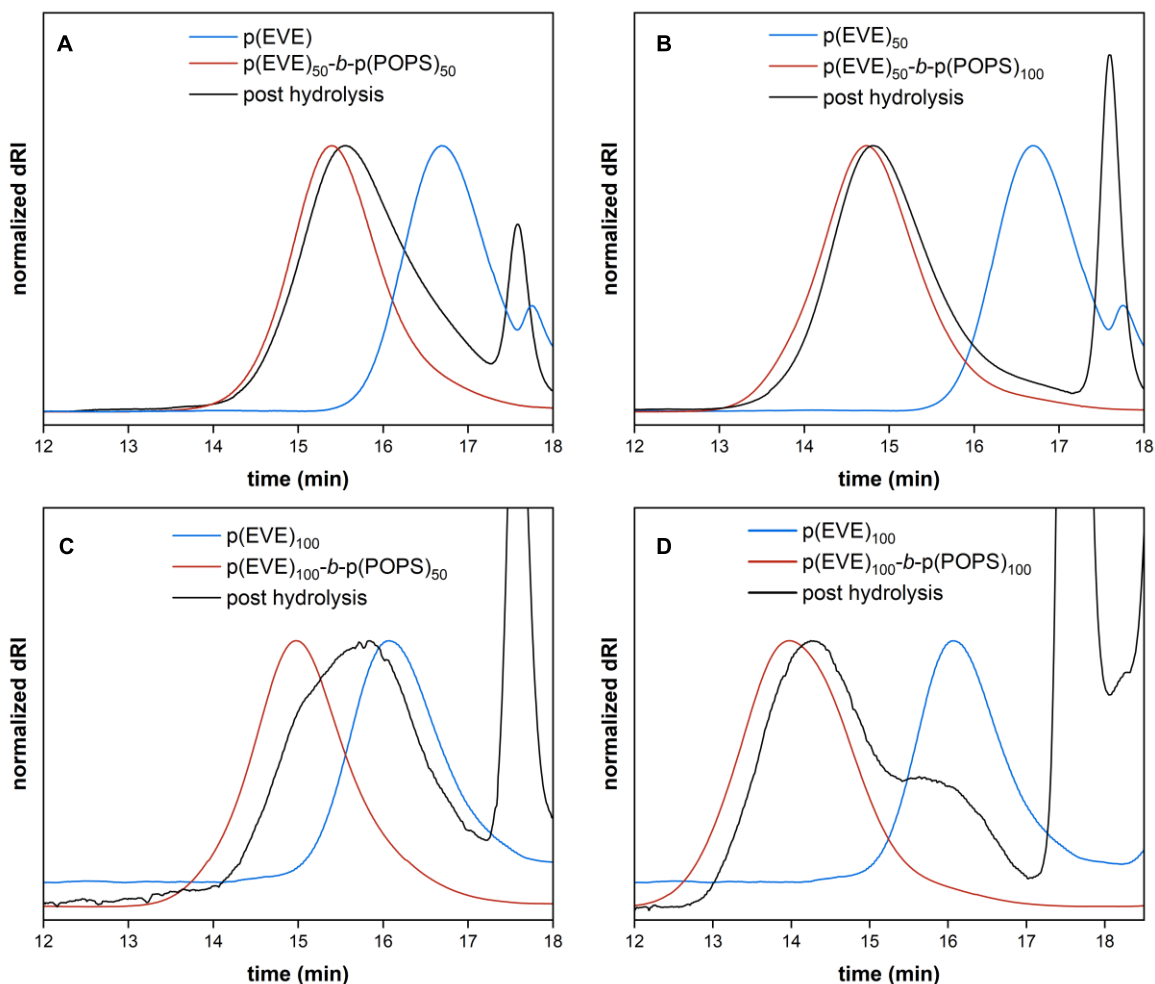


Figure S18. SEC traces of BCPs hydrolyzed with AgNO₃.

Table S6. Hydrolysis of p(EVE)-*b*-p(POPS) with AgNO₃

entry	diblock copolymer	p(EVE) M_n (kDa) ^[a]	p(EVE) $\bar{D}^{[a]}$	diblock M_n (kDa) ^[a]	diblock $\bar{D}^{[a]}$	post-hydrolysis M_n (kDa) ^[a]	post-hydrolysis $\bar{D}^{[a]}$
1	p(EVE) ₅₀ - <i>b</i> -p(POPS) ₅₀	4.1	1.23	11.9	1.44	9.9	1.44
2	p(EVE) ₅₀ - <i>b</i> -p(POPS) ₁₀₀	4.1	1.23	21.4	1.53	18.9	1.48
3	p(EVE) ₁₀₀ - <i>b</i> -p(POPS) ₅₀	6.29	1.38	17.6	1.46	10.1	1.51
4	p(EVE) ₁₀₀ - <i>b</i> -p(POPS) ₁₀₀	6.29	1.38	36.9	1.7	42.1, 8.22	1.27, 1.12

[a] Determined via SEC in DMF with 0.025 M LiBr against PMMA standards. Reaction conditions: p(EVE)-*b*-p(POPS) (10-15 mg, 1 eq), THF (1.5 mL), AgNO₃ (30–50 eq), rt, 72 hr.

For each diblock tested, a shift in the SEC trace is observed, indicating that hydrolysis has taken place. Gratifyingly, the post-hydrolysis M_n of p(EVE)₅₀-*b*-p(POPS)₅₀, p(EVE)₅₀-*b*-p(POPS)₁₀₀, and p(EVE)₁₀₀-*b*-p(POPS)₅₀ samples (Figure S18A–C; Table S6, entries 1–3) were reduced by the amount that approximately corresponds to the M_n of the p(EVE) block (with the caveat of determining M_n against PMMA standards). The M_n of the post-hydrolysis p(EVE)₁₀₀-*b*-p(POPS)₁₀₀ (Table S6, entry 4) is reported higher than the diblock, but the trace is clearly shifted toward a longer retention time (Figure S18D). In the same post-hydrolysis polymer, a peak aligning with the starting p(EVE) homopolymer can be observed, which is an encouraging piece of evidence that cleavage of the thioacetal bond has occurred. Comparing these shifts in SEC traces to the largely unchanging traces of our BCPs pre- and post-precipitation, we conclude that it is unlikely precipitation in methanol is causing cleavage of the thioacetal linkage between the p(EVE) and p(POPS) blocks.

Another hypothesis is that the p(EVE)-*b*-p(POPS) is fractionating in the precipitation solvent on the basis of the increased solubility of p(EVE). As noted in the main text, p(EVE) is soluble in a large number of organic solvents, including methanol, out of which p(POPS) precipitates. We hypothesize that the BCPs with an appreciable % composition of p(EVE) are being solubilized in the precipitation solvent while the BCPs with a very high p(POPS) fraction are being precipitated out. This fractionation explains the change in ¹H NMR peak intensity of the p(EVE) relative to p(POPS) while the average molar masses remain the same. To solve this problem of fractionation, all future BCPs were purified using prepSEC.

G. SEC traces of block copolymers purified by prepSEC

Upon discovering the fractionation of the BCPs when precipitated, we repeated the BCP synthesis and purified the final polymers using prepSEC to avoid fractionation. Below are the SEC traces of these prepSEC-purified polymers.

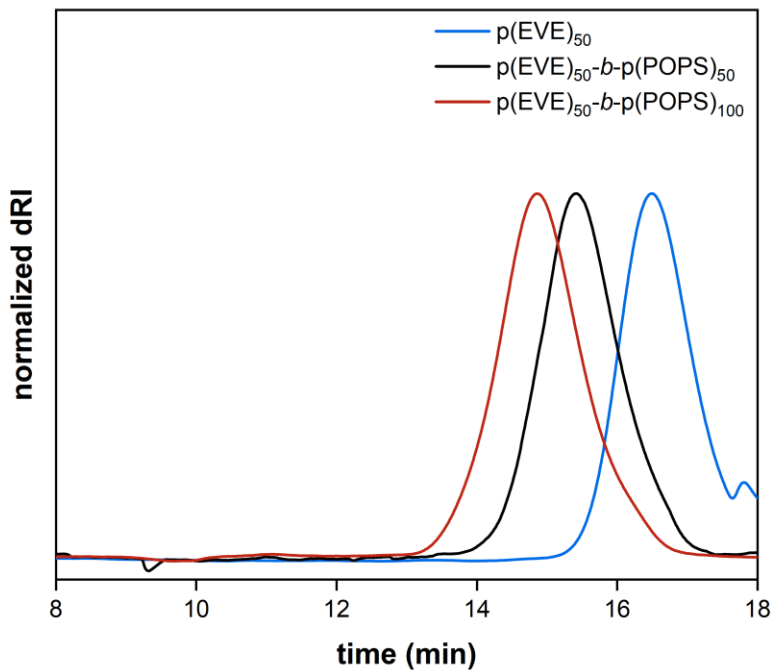


Figure S19. SEC traces of $p(\text{EVE})_{50}$ - b - $p(\text{POPS})_n$ purified by prepSEC.

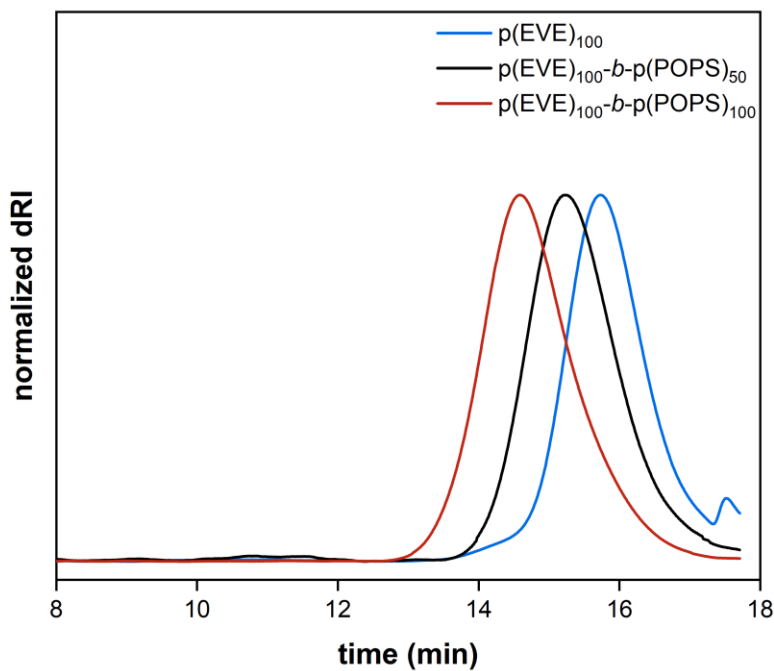


Figure S20. SEC traces of $p(\text{EVE})_{100}$ - b - $p(\text{POPS})_n$ purified by prepSEC.

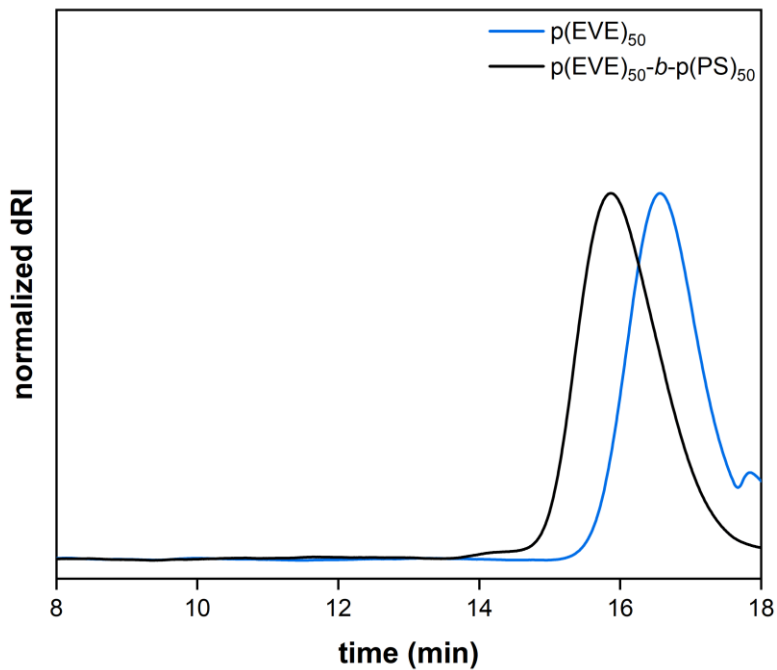


Figure S21. SEC traces of $p(EVE)_{50}-b-p(PS)_{50}$ purified by prepSEC.

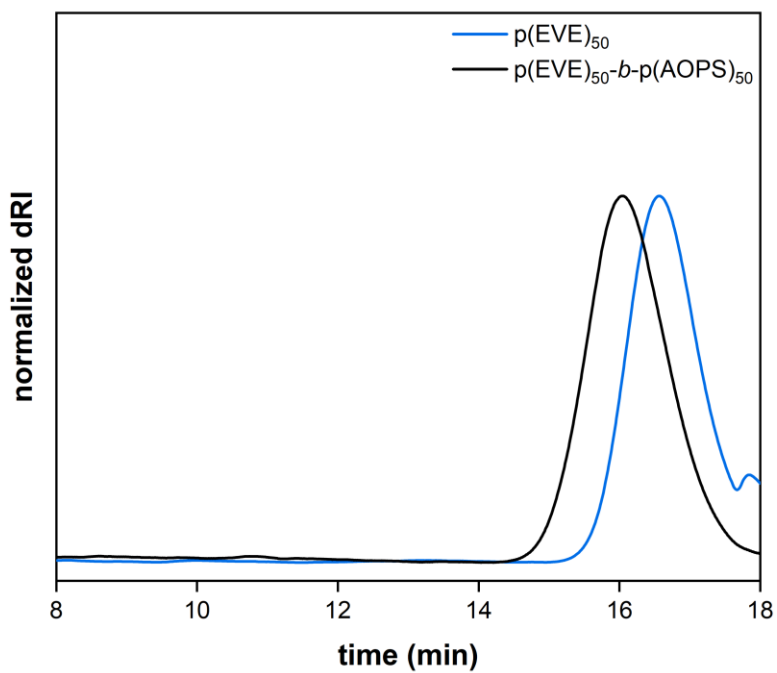


Figure S22. SEC traces of $p(EVE)_{50}-b-p(AOPS)_{50}$ purified by prepSEC.

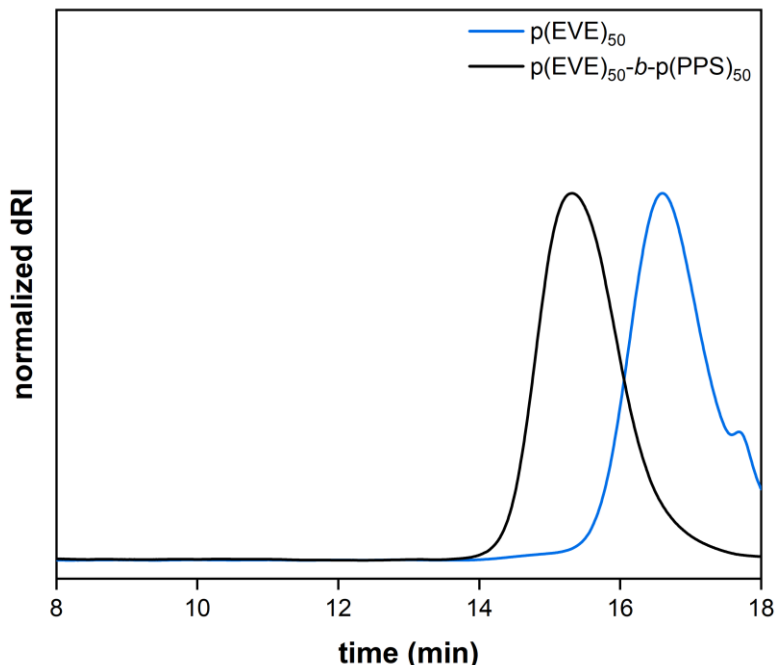


Figure S23. SEC traces of p(EVE)₅₀-b-p(PPS)₅₀ purified by prepSEC.

H. Verification of polymer end-groups

To demonstrate the fidelity of the trithiocarbonate end-group, p(EVE)₁₀ and p(EVE)₁₀-b-p(POPS)₁₀ were synthesized and characterized with COSY, HSQC, and HMBC NMR spectroscopy.

Starting with p(EVE)₁₀, COSY (Figure S24), HSQC (Figure S25), and HMBC (Figure S26) NMR spectra were used to assign the structure of the end-groups and repeat units. HMBC was used to confirm that the trithiocarbonate end-group is attached to the polymer by the correlation between the thiocarbonyl carbon **P** with the methylene **B** of the Z group and with the neighboring methine **C** of the adjacent repeat unit in the chain. Note that the thiocarbonyl carbon is not observed in the 1D ¹³C NMR spectrum, even with increased scans (up to 1024 scans) and relaxation delays (up to 20 seconds).

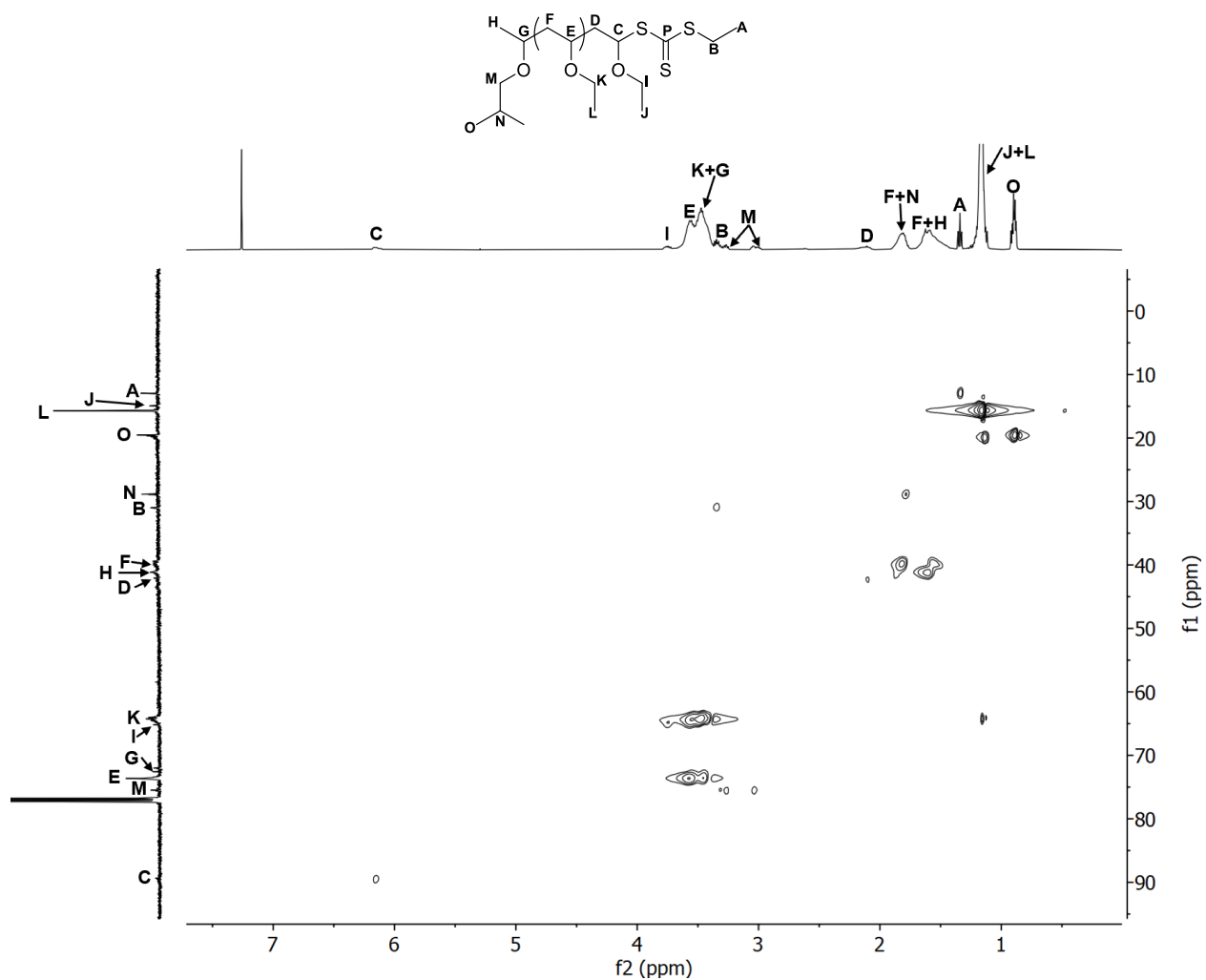


Figure S25. HSQC NMR spectrum (500 and 126 MHz, CDCl₃) of p(EVE)₁₀.

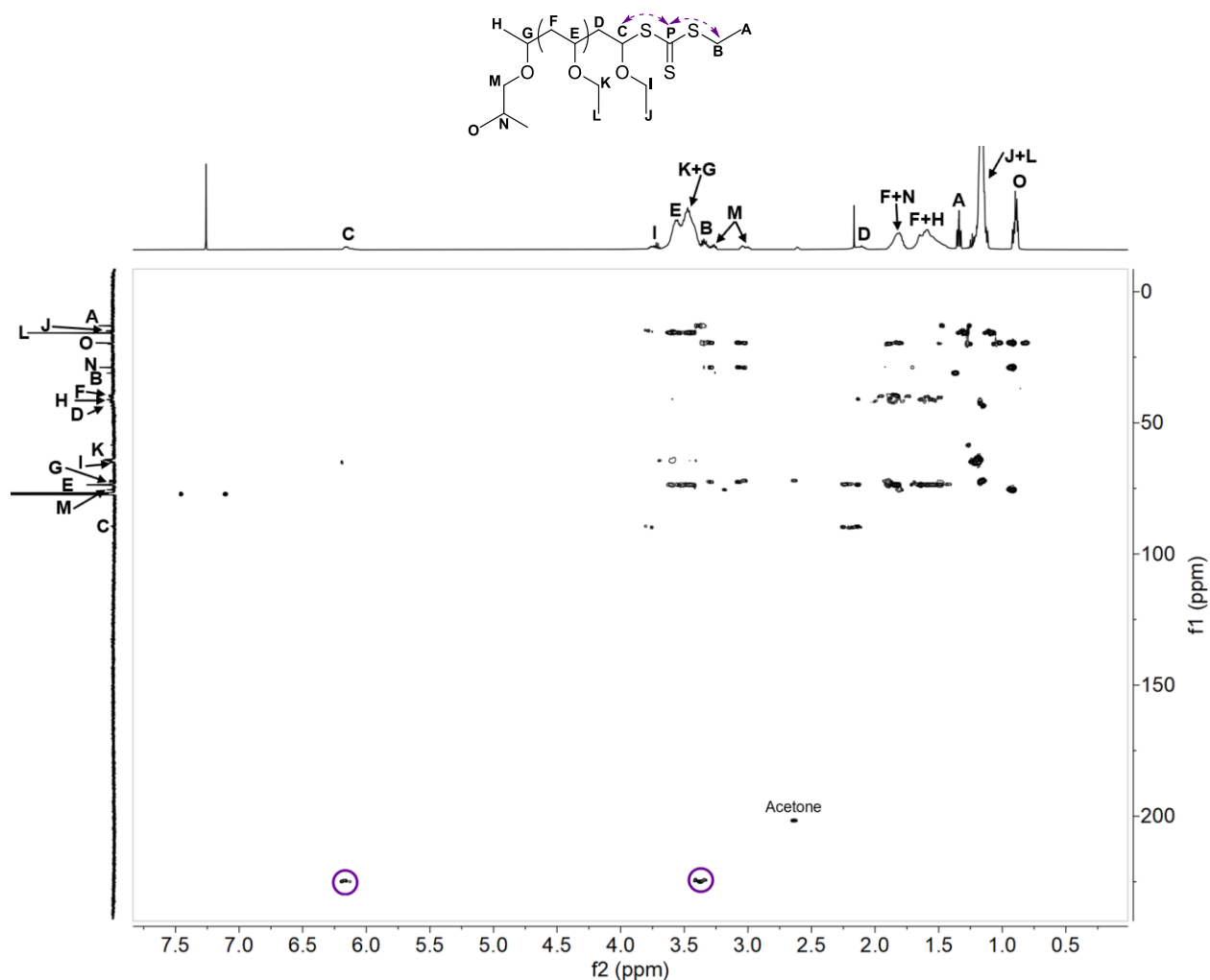


Figure S26. HMBC NMR spectrum (600 and 151 MHz, CDCl_3) of p(EVE)_{10} with cross peaks of the thiocarbonyl carbon **P** with protons **B** of the end-group and **C** of the repeat unit circled in purple.

For p(EVE)_{10} -*b*- p(POPS)_{10} , COSY (Figure S27), HSQC (Figure S28), and HMBC (Figure S29) spectroscopy were used to verify the structure of the diblock copolymer. HMBC spectroscopy was useful to verify the presence of the TCT end-group due to the correlation of the thiocarbonyl carbon with the methylene protons **X** of the adjacent POPS repeat unit. The combination of the HMBC correlations between the thiocarbonylthio carbon **P** and the respective adjacent repeat units for both the homopolymer and diblock as well as successful chain extension at each of these steps serves as evidence of the fidelity of the TCT end-group through multiple polymerizations.

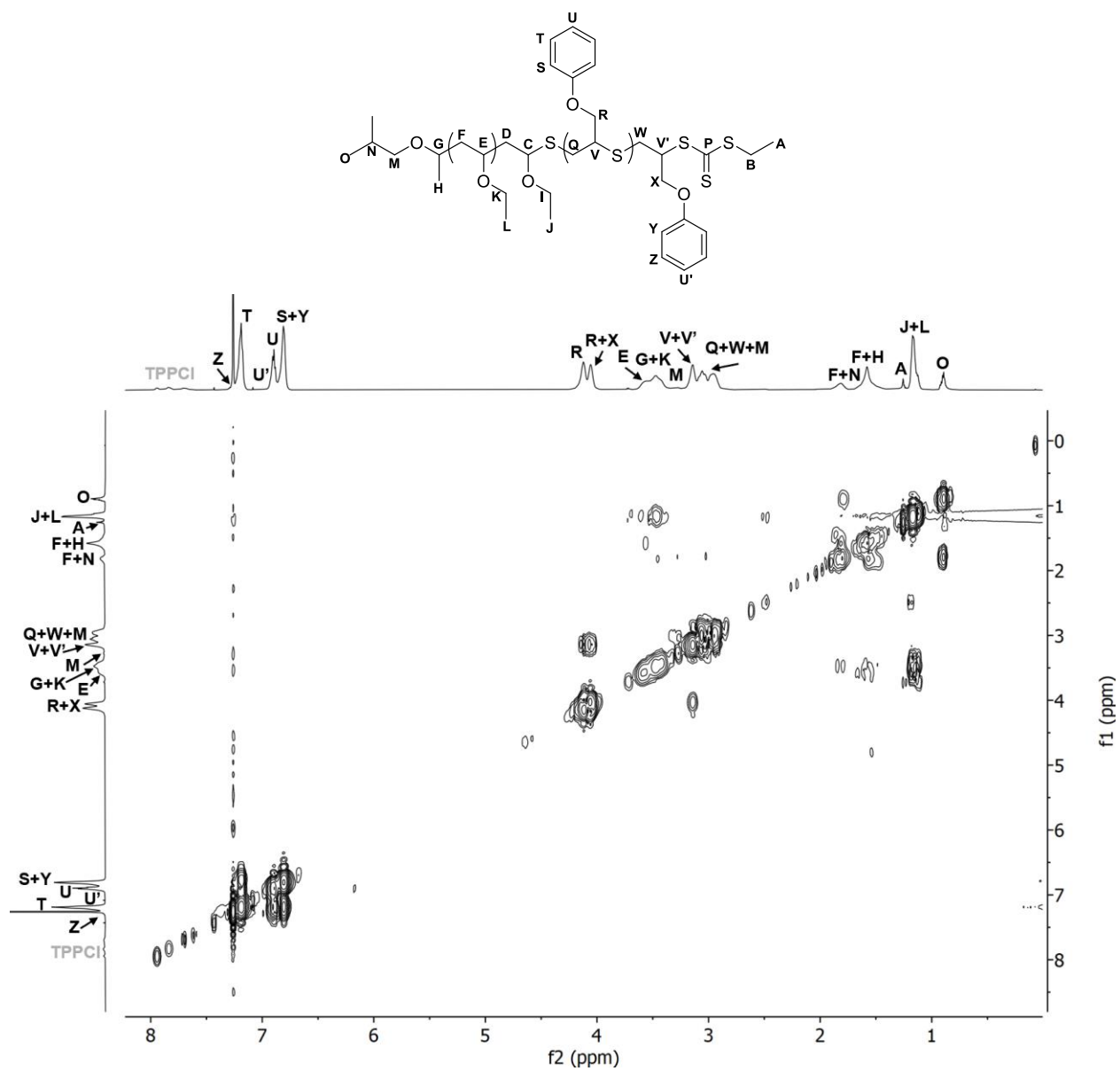


Figure S27. COSY NMR spectrum (600 MHz, CDCl_3) of $p(\text{EVE})_{10}\text{-}b\text{-}p(\text{POPS})_{10}$.

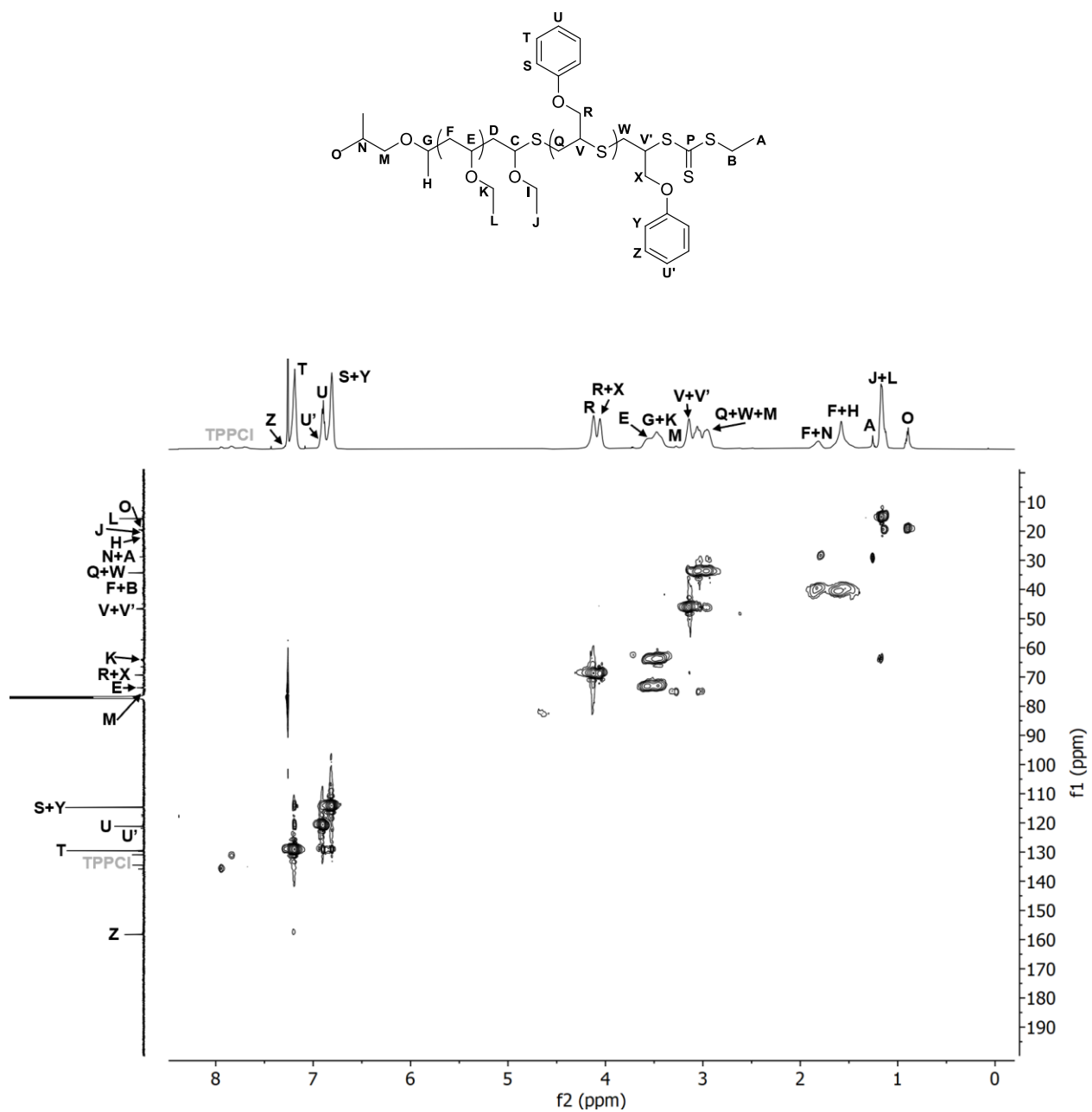


Figure S28. HSQC NMR spectrum (600 and 151 MHz, CDCl_3) of $p(\text{EVE})_{10}\text{-}b\text{-}p(\text{POPS})_{10}$.

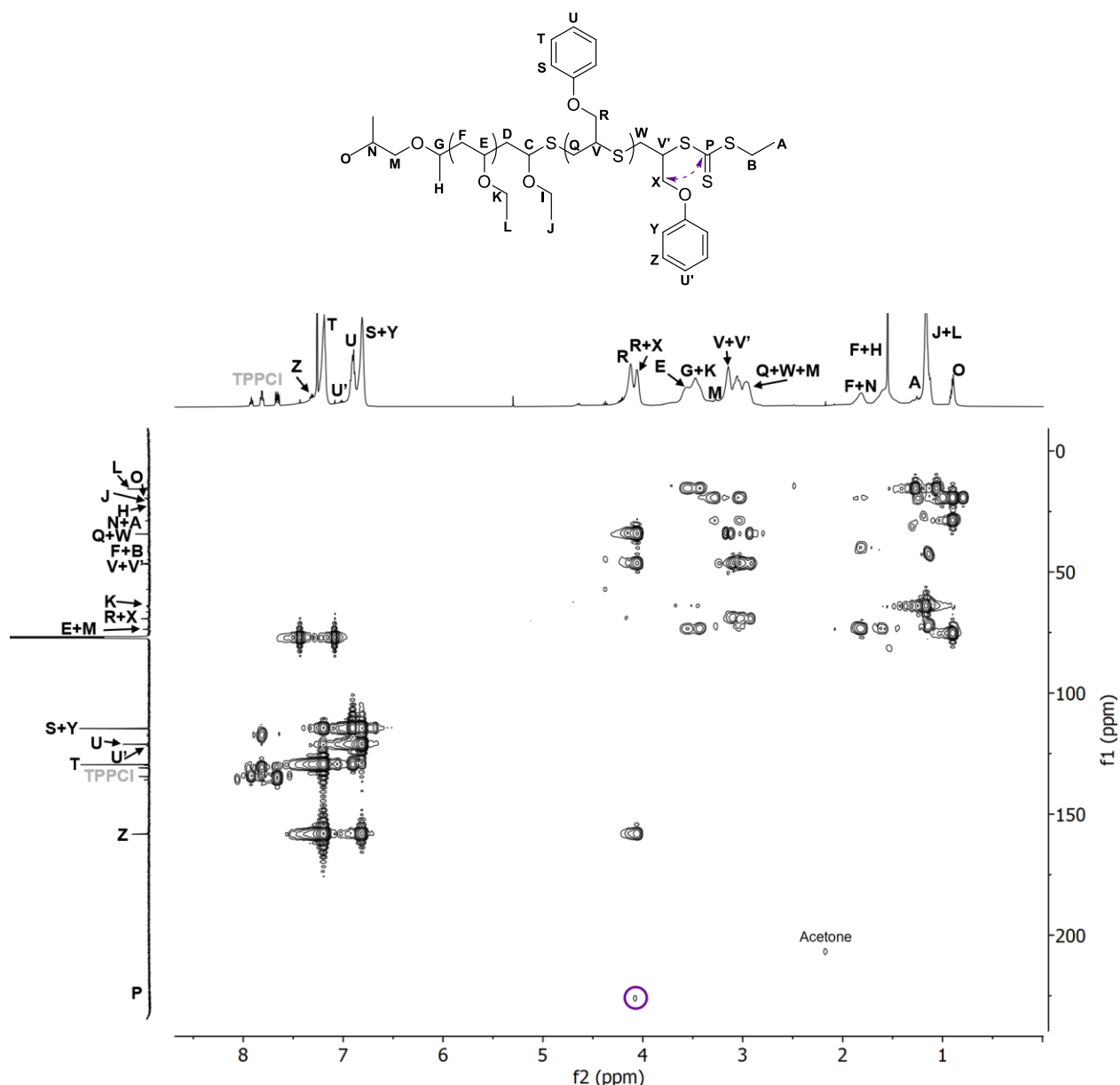
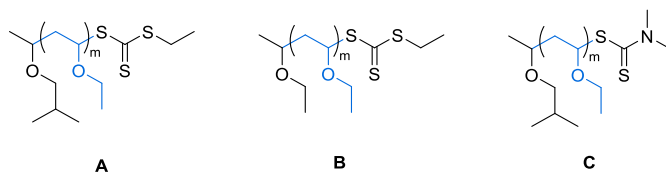


Figure S29. HMBC NMR spectrum (600 and 151 MHz, CDCl_3) of $\text{p(EVE)}_{10}\text{-}b\text{-p(POPS)}_{10}$ with the correlation between TCT carbon **P** with adjacent repeat unit methylene **R** circled in purple.

To additionally confirm that the isobutoxyethyl and trithiocarbonate end-groups are present, MALDI-TOF MS was performed on p(EVE)_{50} . The spectrum showed 4 major populations, 3 of which (Table S7, entries 1, 3, and 4; Figure S31) were different ion adducts of p(EVE) with the expected isobutoxyethyl and trithiocarbonate end-groups (structure **A**). The remaining population (Table S7, entry 2; Figure S31) was analogous to population 4 except the end-group at the alpha chain-end was ethoxyethyl instead of isobutoxyethyl (structure **B**). An ethoxyethyl end-group is evidence of initiation via direct monomer oxidation of the ethyl vinyl ether monomer. Entry 5 is included in Table S7 to show that the $\Delta(m/z)$ matched the repeat unit of ethyl vinyl ether ($m/z =$

72). Unfortunately, we did not observe signal for any polymer containing p(POPS) (i.e., homopolymer or diblock copolymer).

Table S7. Representative MALDI-TOF data of p(EVE)₅₀



entry	population	DP of EVE	adduct	expected <i>m/z</i>	observed <i>m/z</i> ^[a]
1	1	17	A + NH ₄ ⁺	1481.06	1480.14
2	2	17	B + MeCN + Na ⁺	1499.02	1498.14
3	3	17	A + 2 Na ⁺ - H ⁺	1508.00	1508.17
4	4	17	A + MeCN + Na ⁺	1527.05	1526.17
5	1	18	A + NH ₄ ⁺	1553.12	1552.19

[a] Observed using reflectron mode.¹² The left most peak of each distribution was chosen as the monoisotopic peak.

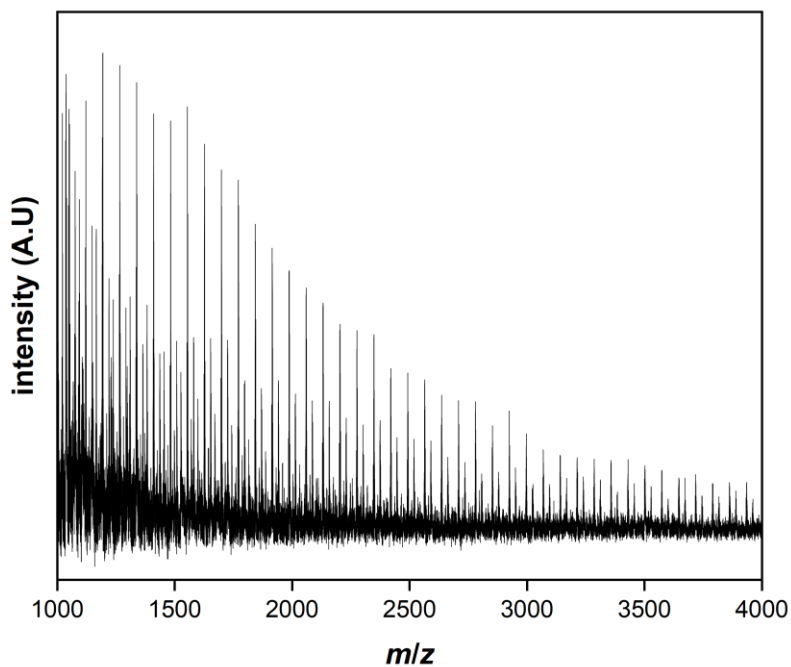


Figure S30. Full MALDI-TOF spectrum of p(EVE)₅₀.

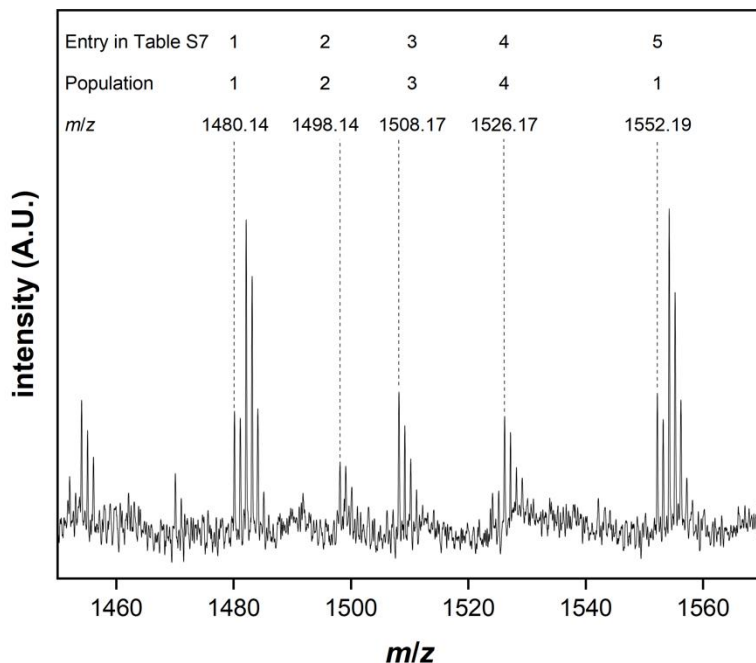


Figure S31. Zoomed-in MALDI-TOF spectrum of p(EVE)₅₀ in the DP 17–18 region.

Note: When analyzing a p(EVE)₅₀ sample stored in DMAc for 3 days, an additional minor population ($C + 2 Na^+ - H^+$) was observed in the MALDI-TOF spectrum corresponding to the substitution of the thiyl Z group with a dimethylamino group. DMAc can contain trace amounts of dimethylamine (from the synthesis and/or trace degradation) which we hypothesize is slowly attacking the trithiocarbonate to undergo this exchange over time. Therefore, any polymer with a trithiocarbonate end-group should not be exposed to DMAc for extended periods of time to avoid end-group degradation.

I. Thermal characterization of polymers

TGA of the p(EVE) homopolymer exhibits a multi-stage degradation (Figure S32; Table S8 entry 1) with the largest mass loss event occurring at $T_o = 375$ °C. Two smaller degradations were also observed at $T_o = 148$ °C and 266 °C. ¹H NMR spectroscopy showed no residual solvent, and the thermogram does not change after drying in a vacuum oven at 70 °C for 3 days. Therefore, we do not believe these early mass losses are due to the presence of solvent or other small molecules, but we have not been able to identify their origin. The p(POPS) homopolymer exhibits a single-stage degradation with a T_o of 284 °C (Figure S33; Table S8 entry 2). TGA of p(CHVE) homopolymer shows a T_o of 95 °C and 400 °C (Figure S34; Table S8 entry 3). p(DHF)₅₀ has a 2 stage mass loss: one T_o at 83 °C, and another at 377 °C (Figure S35; Table S8 entry 4). The p(PS), p(AOPS), and p(PPS) homopolymers exhibit a single-stage mass losses with a T_o of 278 °C, 288 °C, and 297 °C, respectively (Figure S36–Figure S38; Table S8 entries 5–7).

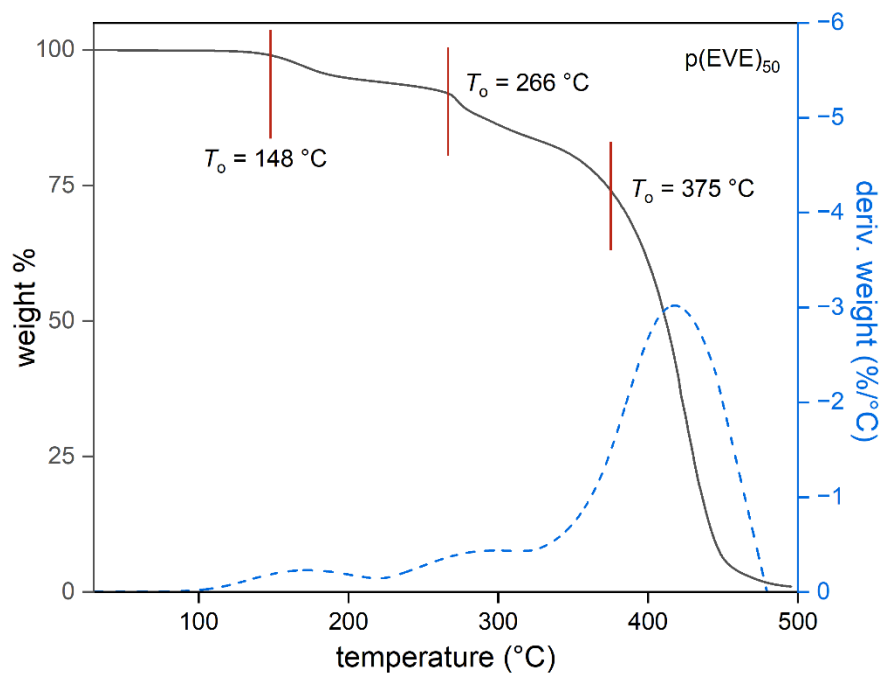


Figure S32. TGA thermogram of p(EVE)₅₀.

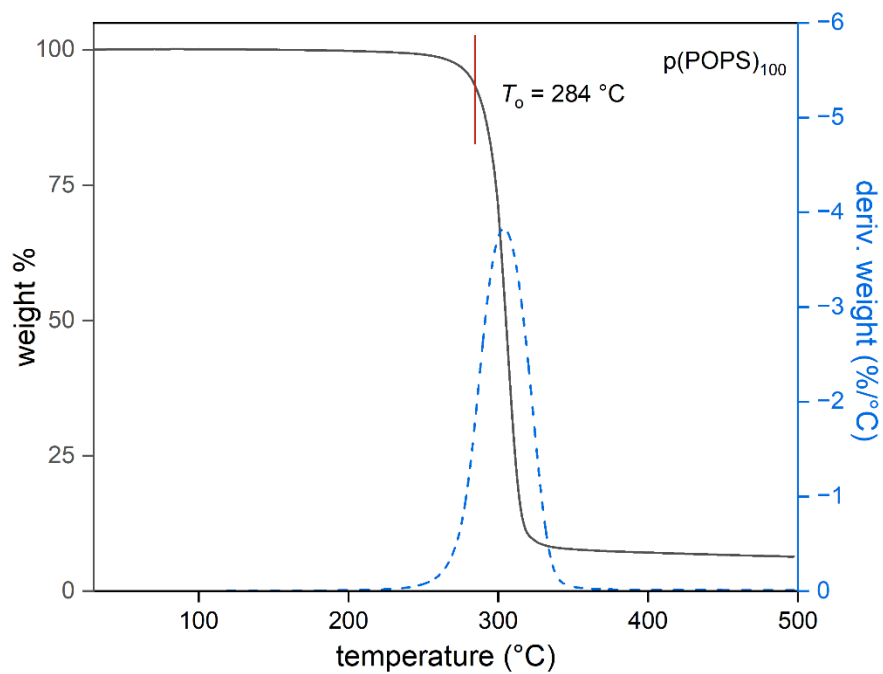


Figure S33. TGA thermogram of p(POPS)₁₀₀.

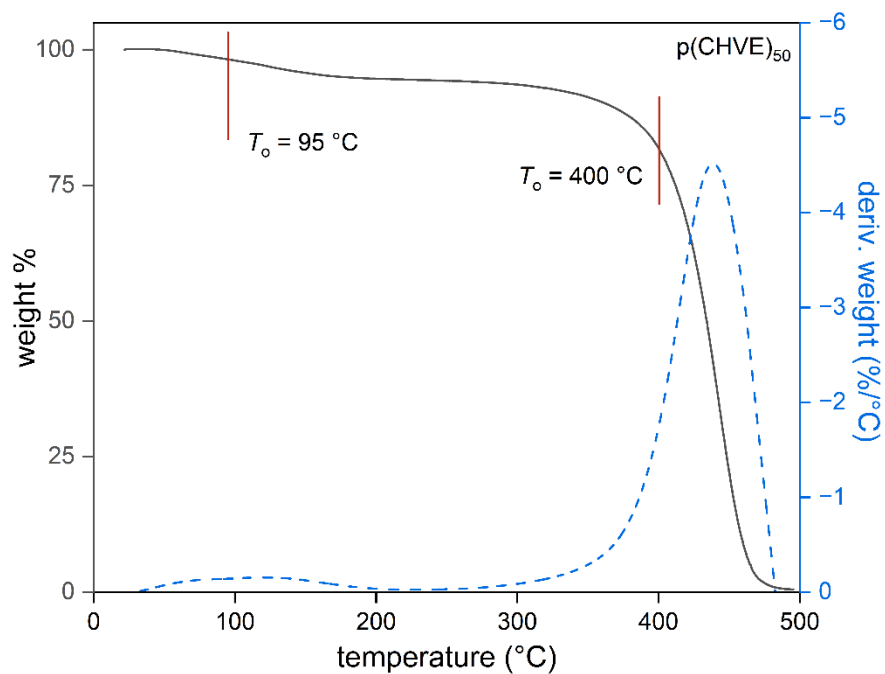


Figure S34. TGA thermogram of p(CHVE)₅₀.

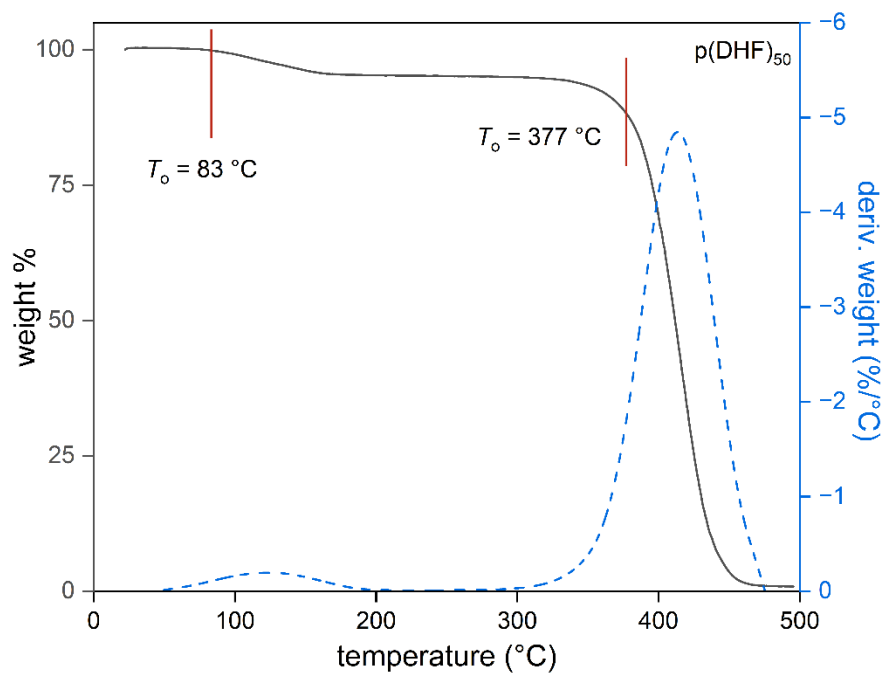


Figure S35. TGA thermogram of p(DHF)₅₀.

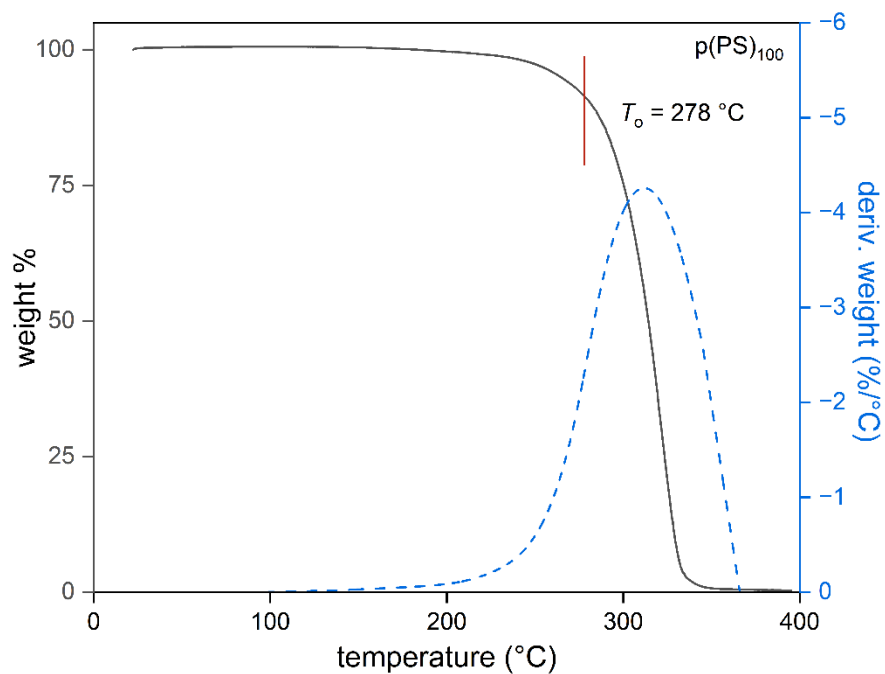


Figure S36. TGA thermogram of p(PS)₁₀₀.

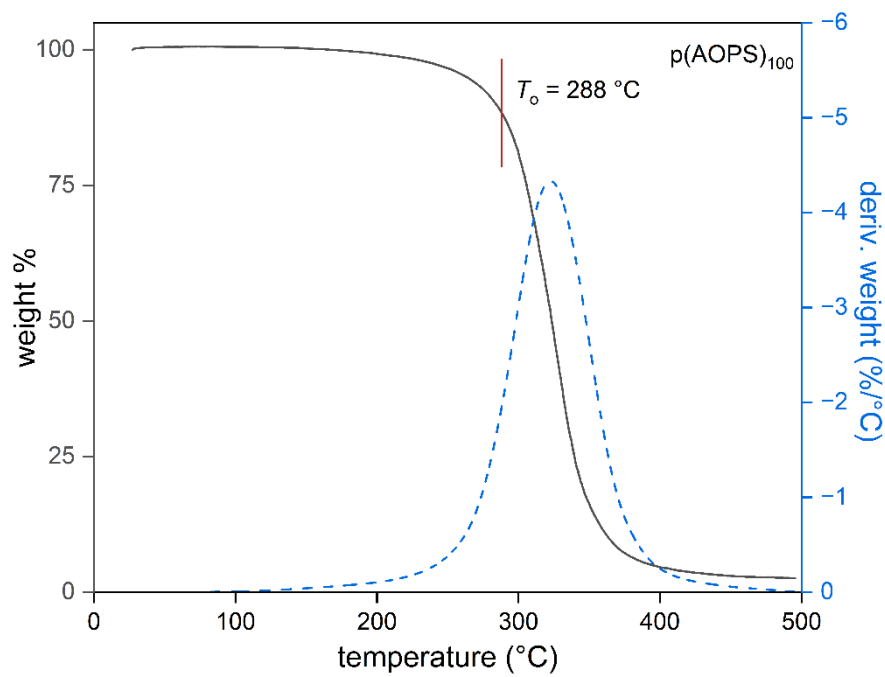


Figure S37. TGA thermogram of p(AOPS)₁₀₀.

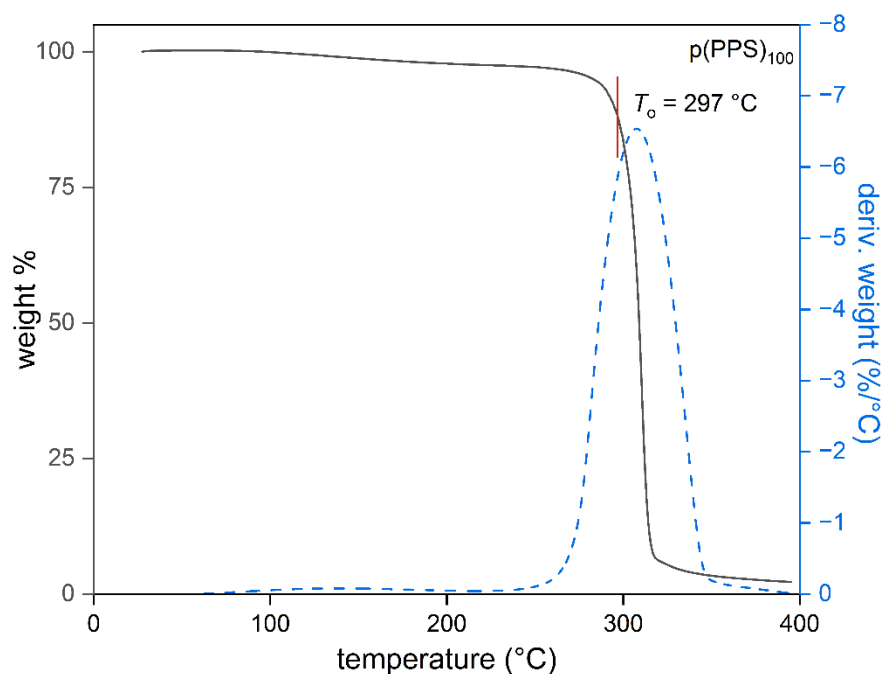


Figure S38. TGA thermogram of p(PPS)₁₀₀.

TGA of the prepSEC-purified p(EVE)-*b*-p(POPS) BCPs revealed multi-stage degradations corresponding to the different blocks – one T_o at 271–283 °C corresponding to the p(POPS) block and another around 373–379 °C corresponding to the p(EVE) block (Table S8, entries 8–11). As expected, the % mass loss attributed to each of these degradation events corresponds to the size of the respective blocks (Figure S39–Figure S42). Similar to the p(EVE) homopolymer, a small mass loss event is seen for each BCP around 150 °C. The same trend can be seen for the BCPs formed using the expanded thiirane scope (Figure S43–Figure S45; Table S8 entries 12–14). The T_o corresponding to the p(EVE) blocks for these BCPs are higher compared to the p(EVE)-*b*-p(POPS) samples, but this can be attributed to the method of determining T_o and its strong reliance on the slopes of the mass-loss features.

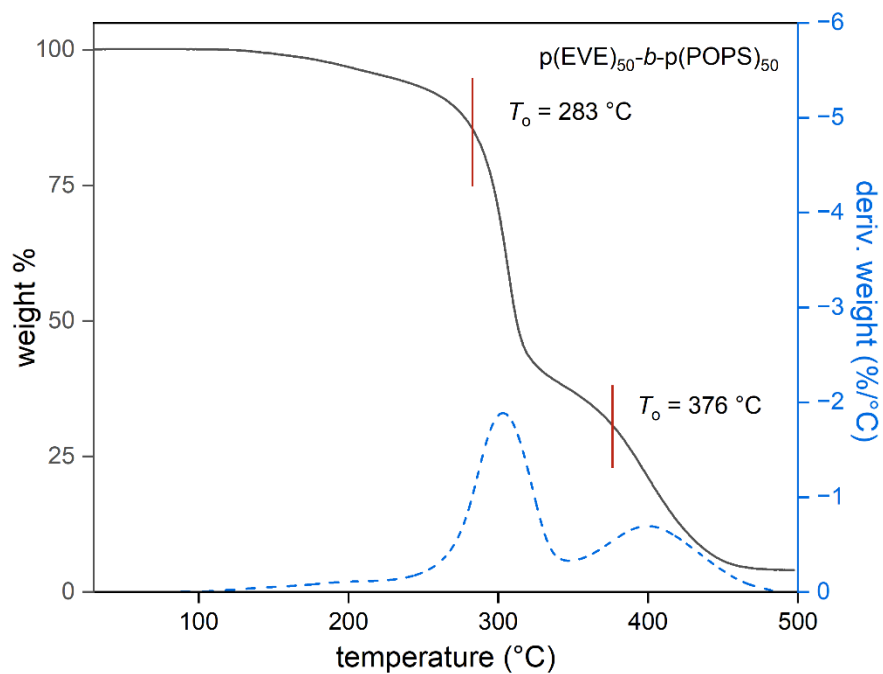


Figure S39. TGA thermogram of $p(\text{EVE})_{50}\text{-}b\text{-}p(\text{POPS})_{50}$ purified by prepSEC.

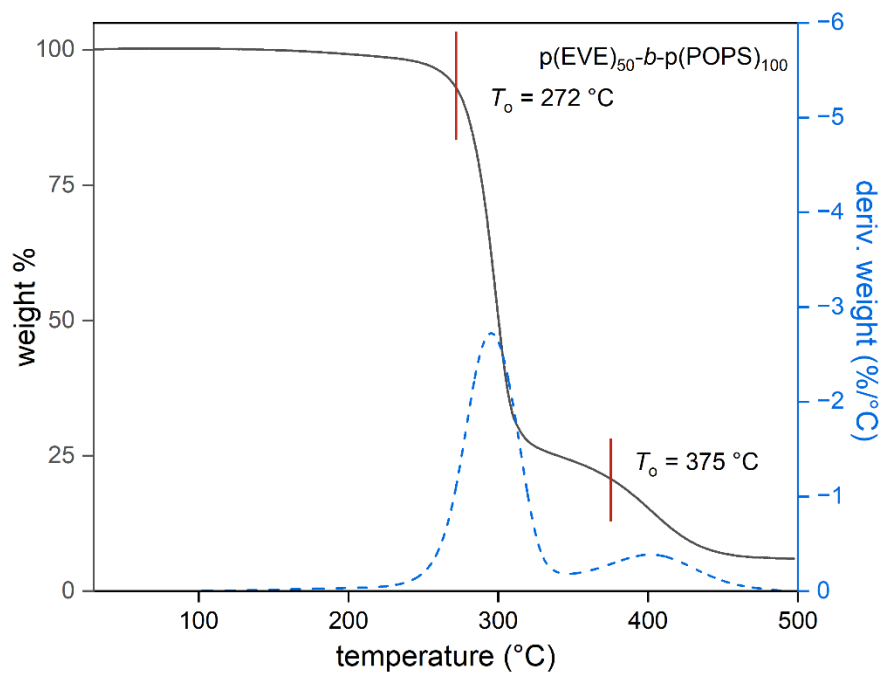


Figure S40. TGA thermogram of $p(\text{EVE})_{50}\text{-}b\text{-}p(\text{POPS})_{100}$ purified by prepSEC.

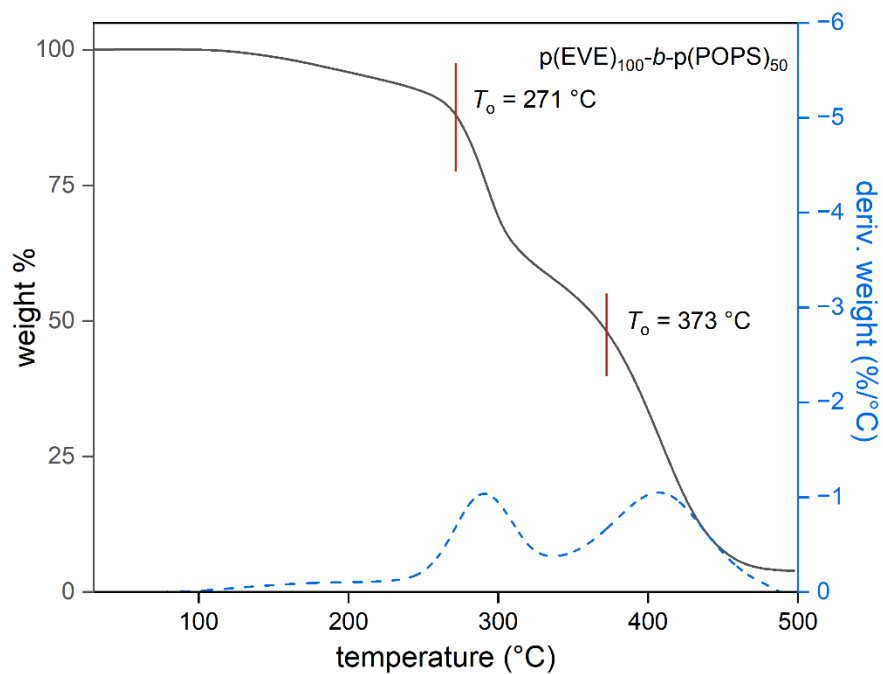


Figure S41. TGA thermogram of p(EVE)₁₀₀-b-p(POPS)₅₀ purified by prepSEC.

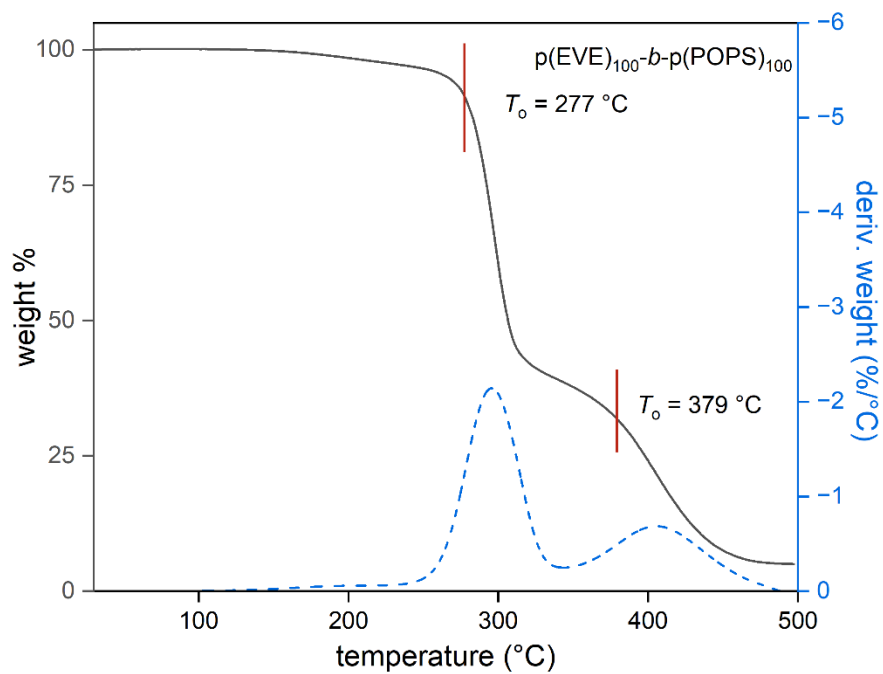


Figure S42. TGA thermogram of p(EVE)₁₀₀-b-p(POPS)₁₀₀ purified by prepSEC.

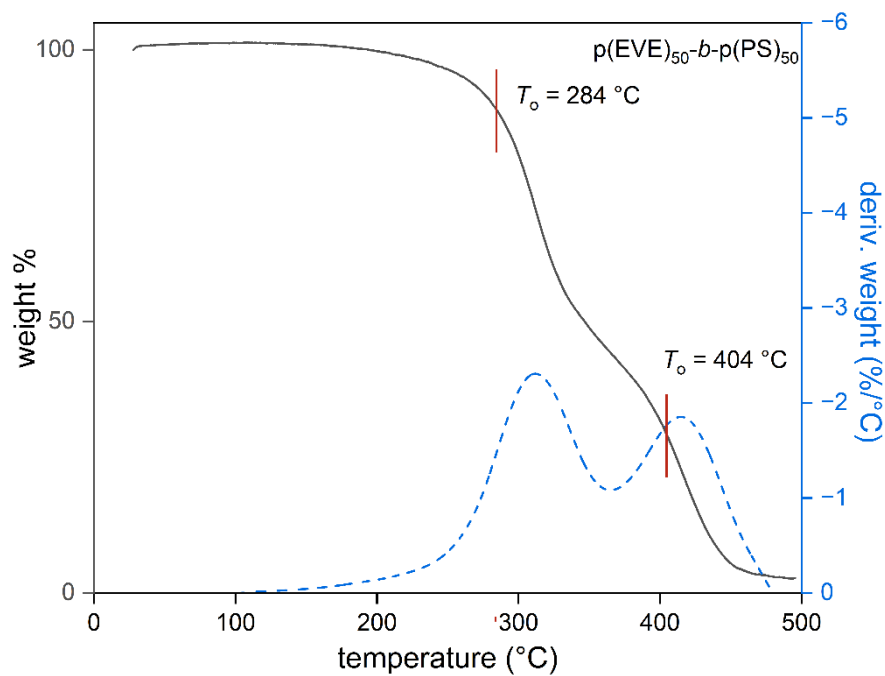


Figure S43. TGA thermogram of p(EVE)₅₀-b-p(PS)₅₀ purified by prepSEC.

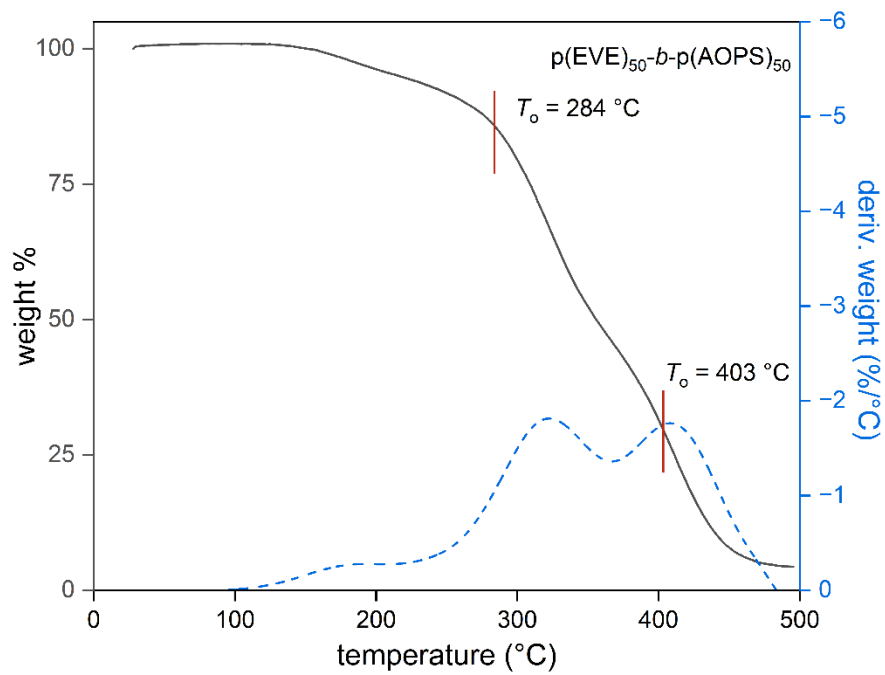


Figure S44. TGA thermogram of p(EVE)₅₀-b-p(AOPS)₅₀ purified by prepSEC.

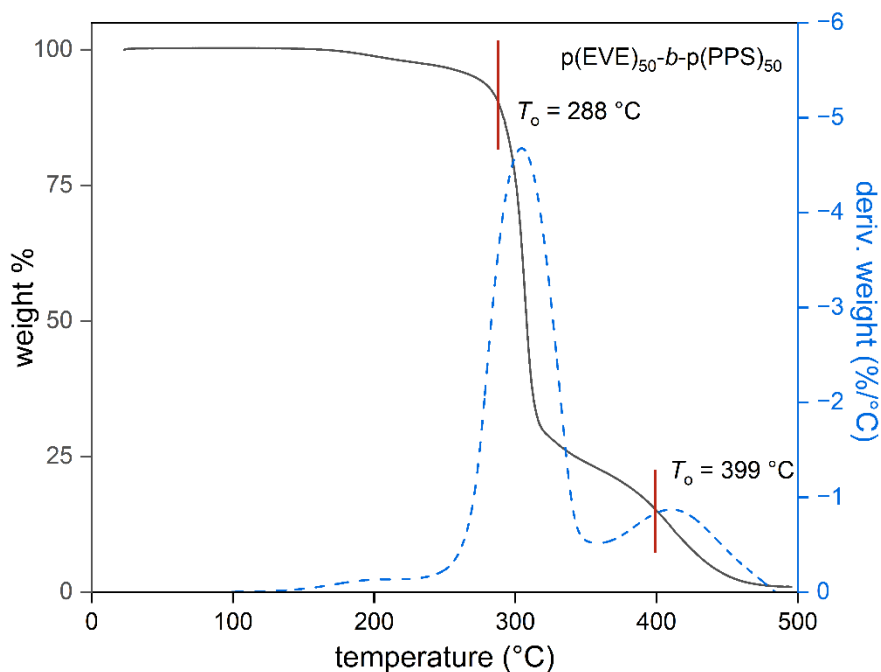


Figure S45. TGA thermogram of p(EVE)₅₀-b-p(PPS)₅₀ purified by prepSEC.

Next, the homopolymers and prepSEC BCPs were analyzed by DSC. The observed glass transition temperatures of the p(EVE) (Figure S46; Table S8, entry 1) and p(POPS) (Figure S47; Table S8, entry 2) homopolymers were close to previously reported values of $-30\text{ }^{\circ}\text{C}$ ¹ and $9\text{ }^{\circ}\text{C}$,² respectively. The other vinyl ether homopolymers tested, p(CHVE) and p(DHF), have glass transition temperatures of 55 and 100 °C, respectively. The glass transition temperatures for the other thirane homopolymers; p(PS), p(AOPS), and p(PPS); were measured to be $-43\text{ }^{\circ}\text{C}$, $-54\text{ }^{\circ}\text{C}$, and $17\text{ }^{\circ}\text{C}$, respectively (Figure S50–Figure S52; Table S8 entries 5–7). For all of the BCPs, two T_g features were observed (Figure S53–Figure S59; Table S8 entries 8–14), which correspond to the T_g of their respective homopolymers. The presence of these two T_g features is evidence for microphase separation of the two blocks.¹³

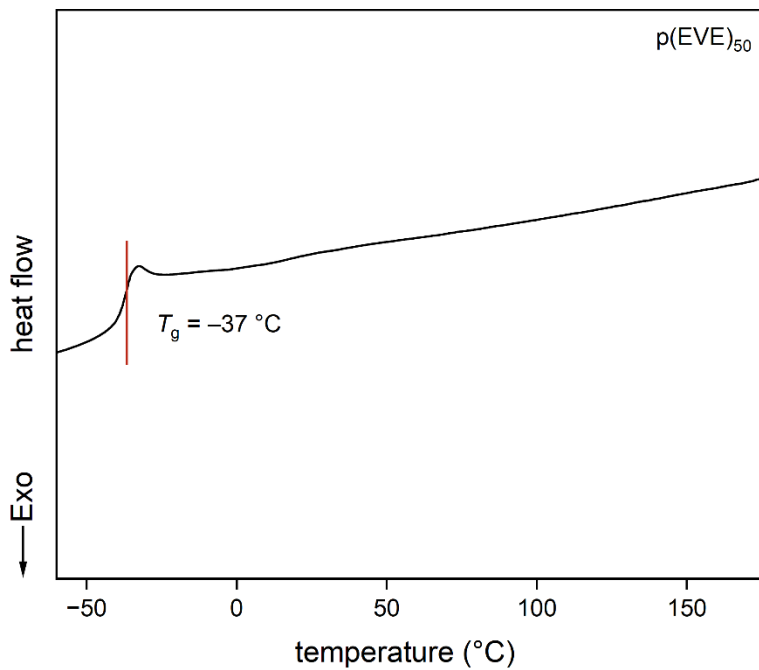


Figure S46. DSC thermogram of p(EVE)₅₀.

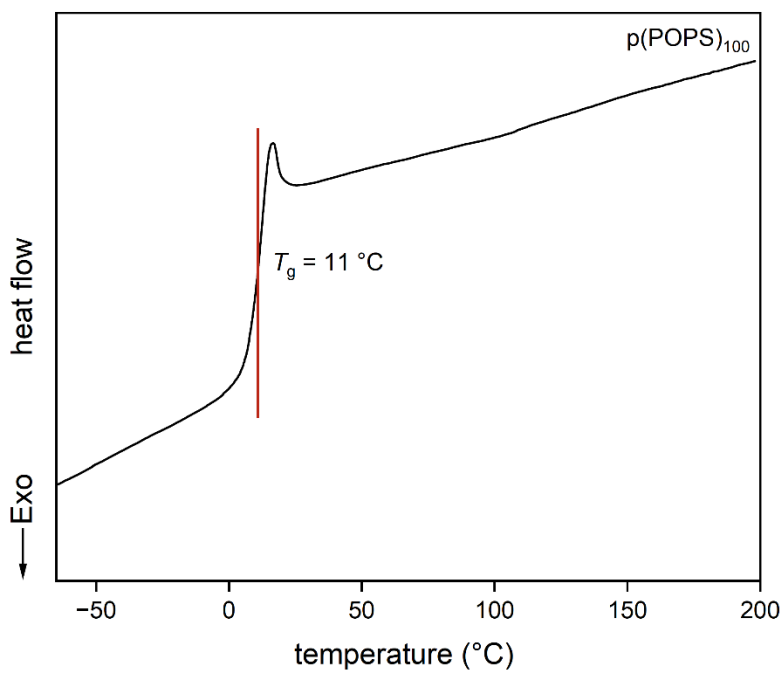


Figure S47. DSC thermogram of p(POPS)₁₀₀.

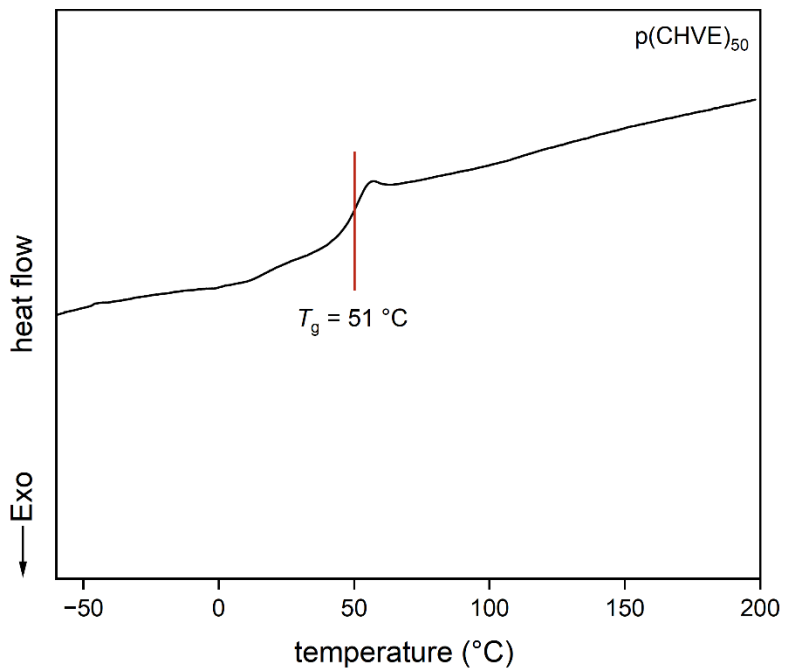


Figure S48. DSC thermogram of p(CHVE)₅₀.

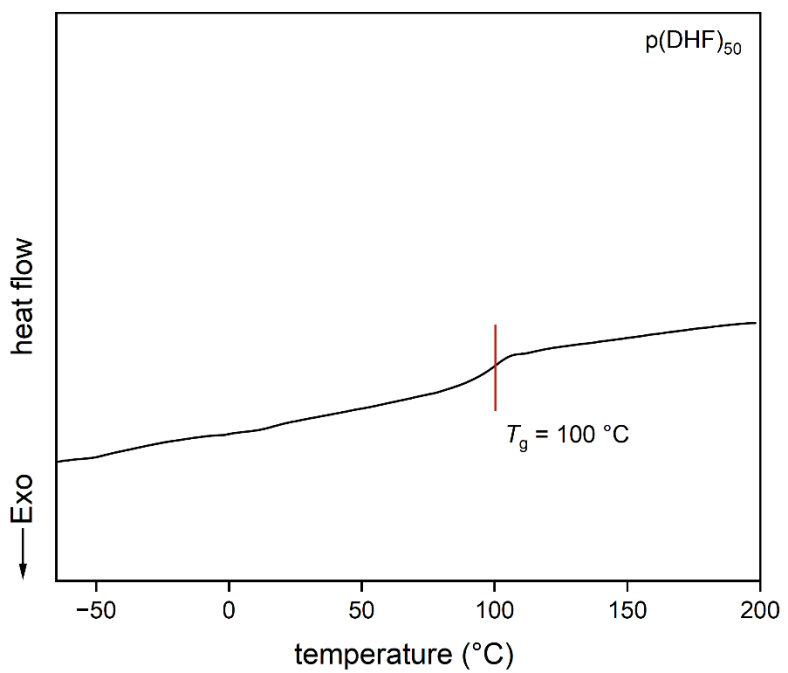


Figure S49. DSC thermogram of p(DHF)₅₀.

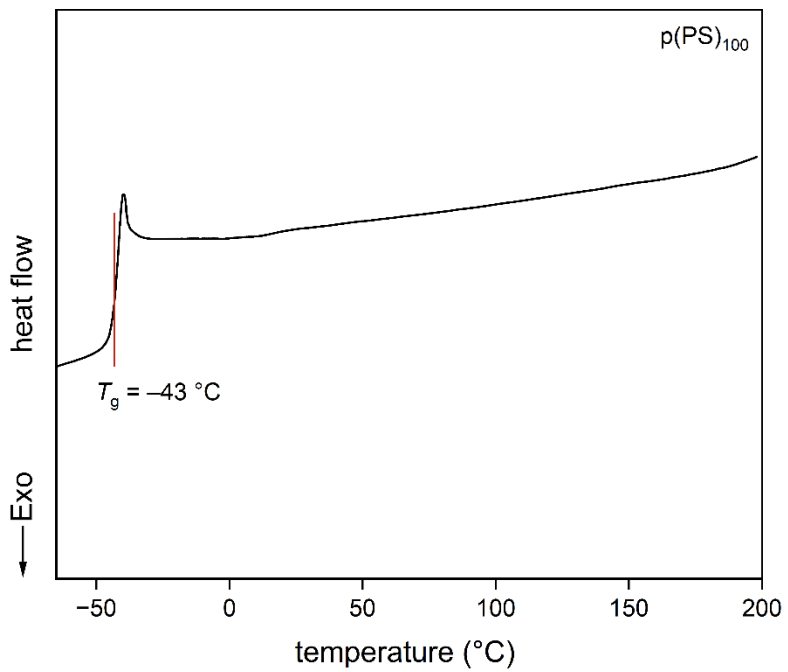


Figure S50. DSC thermogram of p(PS)₁₀₀.

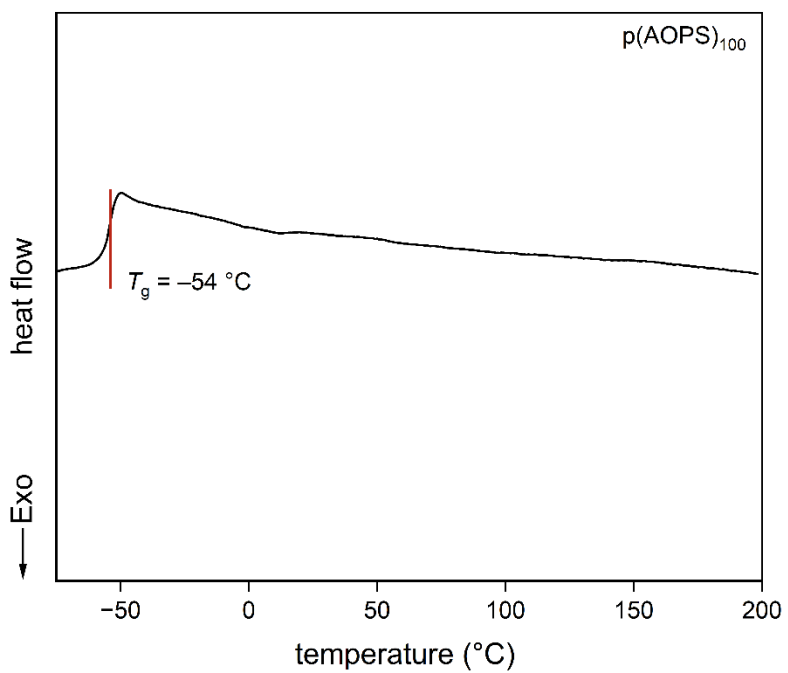


Figure S51. DSC thermogram of p(AOPS)₁₀₀.

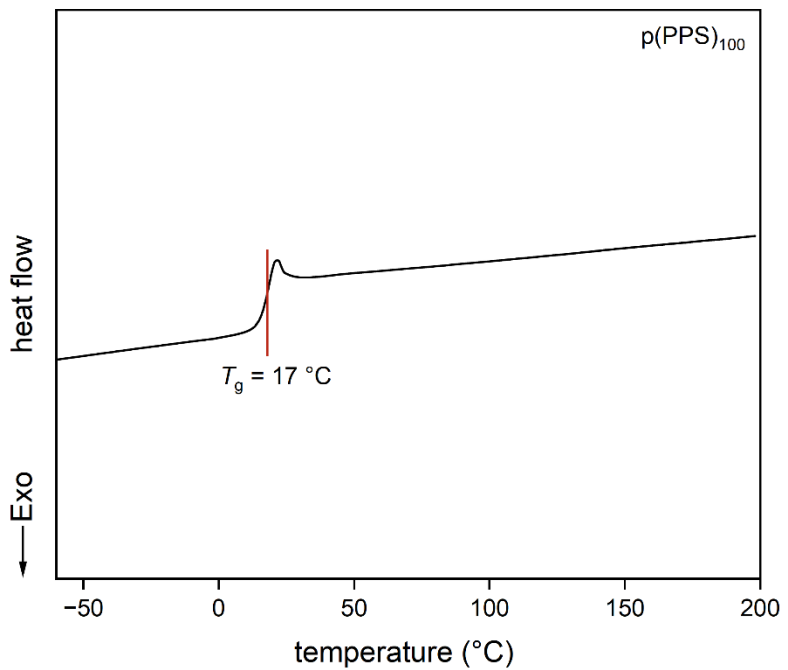


Figure S52. DSC thermogram of p(PPS)₁₀₀.

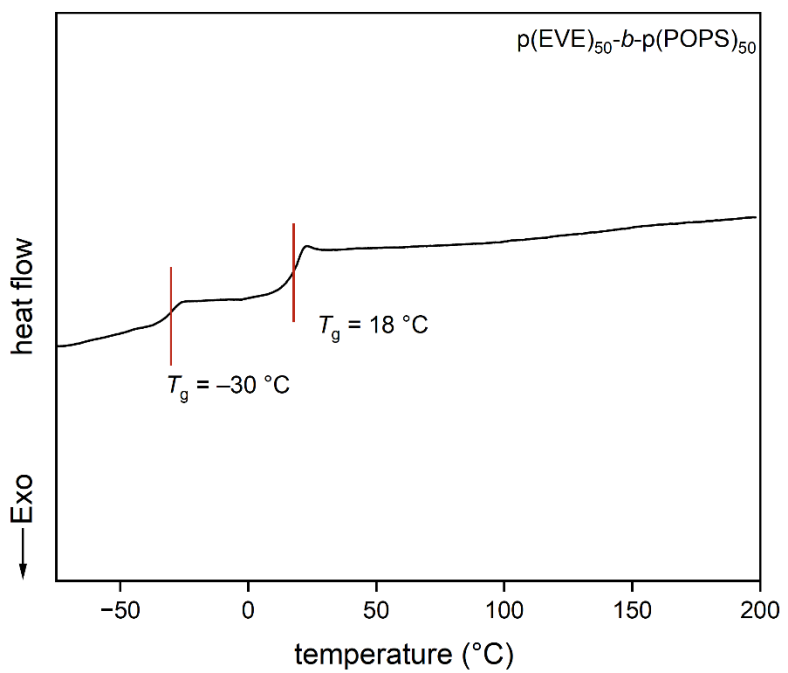


Figure S53. DSC thermogram of p(EVE)₅₀-b-p(POPS)₅₀ purified by prepSEC.

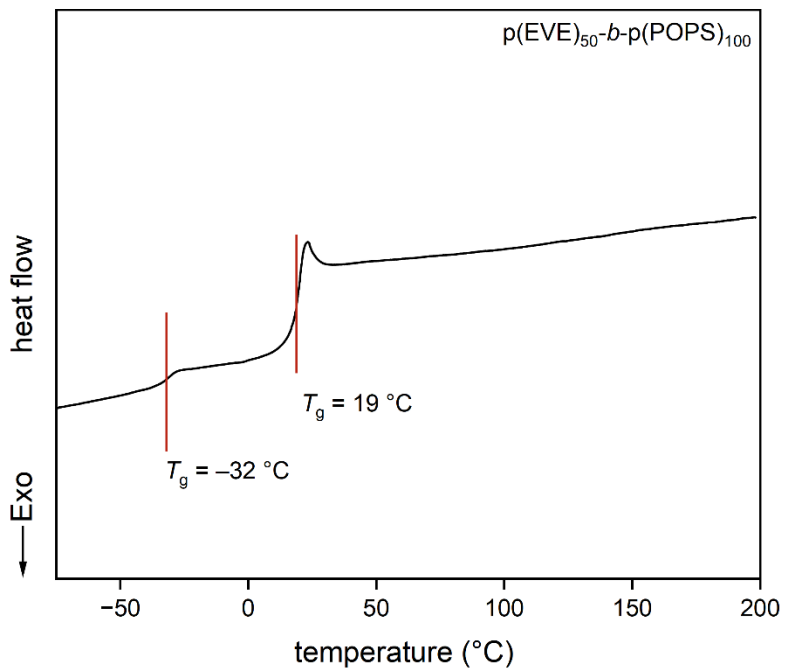


Figure S54. DSC thermogram of p(EVE)₅₀-b-p(POPS)₁₀₀ purified by prepSEC.

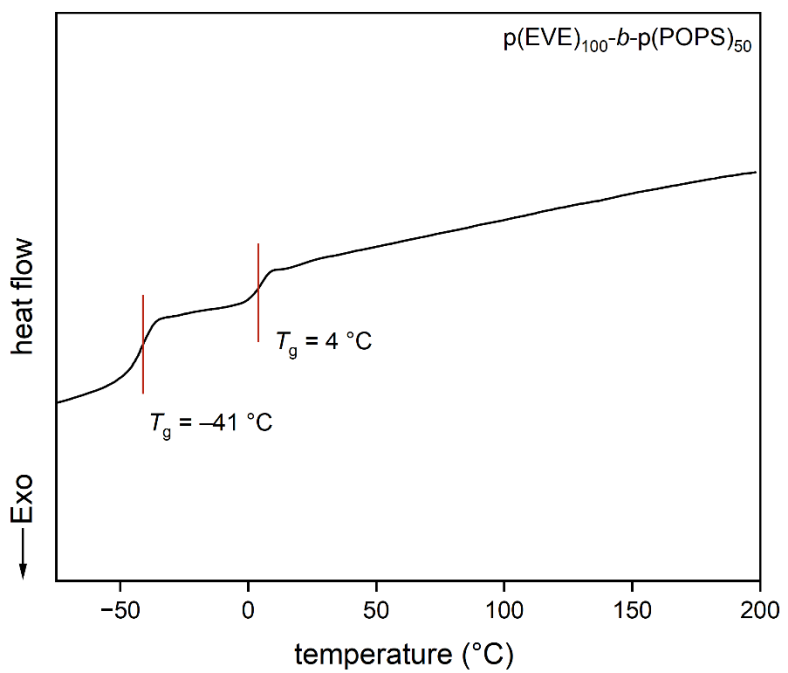


Figure S55. DSC thermogram of p(EVE)₁₀₀-b-p(POPS)₅₀ purified by prepSEC.

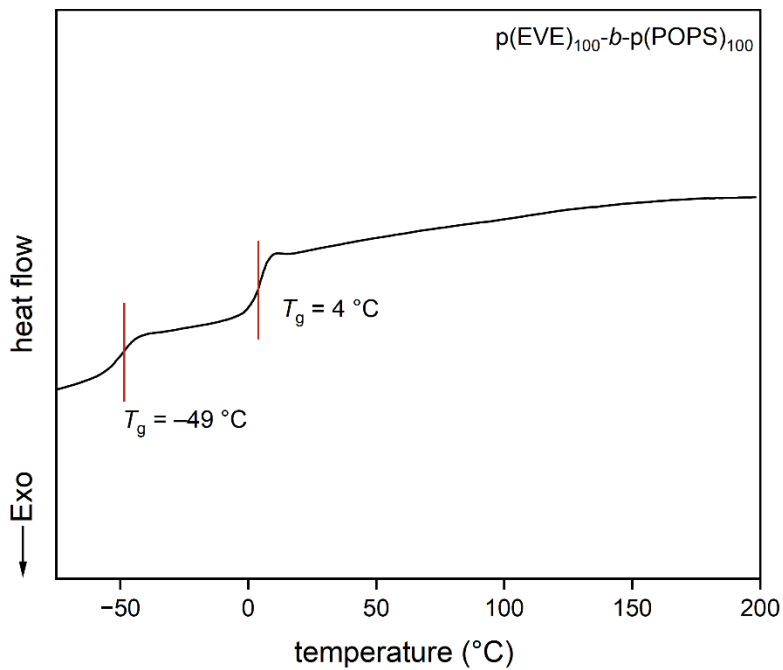


Figure S56. DSC thermogram of p(EVE)₁₀₀-b-p(POPS)₁₀₀ purified by prepSEC.

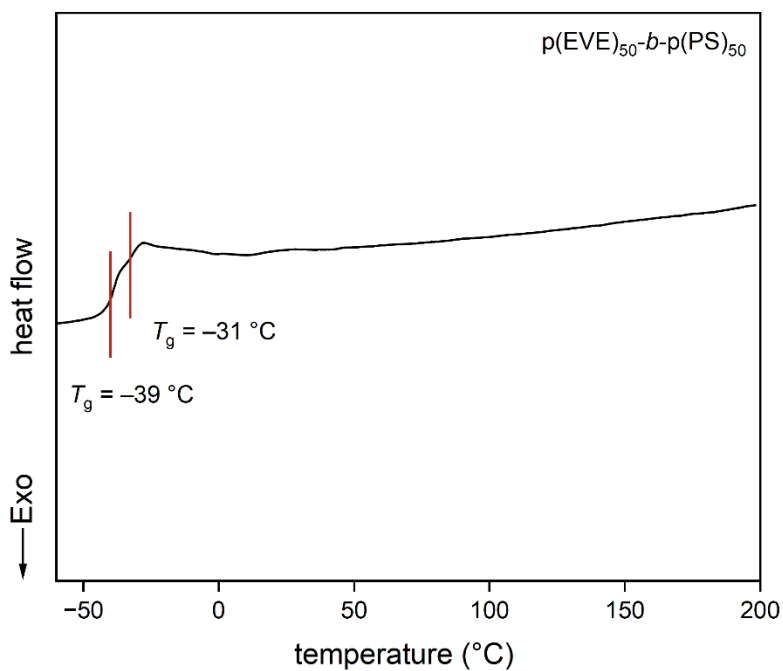


Figure S57. DSC thermogram of p(EVE)₅₀-b-p(PS)₅₀ purified by prepSEC.

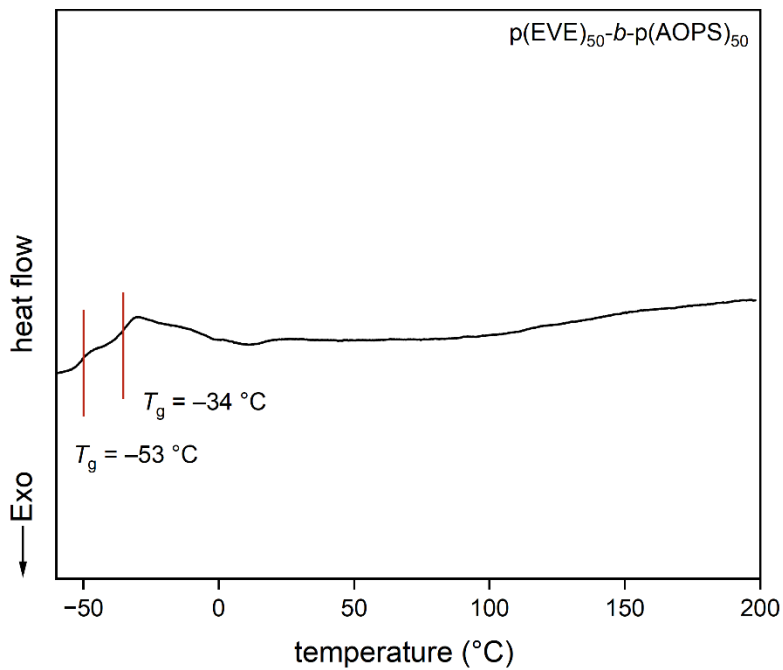


Figure S58. DSC thermogram of p(EVE)₅₀-b-p(AOPS)₅₀ purified by prepSEC.

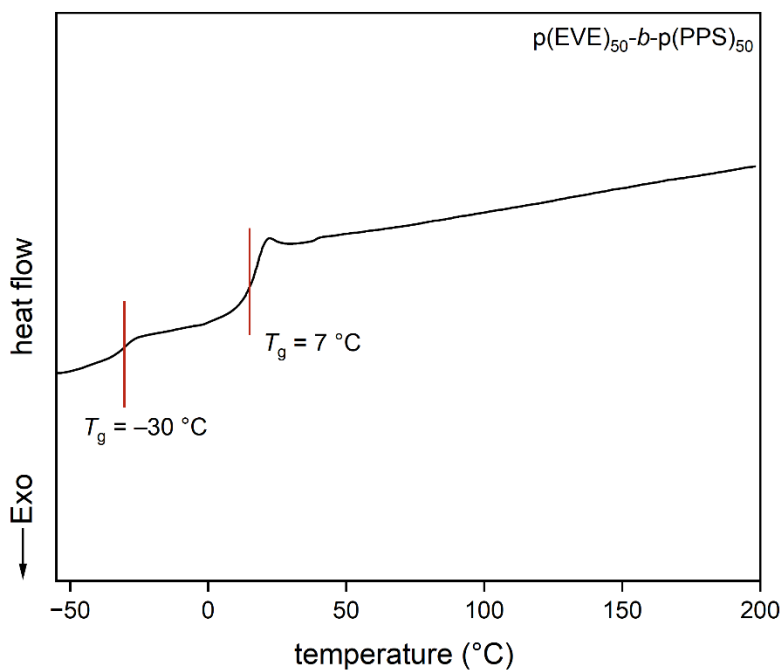


Figure S59. DSC thermogram of p(EVE)₅₀-b-p(PPS)₅₀ purified by prepSEC.

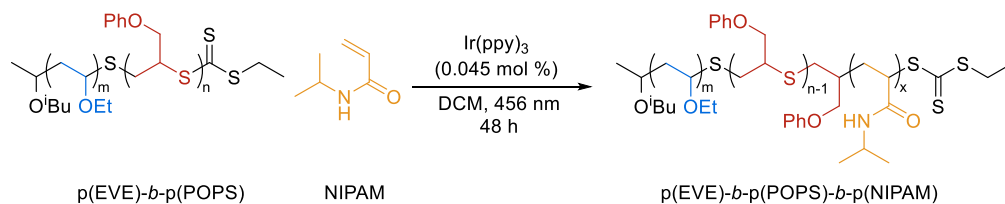
Table S8. Thermal characterization data of homopolymers and BCPs purified by prepSEC

entry	polymer	first T_o ($^{\circ}\text{C}$) ^[a]	second T_o ($^{\circ}\text{C}$) ^[a]	T_g ($^{\circ}\text{C}$) ^[b]
1	p(EVE) ₅₀	266	375	-37
2	p(POPS) ₁₀₀	284	-	11
3	p(CHVE) ₅₀	95	400	51
4	p(DHF) ₅₀	83	377	100
5	p(PS) ₁₀₀	278	-	-43
6	p(AOPS) ₁₀₀	288	-	-54
7	p(PPS) ₁₀₀	297	-	17
8	p(EVE) ₅₀ - <i>b</i> -p(POPS) ₅₀	283	376	-30, 18
9	p(EVE) ₅₀ - <i>b</i> -p(POPS) ₁₀₀	272	375	-32, 19
10	p(EVE) ₁₀₀ - <i>b</i> -p(POPS) ₅₀	271	373	-41, 4
11	p(EVE) ₁₀₀ - <i>b</i> -p(POPS) ₁₀₀	277	379	-49, 4
12	p(EVE) ₅₀ - <i>b</i> -p(PS) ₁₀₀	284	404	-39, -31
13	p(EVE) ₅₀ - <i>b</i> -p(AOPS) ₁₀₀	284	403	-53, -34
14	p(EVE) ₅₀ - <i>b</i> -p(PPS) ₁₀₀	288	399	-30, 7

[a] Calculated from TGA thermograms. [b] Determined by DSC.

J. Triblock terpolymer synthesis and associated SEC traces

We performed second extensions of p(EVE)₅₀-*b*-p(POPS)₅₀ and p(EVE)₁₀₀-*b*-p(POPS)₁₀₀ using photocontrolled radical polymerization of NIPAM to make novel triblock terpolymers (see Section 3.E for procedure).



Scheme S2. Radical chain extension of p(EVE)-*b*-p(POPS) BCPs.

For p(EVE)₅₀-*b*-p(POPS)₅₀-*b*-p(NIPAM)₅₀, there is complete chain extension from the diblock as evidenced by a clean shift of the SEC peak to a lower retention time (Figure S60) and a significant increase in M_n from 14.3 kDa to 21.6 kDa.

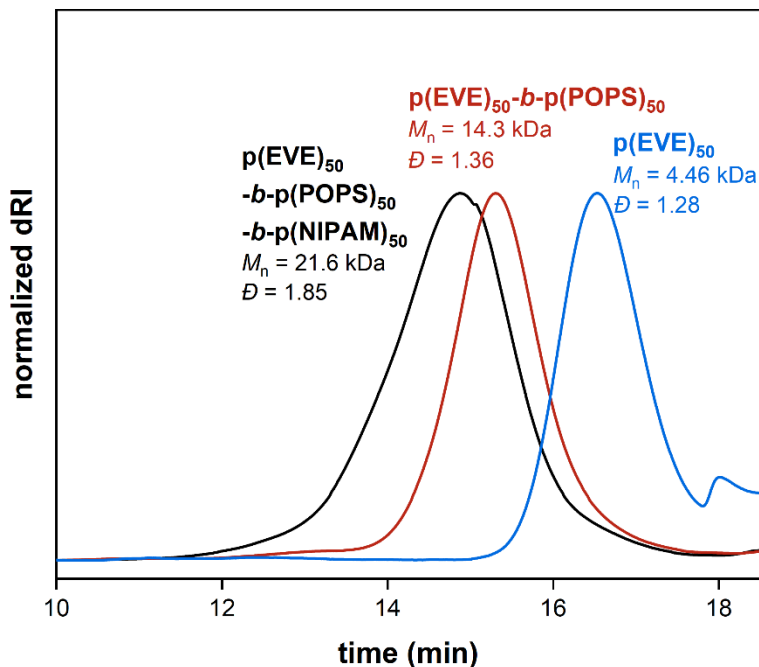


Figure S60. SEC traces from the synthesis of $p(\text{EVE})_{50}\text{-}b\text{-}p(\text{POPS})_{50}\text{-}b\text{-}p(\text{NIPAM})_{50}$.

The extension of $p(\text{EVE})_{100}\text{-}b\text{-}p(\text{POPS})_{100}\text{-}b\text{-}p(\text{NIPAM})_{100}$ also proceeded cleanly with a significant shift in the SEC trace (Figure S61), albeit of a smaller magnitude, with M_n increasing from 18.3 kDa to 20.4 kDa. These extensions are the first examples of a triblock terpolymer formed from the combination of cationic, anionic, and radical polymerizations of three unique monomer classes without the need for intermediate compatibilization steps or end-group modification. We believe that further optimization of these conditions will result in even more well-controlled materials.

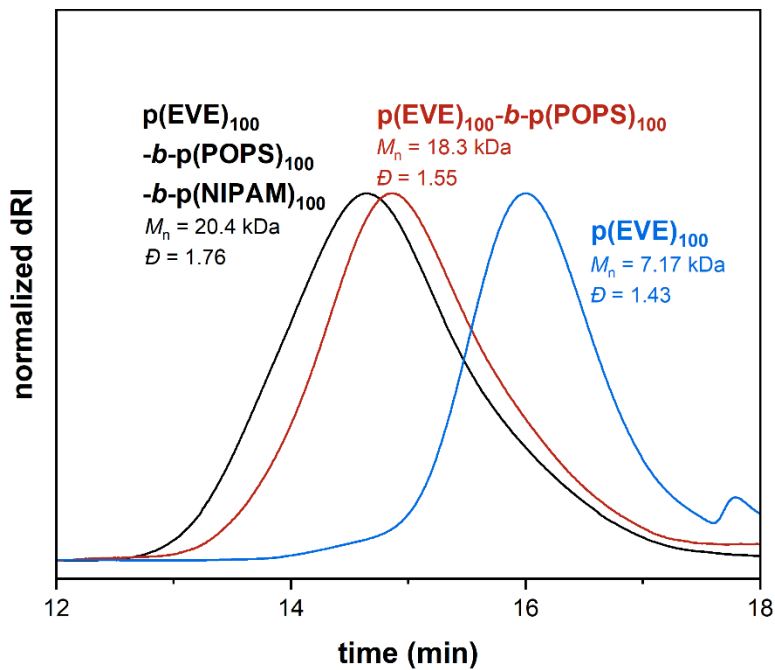
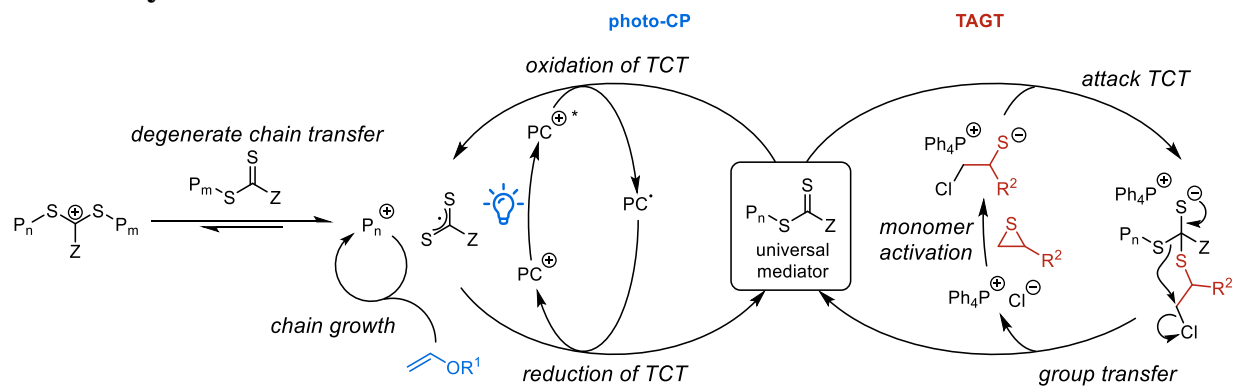


Figure S61. SEC traces from the synthesis of p(EVE)₁₀₀-b-p(POPS)₁₀₀-b-p(NIPAM)₁₀₀.

K. Polymerization mechanisms



Scheme S3. Mechanisms of photo-CP and TAGT.

3. General synthetic procedures

A. Photoreactor setup

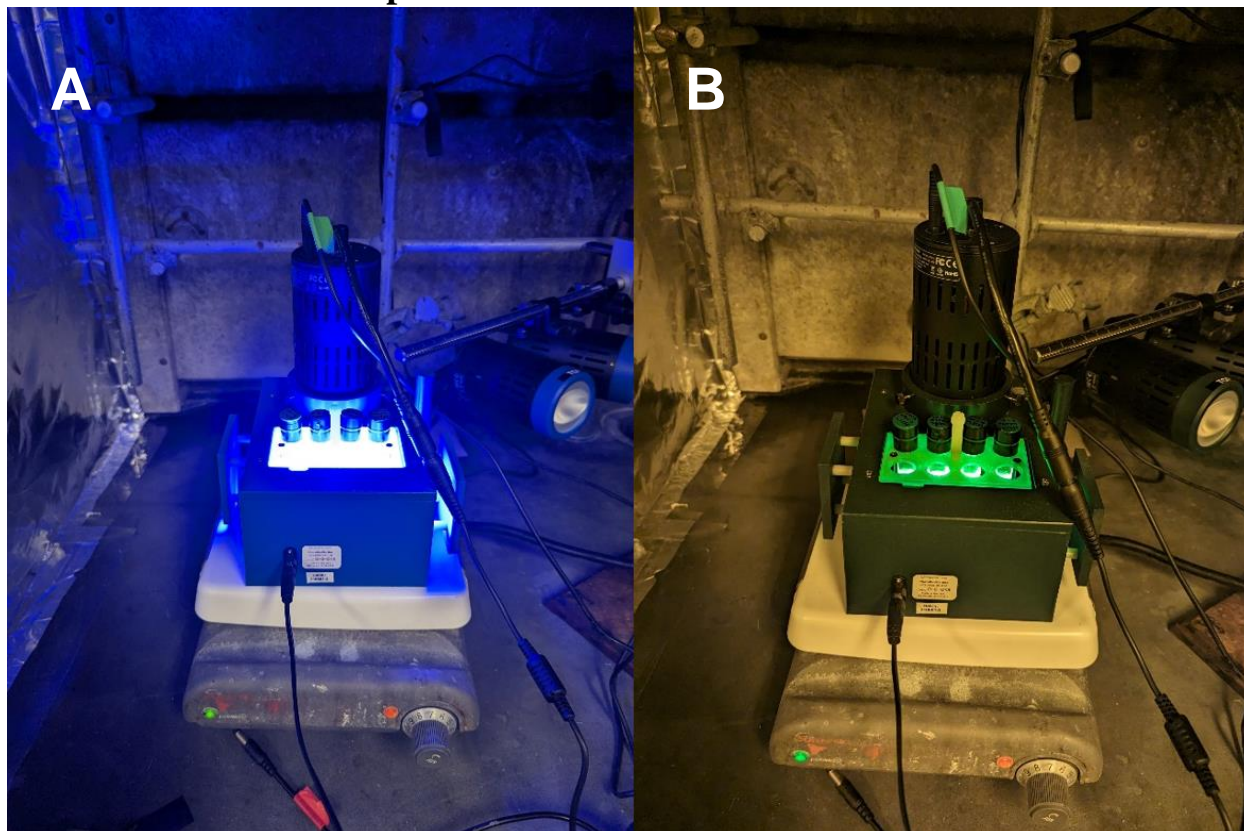
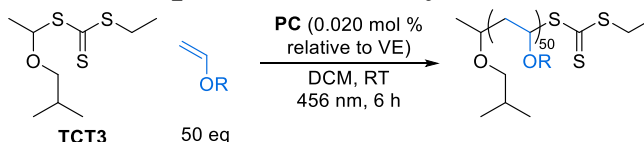


Figure S62. Images of the photoreactor setup (A) with the bulb on and (B) with bulb on looking through HepatoChem UVEX Amber Safety Glasses.

All photochemical reactions were performed using an EvoluChem PhotoRedOx Box equipped with a single Kessil PR160L 50W 456 nm lamp at 100% power. A Kessil lamp was chosen over the EvoluChem 18W 450 nm LED bulbs sold with the box in order to achieve a higher light intensity. The embedded cooling fan in the box was powered and the whole box was placed on a magnetic stirrer. This setup was placed inside of a fume hood with the sash fully closed and covered in foil to ensure the highest airflow and to prevent light leaking. Always be careful to wear appropriate UV- and blue-light blocking safety glasses while working with this setup.

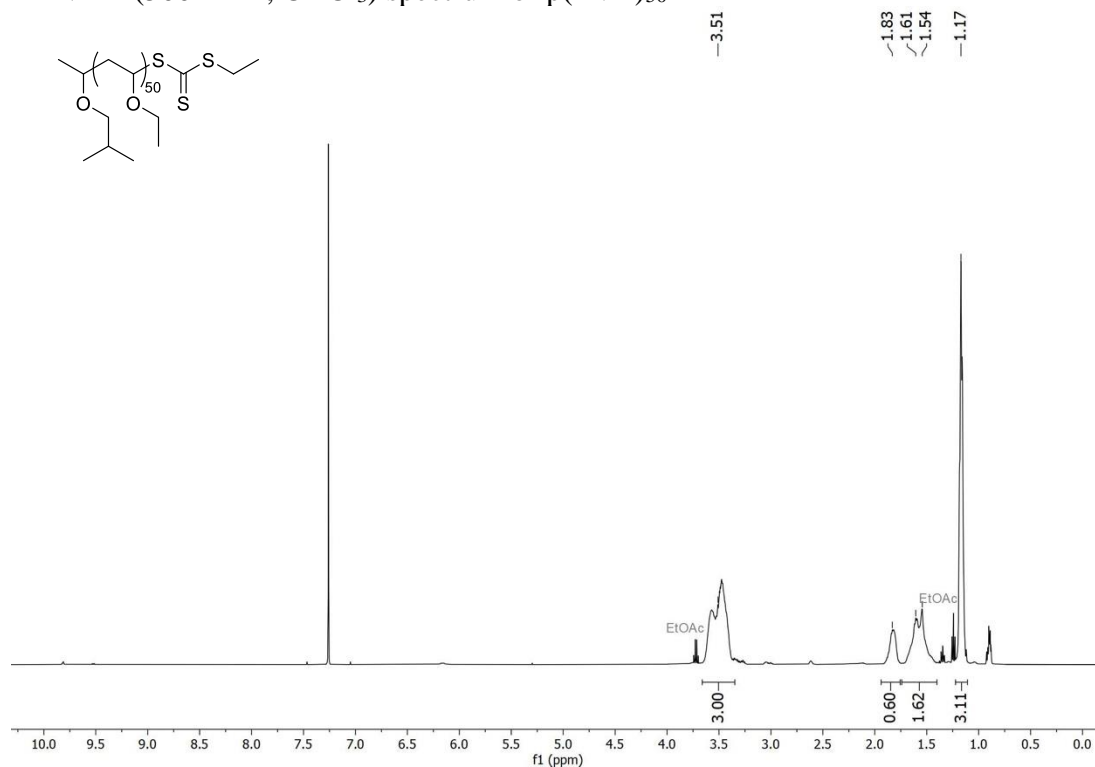
B. General procedure for photo-CP of vinyl ethers



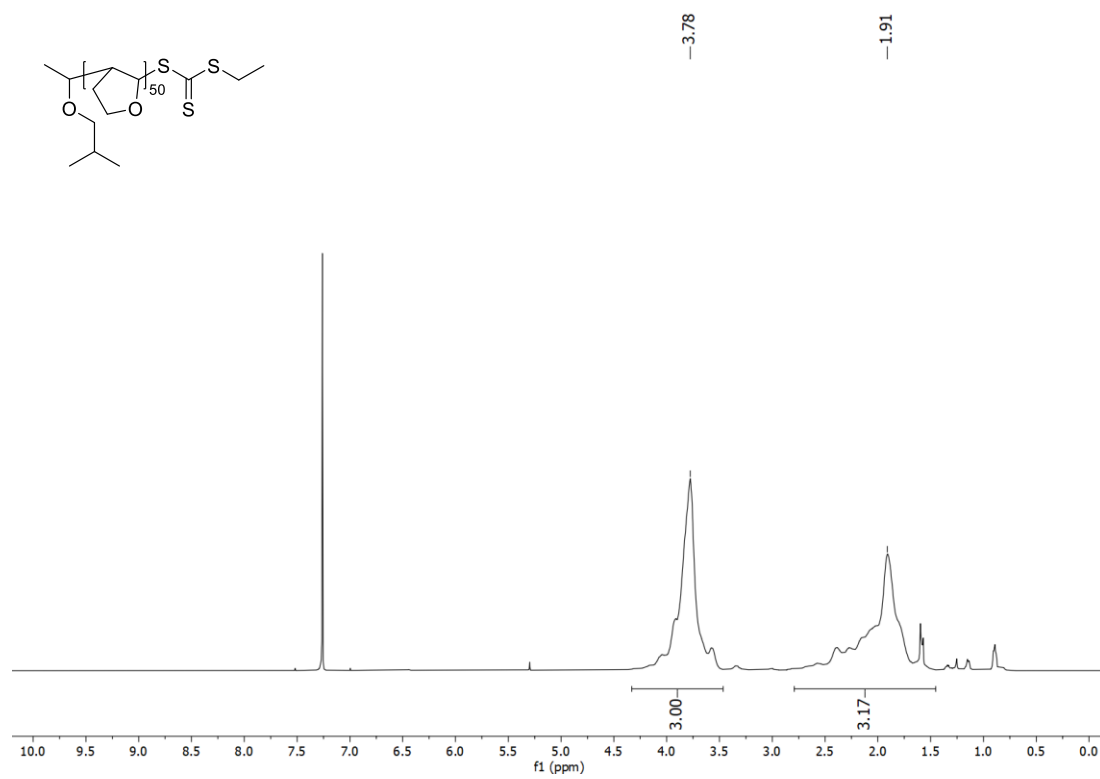
This synthesis was adapted from a previous literature procedure.³ Inside a nitrogen glovebox, a 1 dram screw-top vial was equipped with a stir bar and charged with 20 μ L of a solution of **TCT3** in DCM (1.0 M, 0.020 mmol, 1 eq). Vinyl ether (1.0 mmol, 50 eq) was added to the vial, followed

by 100 μL of a solution of **PC** in DCM (2.0 mM, 0.20 μmol , 0.020 mol % relative to VE monomer). The vial was capped and electrical tape was wrapped around the cap-vial interface to ensure a good seal. The vial was removed from the glovebox and placed into the photoreactor (see Section S3.A). The reaction was irradiated at 456 nm for 6 hours, at which point 98% conversion was typically reached. Solvent and any unreacted monomer were removed via drying overnight in a vacuum oven set at 70 $^{\circ}\text{C}$. Residual **PC** was not removed from these samples prior to characterization or chain extension due to the high solubility of p(EVE) precluding the ability to purify by precipitation.

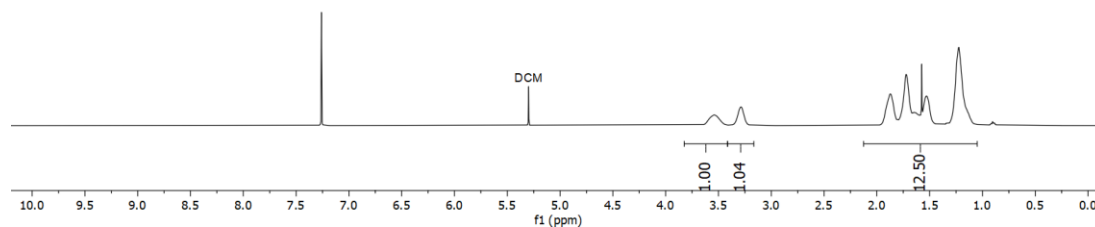
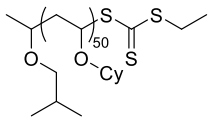
^1H NMR (500 MHz, CDCl_3) spectrum of p(EVE)₅₀



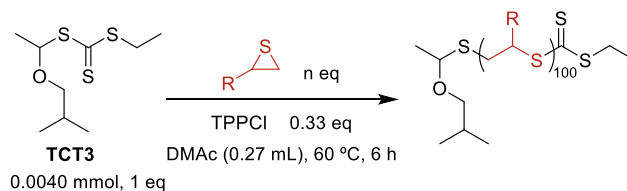
^1H NMR (500 MHz, CDCl_3) spectrum of $\text{p}(\text{DHF})_{50}$



^1H NMR (500 MHz, CDCl_3) spectrum of $\text{p}(\text{CHVE})_{50}$

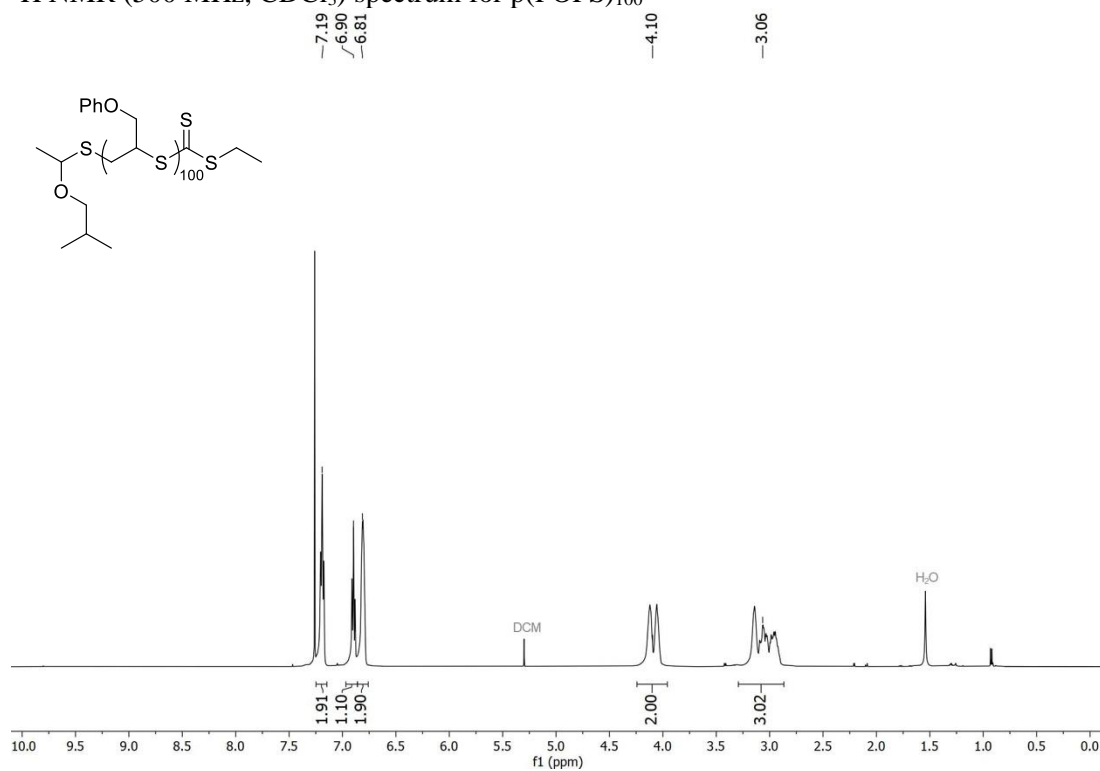


C. General procedure for TAGT of thiiranes

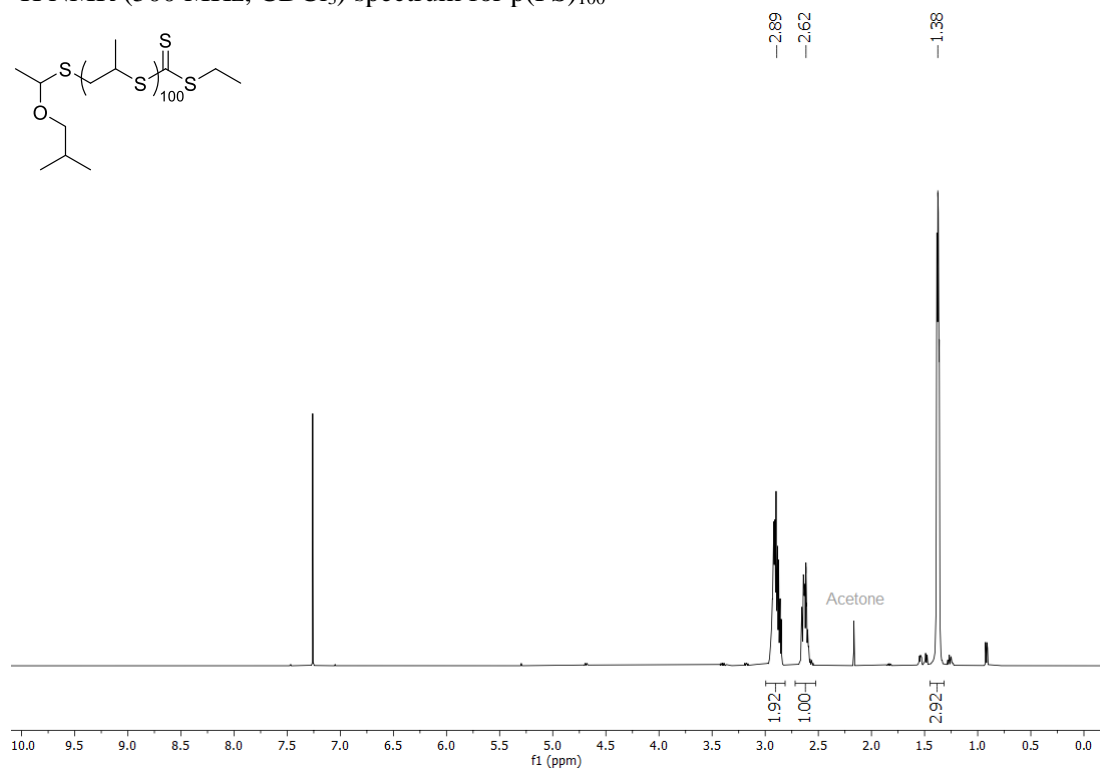


This synthesis was adapted from a previous literature procedure.⁴ A 1 dram screw-top vial was charged with 130 μL of a stock solution of **TCT3** in DMAc (0.50 M, 0.0040 mmol, 1 eq) and a stir bar. Thiirane (50–300 eq) was added to the vial by weight followed by 110 μL of a stock solution of TPPCI in DMAc (12 mM, 0.0013 mmol, 0.33 eq). More solvent was added until the total amount of DMAc was 270 μL . The solution was placed in a pre-heated reaction block at 60 °C. After stirring for 6 hours, the vial was removed from the glovebox, and an aliquot was taken for ^1H NMR analysis. The polymerization was then quenched with the addition of DCM (~100 μL), followed by isolation via precipitation in cold methanol. The pellet was redissolved in DCM to transfer to a tared vial. Additionally, an aliquot was taken for SEC analysis. The solvent was removed via drying overnight in a vacuum oven set at 70 °C.

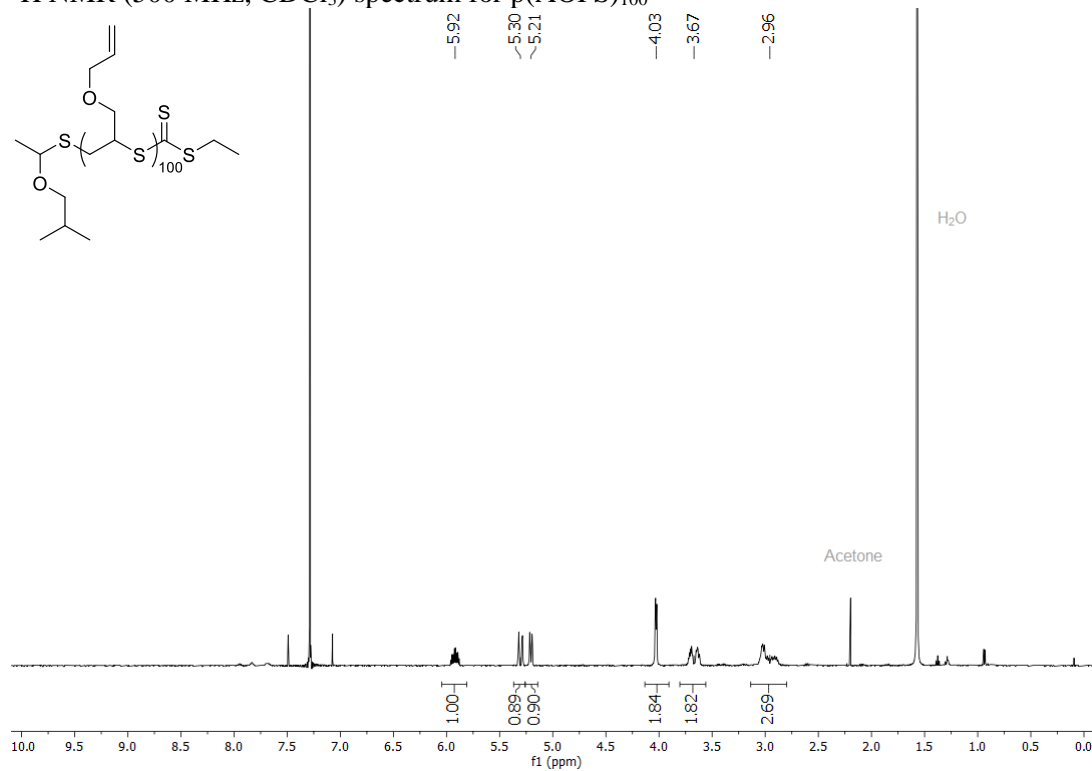
^1H NMR (500 MHz, CDCl_3) spectrum for $\text{p}(\text{POPS})_{100}$



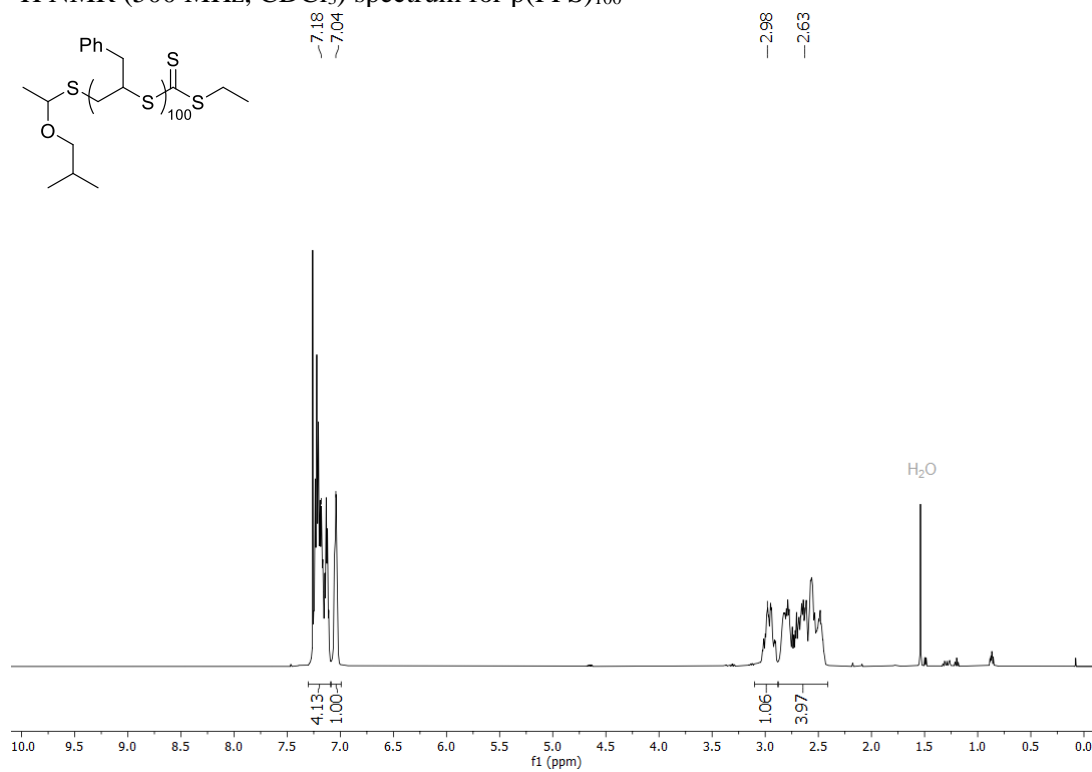
^1H NMR (500 MHz, CDCl_3) spectrum for $\text{p}(\text{PS})_{100}$



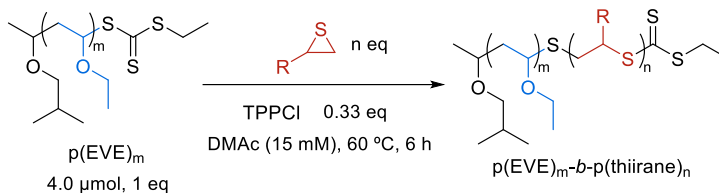
^1H NMR (500 MHz, CDCl_3) spectrum for p(AOPS) $_{100}$



^1H NMR (500 MHz, CDCl_3) spectrum for p(PPS) $_{100}$

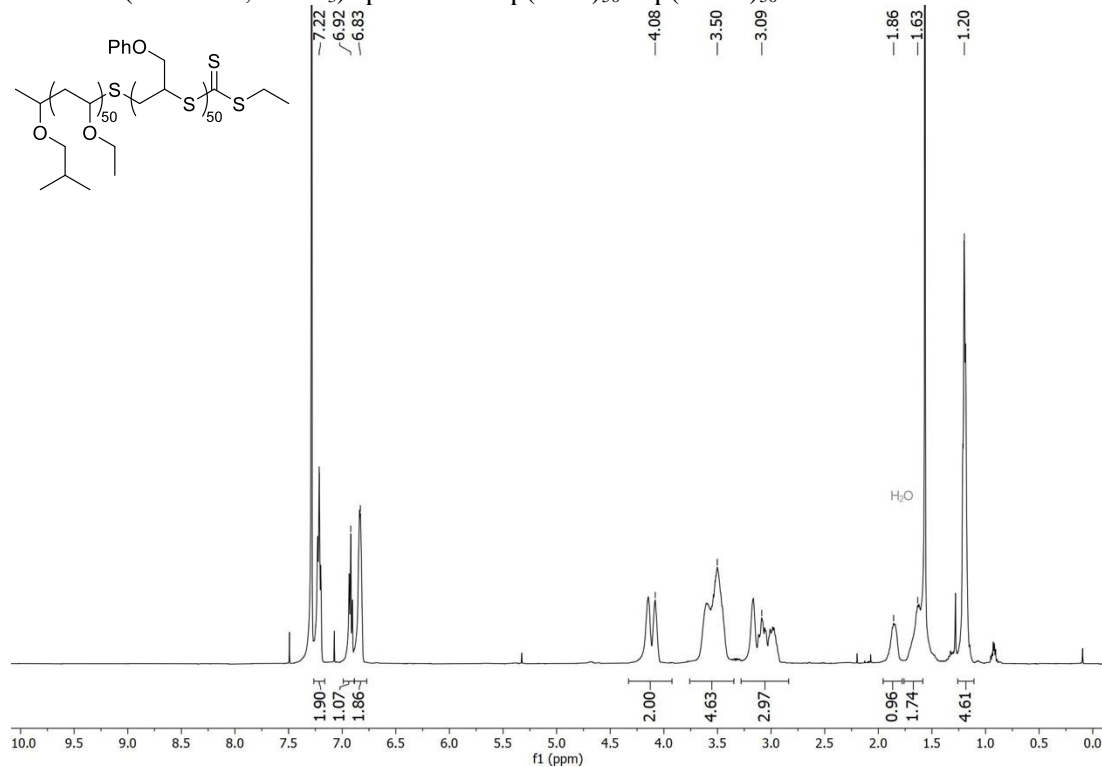


D. General procedure for anionic chain extensions of p(EVE)

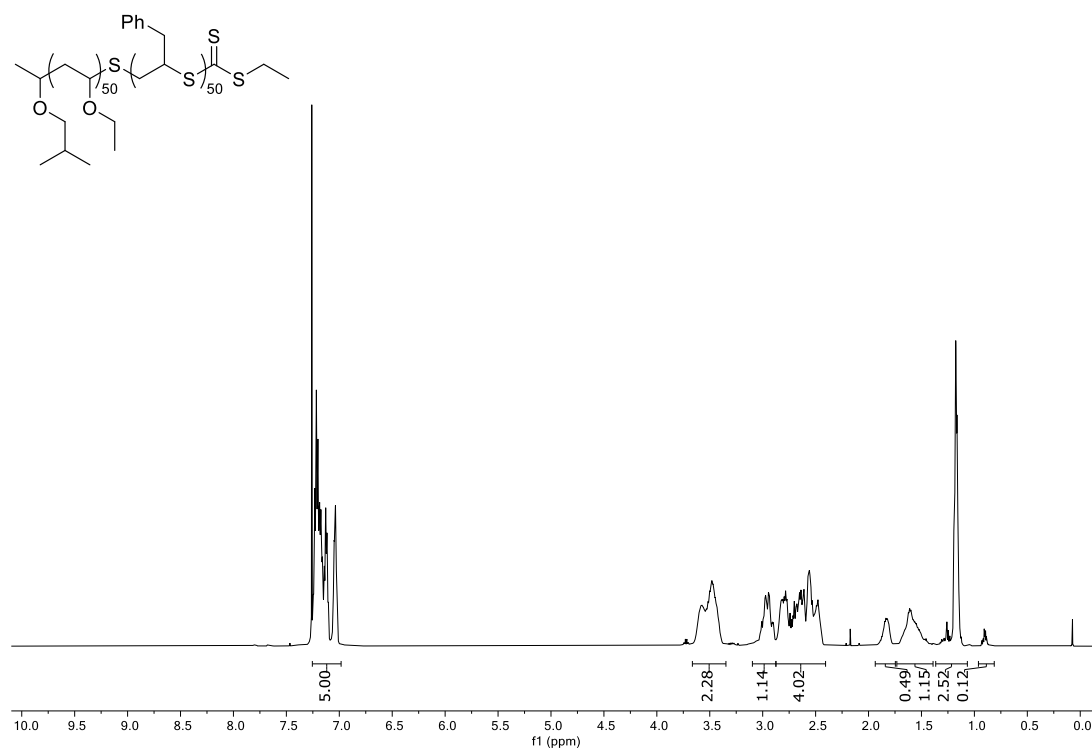


A 1 dram screw-top vial was charged with 130 μL of a stock solution of p(EVE) in DMAc (30 mM, 0.0040 mmol, 1 eq) and a stir bar. Thiirane (50–100 eq) was added to the vial by weight followed by 110 μL of a solution of TPPCl in DMAc (1.2 mM, 0.0013 mmol, 0.33 eq). Additional solvent was added until the total amount of DMAc was 270 μL (15 mM relative to p(EVE)). The solution was placed in a pre-heated reaction block at 60 $^\circ\text{C}$. After stirring for 6 hours, the vial was removed from the glovebox, and aliquots were taken for ^1H NMR and SEC analyses. The polymerization was then quenched with the addition of DCM (\sim 100 μL). The solvent was removed via drying overnight in a vacuum oven set at 70 $^\circ\text{C}$. The polymers were purified via prepSEC and dried under high vac.

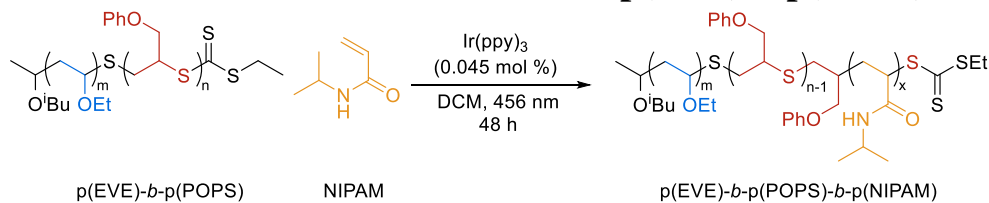
^1H NMR (500 MHz, CDCl_3) spectrum for p(EVE)₅₀-b-p(POPS)₅₀



^1H NMR (500 MHz, CDCl_3) spectrum for $\text{p(EVE)}_{50}\text{-}b\text{-p(PPS)}_{50}$

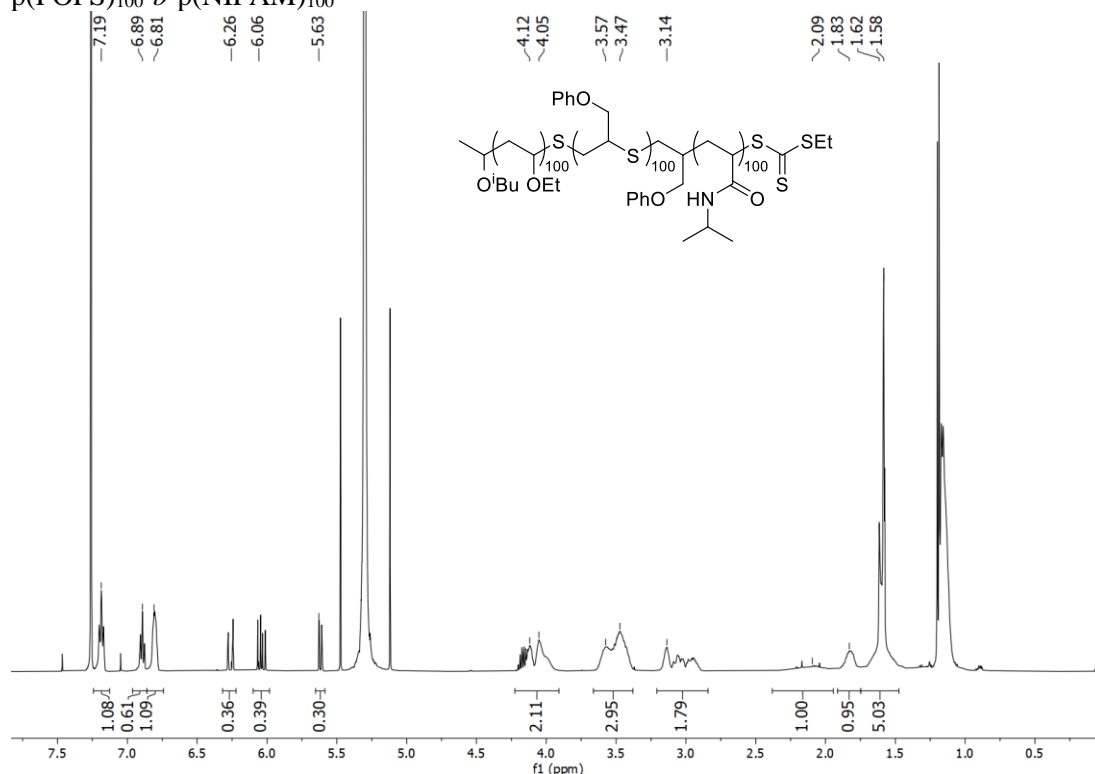


E. Procedure for radical chain extension of $\text{p(EVE)-}b\text{-p(POPS)}$



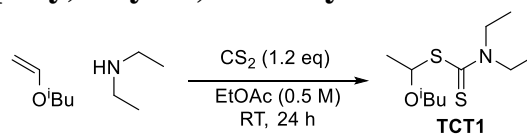
Inside a nitrogen-filled glovebox, a 1 dram screw-top vial was charged with $\text{p(EVE)-}b\text{-p(POPS)}$ (1 eq), a stir bar, and NIPAM (50 or 100 eq). DCM (3 mM) was added, and the solution was allowed to stir for 5 minutes to fully dissolve the components. To this solution, Ir(ppy)_3 (1.5 mM in DCM, 0.045 mol % relative to NIPAM) was added. The vial was capped and electrical tape was wrapped around the cap-vial interface to ensure a good seal. The vial was removed from the glovebox and placed into the photoreactor (see Section 3.A). The reaction was irradiated at 456 nm for 48 hours.

^1H NMR (500 MHz, CDCl_3) spectrum of the crude reaction mixture for the synthesis of $p(\text{EVE})_{100}\text{-}b\text{-}p(\text{POPS})_{100}\text{-}b\text{-}p(\text{NIPAM})_{100}$



4. Compound synthesis and characterization

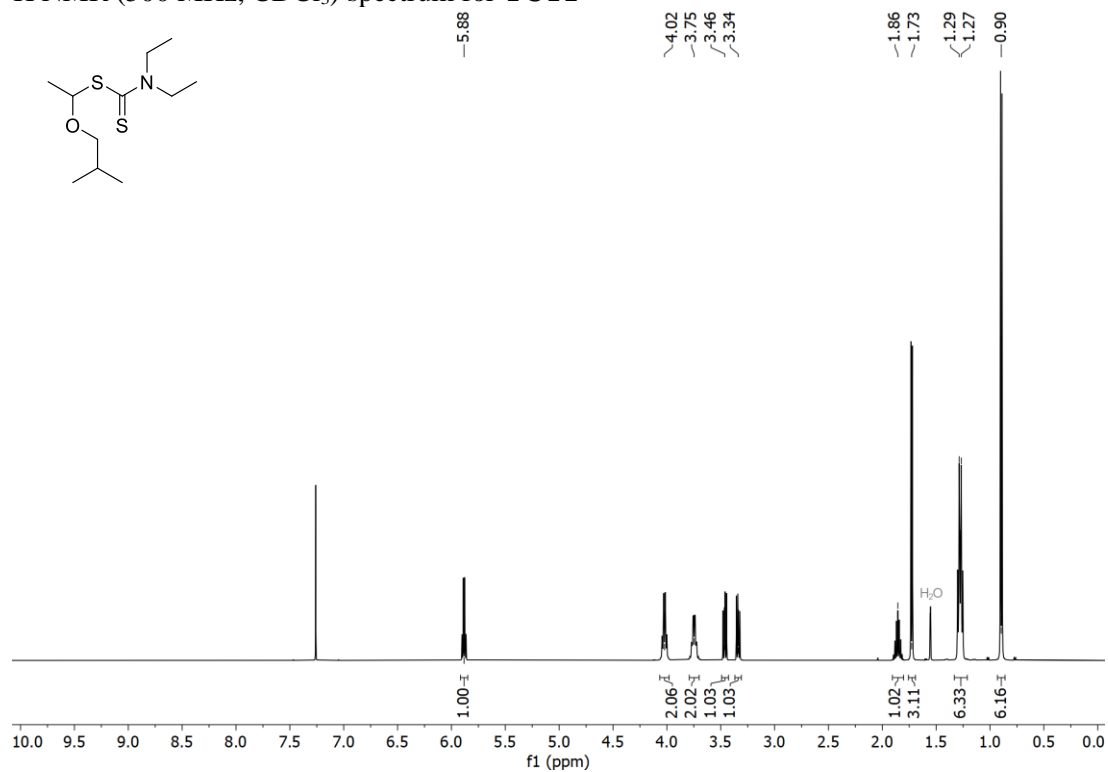
A. 1-(2-Methylpropoxy)ethyl *N,N*-diethylcarbamodithioate (**TCT1**)



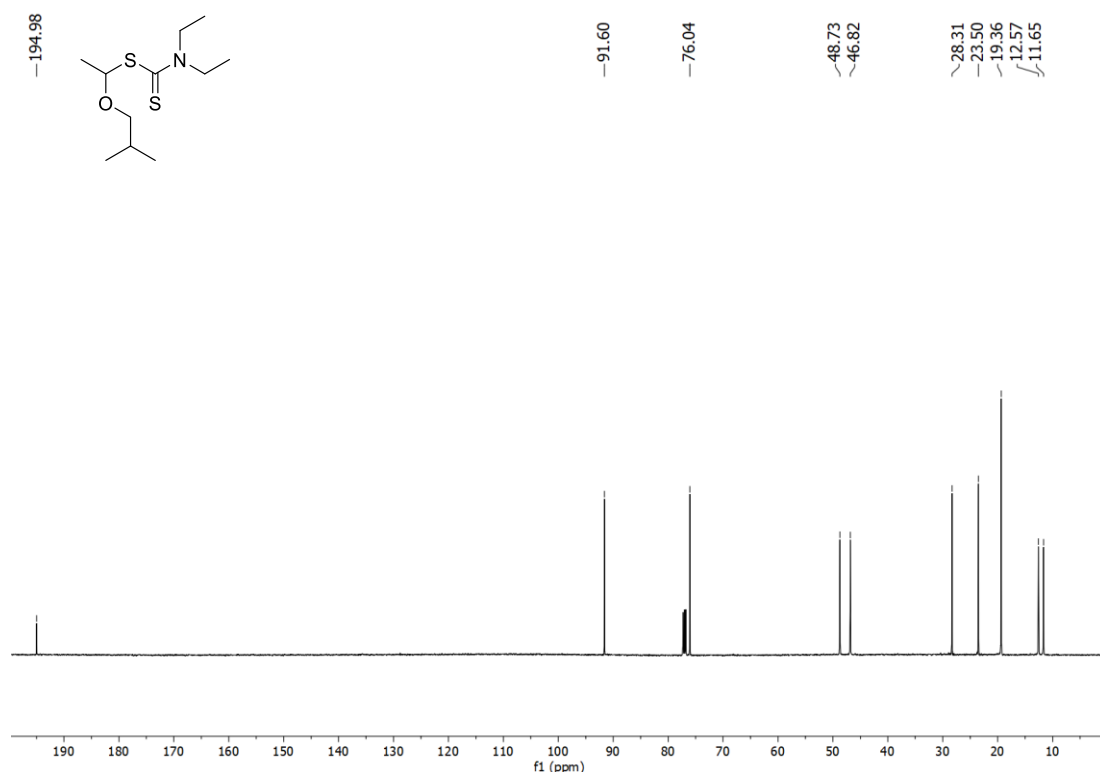
This synthesis was adapted from a previous literature procedure.⁵ To a 25 mL round-bottom flask equipped with a stir bar, EtOAc (10 mL) was added. To this, diethylamine (520 μL , 5.0 mmol, 1 eq) and carbon disulfide (360 μL , 6.0 mmol, 1.2 eq) were added. IBVE (790 μL , 6.0 mmol, 1.2 eq) was filtered through a plug of basic alumina and added to the reaction vessel. The reaction vessel was sealed with a glass stopper using vacuum grease and stirred at room temperature for 24 hours before being quenched with sodium bicarbonate. The aqueous layer was extracted with EtOAc (3 x 3 mL). The combined organic layers were washed with a saturated brine solution and dried over sodium sulfate before being concentrated via rotary evaporation. Exposure to high vacuum over 48 hours resulted in **TCT1** (644 mg, 52% yield) as a pure pale-yellow viscous oil. No further purification was necessary prior to use in polymerizations. The spectroscopic data for this compound were identical to those in the reported literature.^{3,14} ^1H NMR (500 MHz, CDCl_3): δ 5.88 (q, $J = 6.3$ Hz, 1H), 4.02 (q, $J = 7.1$ Hz, 2H), 3.75 (qd, $J = 7.2, 3.0$ Hz, 2H), 3.46 (dd, $J = 9.4, 6.9$ Hz, 1H), 3.34 (dd, $J = 9.4, 6.4$ Hz, 1H), 1.92–1.80 (m, $J = 6.7$ Hz, 1H), 1.73 (d, $J = 6.2$

Hz, 3H), 1.29 (t, $J = 7.2$ Hz, 3H), 1.27 (t, $J = 7.2$ Hz, 3H), 0.90 (d, $J = 6.7$ Hz, 6H). ^{13}C NMR (CDCl₃, 126 MHz): δ 195.0, 91.6, 76.0, 48.7, 46.8, 28.3, 23.5, 19.4, 12.6, 11.7

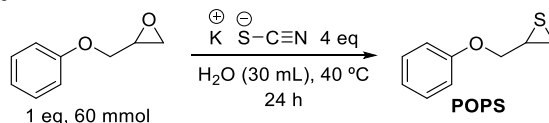
^1H NMR (500 MHz, CDCl₃) spectrum for **TCT1**



¹³C NMR (126 MHz, CDCl₃) Spectrum for TCT1

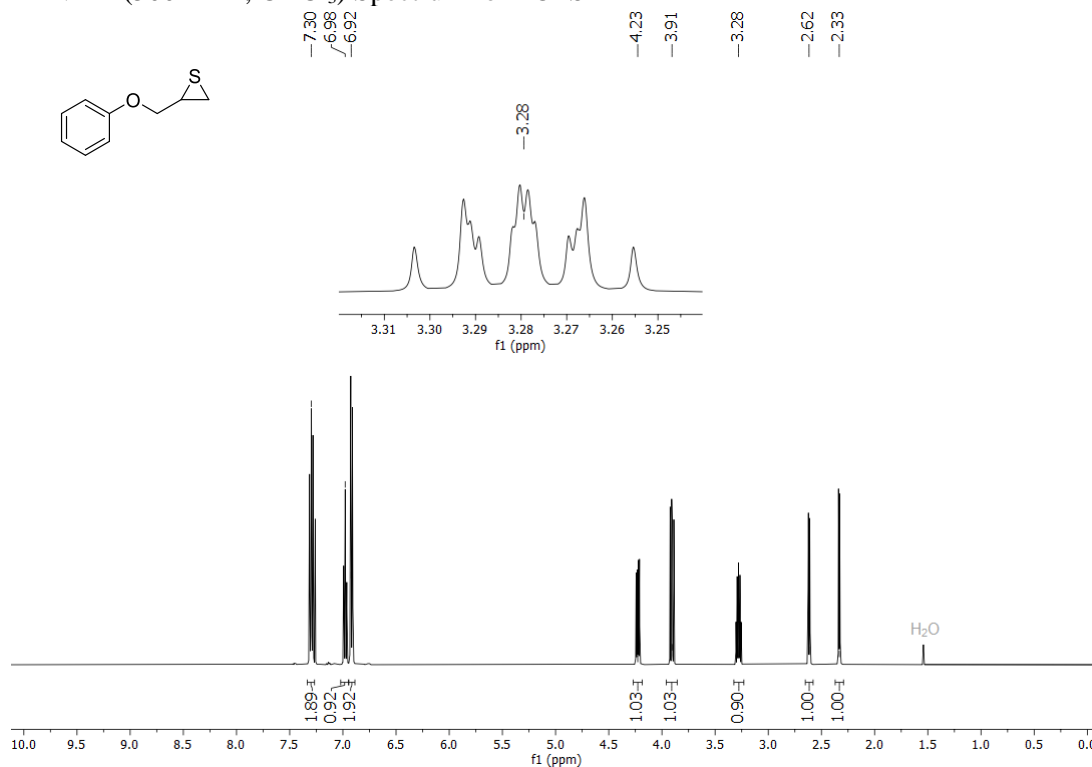


B. 3-Phenoxypropylene sulfide (POPS)

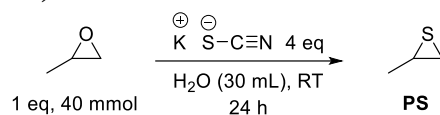


This synthesis was adapted from a previous literature procedure.⁴ A 100 mL round-bottom flask was charged with 2-(phenoxypropylene)oxirane (8.2 mL, 60 mmol, 1 eq), a stirbar, and deionized water (30 mL). Potassium thiocyanate was added to the flask (23.3 g, 240 mmol, 4 eq). The flask was placed in a pre-heated oil bath at 40 °C for 24 hours. The mixture was extracted with ethyl EtOAc (2 x 20 mL). The combined organic layers were then washed with deionized water (2 x 20 mL) and a saturated solution of brine (2 x 20 mL), dried using anhydrous magnesium sulfate, filtered, and concentrated using rotary evaporation. Further purification was carried out via column chromatography (9:1 hexanes:EtOAc, SiO₂) to generate POPS (4.06 g, 41% yield) as a clear, colorless, viscous liquid. The spectroscopic data for this compound matched the reported literature,¹⁵ though previous reports did not fully tabulate the splitting of the peaks. ¹H NMR (500 MHz, CDCl₃): δ 7.30 (m, 2H), 6.98 (m, 1H), 6.92 (m, 2H), 4.23 (ddd, *J* = 10.2, 5.5, 0.8 Hz, 1H), 3.91 (dd, *J* = 10.2, 7.1 Hz, 1H), 3.28 (ddt, *J* = 7.0, 6.2, 5.4 Hz, 1H), 2.62 (dt, *J* = 6.2, 1.1 Hz, 1H), 2.33 (dd, *J* = 5.3, 1.4 Hz, 1H).

¹H NMR (500 MHz, CDCl₃) Spectrum for POPS

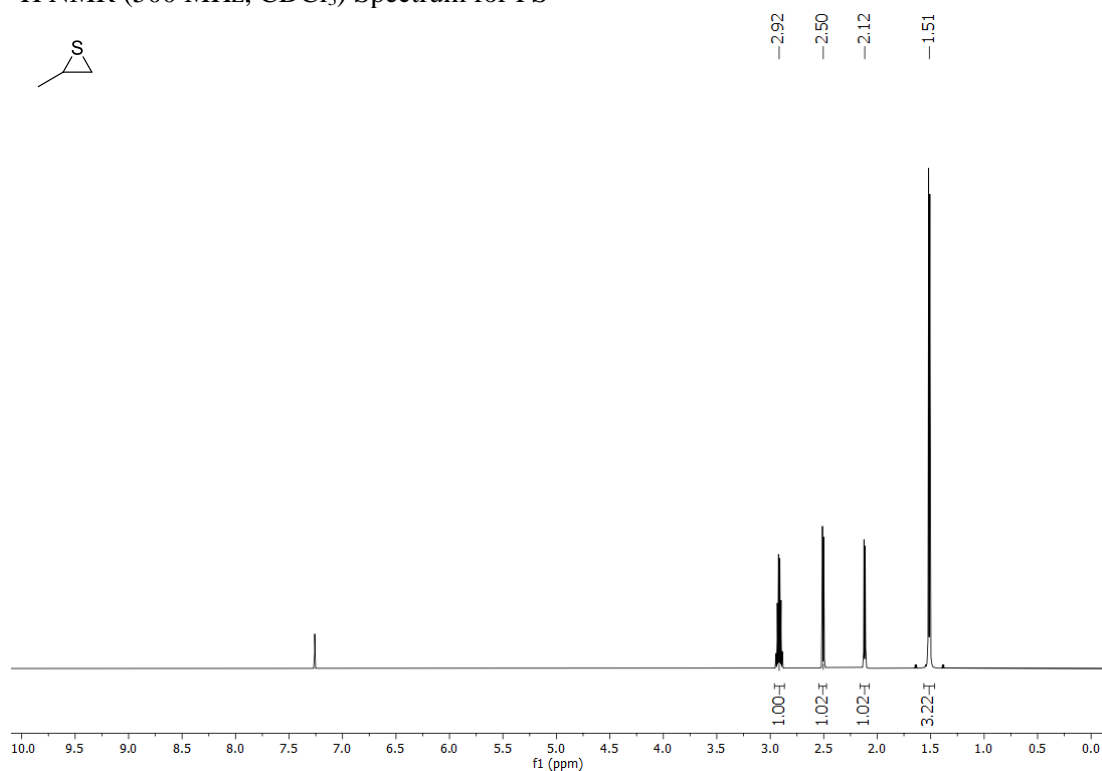


C. Propylene sulfide (PS)

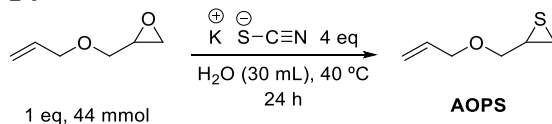


This synthesis was adapted from a previous literature procedure.⁴ A 50 mL round-bottom flask was charged with 2-methyloxirane (2.8 mL, 40 mmol, 1 eq), a stirbar, and deionized water (30 mL). Potassium thiocyanate was added to the flask (16 g, 160 mmol, 4 eq). The flask was stirred at room temperature for 24 hours. The mixture was then separated in a separatory funnel and collected the organic layer to generate PS (1.93 g, 65% yield) as a clear, colorless, viscous liquid. The spectroscopic data for this compound matched the reported literature,¹⁵ though previous reports did not fully tabulate the splitting of the peaks. ¹H NMR (500 MHz, CDCl₃): δ 2.92 (pseudo-h, *J* ≈ 5.8 Hz, 1H), 2.51 (dd, *J* = 6.3, 1.0 Hz, 1H), 2.12 (dd, *J* = 5.7, 0.7 Hz, 1H), 1.51 (d, *J* = 5.8 Hz, 3H).

¹H NMR (500 MHz, CDCl₃) Spectrum for PS

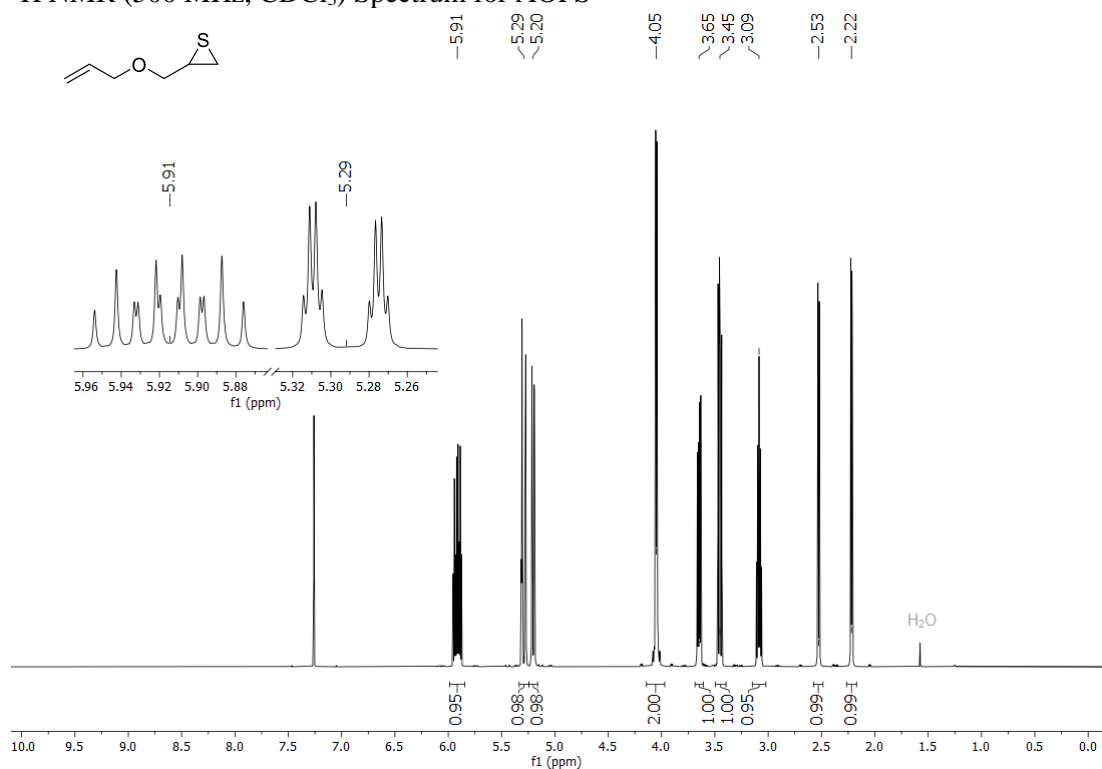


D. 3-(Allyloxy) propylene sulfide (AOPS)

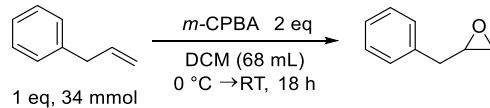


This synthesis was adapted from a previous literature procedure.⁹ A 100 mL round-bottom flask was charged with 2-(prop-2-enoxymethyl)oxirane (5.2 mL, 44 mmol, 1 eq), a stirbar, and deionized water (30 mL). Potassium thiocyanate was added to the flask (12.8 g, 130 mmol, 4 eq). The flask was placed in a pre-heated oil bath at 40 °C for 24 hours. The mixture was extracted with EtOAc (2 x 20 mL). The combined organic layers were then washed with deionized water (2 x 20 mL) and a saturated solution of brine (2 x 20 mL), dried using anhydrous magnesium sulfate, filtered, and concentrated using rotary evaporation. Further purification was carried out via column chromatography (9:1 hexanes:EtOAc, SiO₂) to generate AOPS (2.64 g, 46% yield) as a clear, colorless, viscous liquid. The spectroscopic data for this compound matched the reported literature,¹⁵ though previous reports did not fully tabulate the splitting of the peaks. ¹H NMR (500 MHz, CDCl₃): δ 5.91 (ddt, *J* = 17.2, 10.4, 5.7 Hz, 1H), 5.29 (dq, *J* = 17.2, 1.6 Hz, 1H), 5.20 (dq, *J* = 10.4, 1.3 Hz, 1H), 4.05 (dq, *J* = 5.7, 1.3 Hz, 2H), 3.65 (ddd, *J* = 10.6, 5.7, 0.6 Hz, 1H), 3.45 (dd, *J* = 10.6, 6.8 Hz, 1H), 3.09 (pseudo-quintet, *J* ≈ 6.0 Hz, 1H), 2.53 (dt, *J* = 6.2, 0.8 Hz, 1H), 2.22 (dd, *J* = 5.4, 1.2 Hz, 1H).

¹H NMR (500 MHz, CDCl₃) Spectrum for AOPS

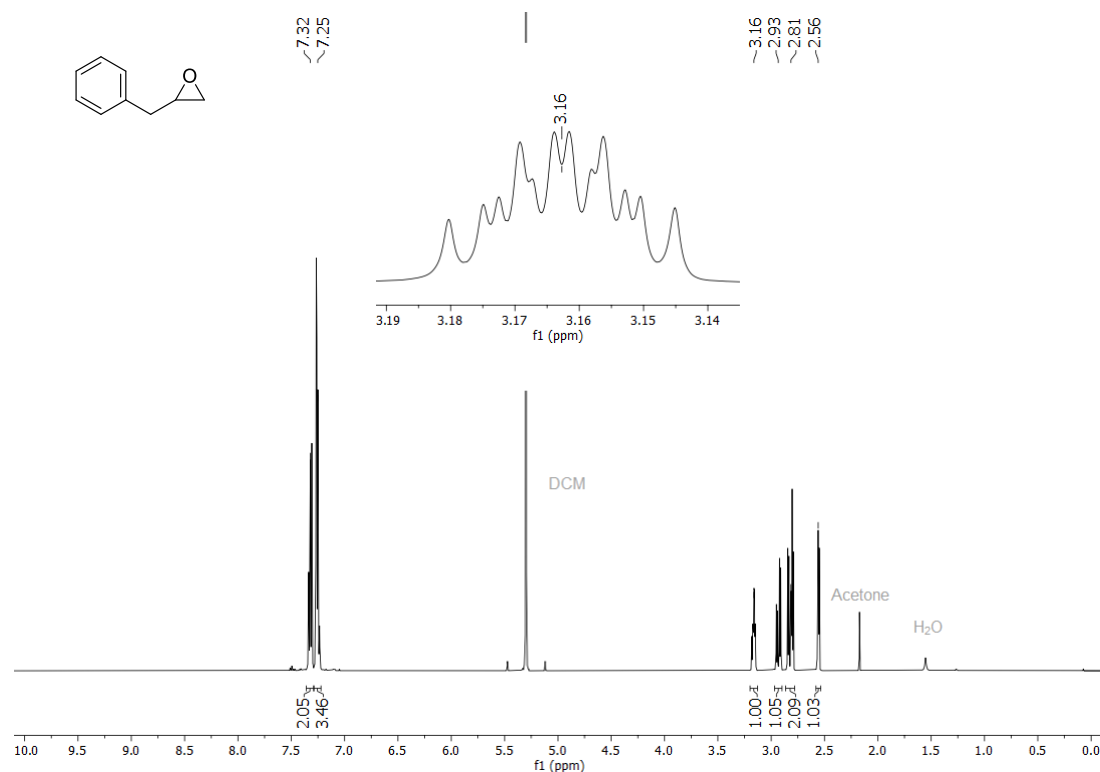


E. 3-Phenylpropylene oxide

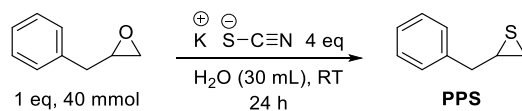


This synthesis was adapted from a previous literature procedure.⁶ A 250 mL round bottom flask was charged with allyl benzene (4.5 mL, 34 mmol, 1 eq), a stirbar, and dichloromethane (30 mL). The flask was cooled to 0 °C for 15 min before *meta*-chloroperoxybenzoic acid (12 g, 68 mmol, 2 eq) over 10 minutes with additional dichloromethane (38 mL). The flask was then warmed up to room temperature and stirred for 18 hours. Afterwards, saturated Na₂S₂O₃ (20 mL) was added dropwise to the flask and allowed to stir for an hour. The resulting mixture was then filtered in a Celite plug and rinsed with deionized water and DCM. The resulting water layer was extracted with DCM twice and all the DCM layers were combined, washed with saturated NaHCO₃ (2 x 30 mL), dried using anhydrous magnesium sulfate, filtered, and concentrated using rotary evaporation. The next step was carried out without further purification. The spectroscopic data for this compound matched the reported literature.⁶ ¹H NMR (500 MHz, CDCl₃): δ 7.31 (m, 2H), 7.24 (m, 3H), 3.16 (tdd, *J* = 5.5, 3.9, 2.7 Hz, 1H), 2.93 (dd, *J* = 14.5, 5.6 Hz, 1H), 2.81 (m, 2H), 2.55 (dd, *J* = 5.0, 2.7 Hz, 1H).

Crude ^1H NMR (500 MHz, CDCl_3) Spectrum for 3-Phenylpropylene oxide

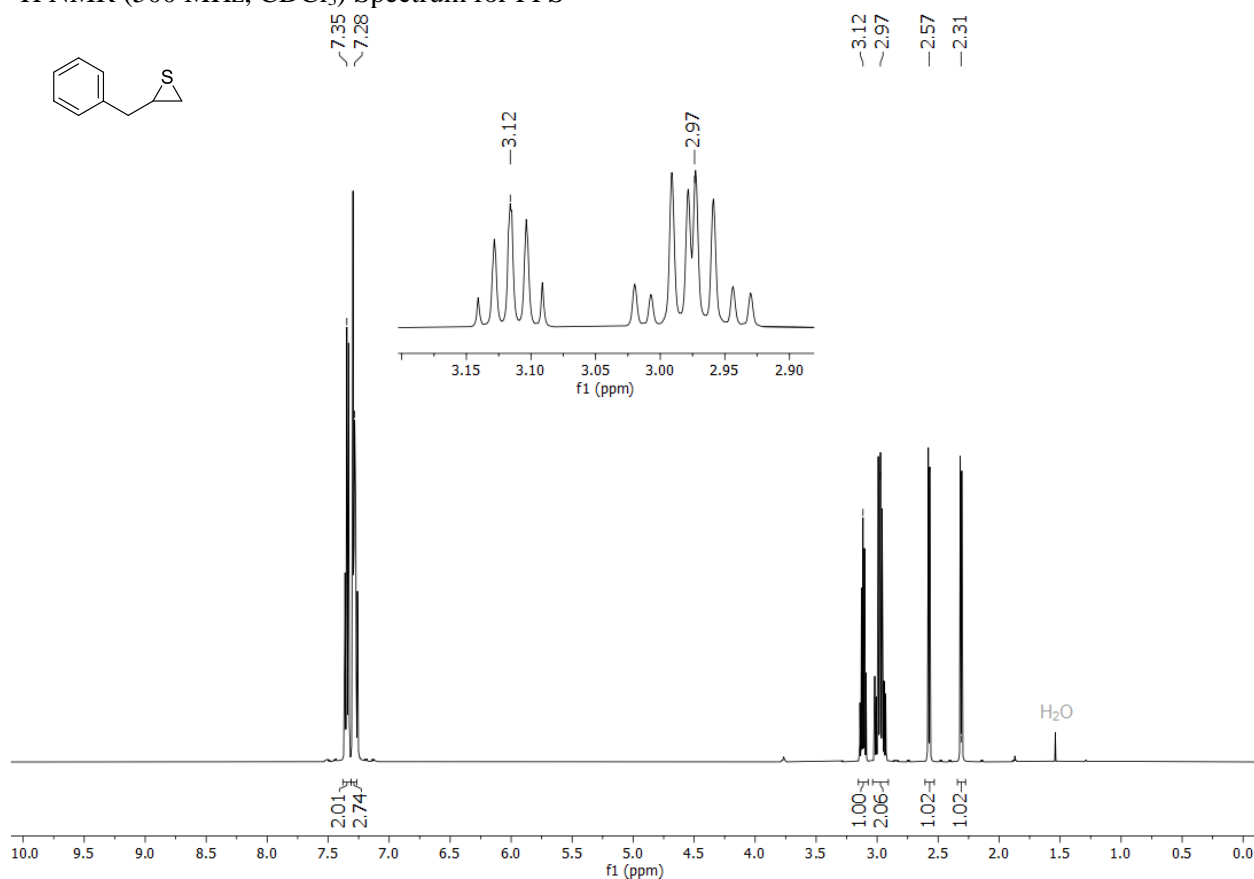


F. 3-Phenylpropylene sulfide (PPS)



This synthesis was adapted from a previous literature procedure.⁷ A 100 mL round bottom flask was charged with 3-phenylpropylene oxide (3.42 g, 25 mmol, 1 eq), a stirbar, and deionized water (32 mL). Potassium thiocyanate was added to the flask (9.33 g, 100 mmol, 4 eq). The flask was placed in a pre-heated oil bath at 40 °C for 24 hours. The mixture was extracted with EtOAc (2 x 20 mL). The combined organic layers were then washed with deionized water (2 x 20 mL) and a saturated solution of brine (2 x 20 mL), dried using anhydrous magnesium sulfate, filtered, and concentrated using rotary evaporation. Further purification was carried out via column chromatography (10:1 petroleum ether:EtOAc, SiO_2) to generate PPS (1.66 g, 33% overall yield over 2 steps) as a clear, colorless, viscous liquid. The spectroscopic data for this compound matched the reported literature,⁷ though previous reports did not fully tabulate the splitting of the peaks. ^1H NMR (500 MHz, CDCl_3): δ 7.35 (m, 2H), 7.28 (m, 3H), 3.12 (pseudo-quintet, 1H), 2.98 (m, 2H), 2.57 (dd, $J = 6.3, 1.1$ Hz, 1H), 2.31 (dd, $J = 5.6, 1.1$ Hz, 1H).

¹H NMR (500 MHz, CDCl₃) Spectrum for PPS



5. References

- 1 Z. Chen, L. Yan, J. J. Rech, J. Hu, Q. Zhang and W. You, *ACS Appl. Polym. Mater.*, 2019, **1**, 804–814.
- 2 J. T. Lai, D. Filla and R. Shea, *Macromolecules*, 2002, **35**, 6754–6756.
- 3 V. Kottisch, Q. Michaudel and B. P. Fors, *J. Am. Chem. Soc.*, 2016, **138**, 15535–15538.
- 4 Z. Zhang, T.-Y. Zeng, L. Xia, C.-Y. Hong, D.-C. Wu and Y.-Z. You, *Nat. Commun.*, 2018, **9**, 2577.
- 5 A. Z. Halimehjani, K. Marjani and A. Ashouri, *Green Chem.*, 2010, **12**, 1306–1310.
- 6 M. H. Shaw, R. A. Croft, W. G. Whittingham and J. F. Bower, *J. Am. Chem. Soc.*, 2015, **137**, 8054–8057.
- 7 J. Dong and J. Xu, *Org. Biomol. Chem.*, 2017, **15**, 836–844.
- 8 V. P. Bogdanov, V. A. Dmitrieva, V. A. Ioutsi, N. M. Belov and A. A. Goryunkov, *Journal of Fluorine Chemistry*, 2019, **226**, 109344.
- 9 J.-W. Li, M. Chen, Z. Zhang, C.-Y. Pan, W.-J. Zhang and C.-Y. Hong, *Polym. Chem.*, 2022, **13**, 402–410.
- 10 M. Martiny, E. Steckhan and T. Esch, *Chem. Ber.*, 1993, **126**, 1671–1682.
- 11 M. Uchiyama, Y. Murakami, K. Satoh and M. Kamigaito, *Angew. Chem., Int. Ed.*, 2023, **62**, e202215021.
- 12 S. Hosseini and S. O. Martinez-Chapa, in *Fundamentals of MALDI-ToF-MS Analysis: Applications in Bio-diagnosis, Tissue Engineering and Drug Delivery*, eds. S. Hosseini and S. O. Martinez-Chapa, Springer, Singapore, 2017, pp. 1–19.

- 13 H. Daimon, H. Okitsu and J. Kumanotani, *Polym. J.*, 1975, **7**, 460–466.
- 14 S. W. Spring, C. S. Cerione, J. H. Hsu, S. L. Shankel and B. P. Fors, *Chin. J. Chem.*, 2023, **41**, 399–404.
- 15 C. M. Kleiner, L. Horst, C. Würtele, R. Wende and P. R. Schreiner, *Org. Biomol. Chem.*, 2009, **7**, 1397–1403.